Available online at www.sciencedirect.com

ScienceDirect

Nuclear Data Sheets 148 (2018) 143–188

Nuclear Data Sheets

www.elsevier.com/locate/nds

Evaluation of the Neutron Data Standards

A.D. Carlson,[1,*] V.G. Pronyaev,[2] R. Capote,[3] G.M. Hale,[4] Z.-P. Chen,[5] I. Duran,[6] F.-J. Hambsch,[7] S. Kunieda,[8] W. Mannhart,[9] B. Marcinkevicius,[3,10] R.O. Nelson,[4] D. Neudecker,[4] G. Noguere,[11] M. Paris,[4] S.P. Simakov,[12] P. Schillebeeckx,[7] D.L. Smith,[13] X. Tao,[14] A. Trkov,[3] A. Wallner,[15,16] and W. Wang[14]

[1] *National Institute of Standards and Technology, 100 Bureau Drive, Stop 8463, Gaithersburg, MD 20899-8463, USA*
[2] *PI Atomstandart, State Corporation Rosatom, 117342, Moscow, Russia*
[3] *NAPC-Nuclear Data Section, International Atomic Energy Agency, Vienna, Austria*
[4] *Los Alamos National Laboratory, Los Alamos, NM 87545, USA*
[5] *Tsinghua University, Beijing, 100084, China*
[6] *Universidad de Santiago de Compostela, Spain*
[7] *EC-JRC-Directorate G, Unit G.2, B-2440 Geel, Belgium*
[8] *Japan Atomic Energy Agency, Nuclear Data Center, Ibaraki 319-1195, Japan*
[9] *Physikalisch-Technische Bundesanstalt, Org. 6.4, 38116 Braunschweig, Germany*
[10] *Uppsala University, Uppsala, Sweden*
[11] *SPRC/LEPh, CEA Cadarache, 13108 Saint Paul Les Durance, France*
[12] *Karlsruhe Institute of Technology, Hermann-von-Helmholtz-Platz 1 76344 Eggenstein-Leopoldshafen, Germany*
[13] *Argonne National Laboratory, Argonne, IL 60439, USA*
[14] *China Nuclear Data Center (CNDC), China Institute of Atomic Energy, Beijing, China*
[15] *Vera Laboratory, Faculty of Physics, University of Vienna, A-1090 Vienna, Austria*
[16] *Dept. of Nuclear Physics, The Australian National University, Canberra ACT 0200, Australia*

(Received 3 September 2017; revised received 30 October and 12 November 2017; accepted 20 November 2017)

With the need for improving existing nuclear data evaluations, (*e.g.*, ENDF/B-VIII.0 and JEFF-3.3 releases) the first step was to evaluate the standards for use in such a library. This new standards evaluation made use of improved experimental data and some developments in the methodology of analysis and evaluation. In addition to the work on the traditional standards, this work produced the extension of some energy ranges and includes new reactions that are called reference cross sections. Since the effort extends beyond the traditional standards, it is called the neutron data standards evaluation. This international effort has produced new evaluations of the following cross section standards: the H(n,n), ^{6}Li(n,t), ^{10}B(n,α), ^{10}B(n,$\alpha_1\gamma$), ^{nat}C(n,n), Au(n,γ), ^{235}U(n,f) and ^{238}U(n,f). Also in the evaluation process the ^{238}U(n,γ) and ^{239}Pu(n,f) cross sections that are not standards were evaluated. Evaluations were also obtained for data that are not traditional standards: the Maxwellian spectrum averaged cross section for the Au(n,γ) cross section at 30 keV; reference cross sections for prompt γ-ray production in fast neutron-induced reactions; reference cross sections for very high energy fission cross sections; the ^{252}Cf spontaneous fission neutron spectrum and the ^{235}U prompt fission neutron spectrum induced by thermal incident neutrons; and the thermal neutron constants. The data and covariance matrices of the uncertainties were obtained directly from the evaluation procedure.

CONTENTS

* Corresponding author: carlson@nist.gov

https://doi.org/10.1016/j.nds.2018.02.002

I. INTRODUCTION

New evaluations of the neutron data standards have been completed. This work was a result of efforts by the Cross Section Evaluation Working Group (CSEWG) and the International Atomic Energy Agency (IAEA). They worked cooperatively to provide these new evaluations of the standards. Important contributions to the evaluation process resulting from this joint international effort have been highlighted at several IAEA meetings. To initiate the evaluation process, an IAEA Consultants' Meeting on International Neutron Cross-Section Standards was held in 2008 at the IAEA Headquarters, Vienna, Austria. In addition to the work on the traditional standards, discussions took place on the possibility of extending the energy ranges and including new reactions that could be considered for adoption as reference cross sections. This work took place under the data development project that had been endorsed by the International Nuclear Data Committee as an important activity to be maintained under the auspices of the Nuclear Data Section of the IAEA. Additional standards related meetings were held in 2010, 2013, 2014, 2016 and 2017. IAEA reports from these meetings provide discussions on the topics as well as the individual presentations given by the attendees at the meetings. INDC(NDS)-0540,-0583, -0641 and -0677 reports are available at the website for the IAEA Nuclear Data Section.

The present work represents an update of the earlier neutron cross section standards evaluation by Carlson *et al.* [1]. That earlier evaluation of the standards will be called the 2006 standards evaluation throughout this paper. Those standards were accepted by the CSEWG as the standards for the ENDF/B-VII.0 library. A short summary of the results of the standards evaluation was contained in the publication describing that evaluation [2]. Changes have been made to the ENDF/B-VII.0 library that led to an update or modification called ENDF/B-VII.1 [3]. The standards must be maintained for a given version of ENDF in order to maintain consistency thus no changes were made to the standards with the introduction of ENDF/B-VII.1. This effort is part of the gradual process of improving the standards. It is hoped that at some point in the future the standards will be evaluated very frequently so they can be used by major nuclear data libraries whenever they decide to produce a new version. The ENDF/B-VIII.0 standards [4], that will be taken from this International Standards Evaluation, represent the most recent outcome of this process. Throughout this paper the present evaluation of the standards will be called the 2017 standards evaluation or the 2017 standards. In this paper the process of obtaining these evaluations will be documented. This should provide adequate guidance so one can better understand how the ENDF/B-VIII.0 standards and their uncertainties were obtained, and should also provide adequate supporting information for assessing their quality. It is essential to devote considerable space in this paper to reviewing this evaluation process, including comprehensive discussions

of the weaknesses in earlier evaluations. It is important to take note of the impact of improvements in computer technology and evaluation methodology in order to understand the progress which has been made leading up to this most recent evaluation.

A. The Need for Standards

Most neutron cross section measurements are made relative to the neutron cross section standards. As such they are the basis for measurements and evaluations. Very few cross sections can be measured absolutely, *i.e.*, without the need to determine the neutron fluence – most cross sections are measured relative to the cross section standards and converted using evaluations of the standards. An important point is that the accuracy of a cross section or fluence measurement is limited by the uncertainty in the standard cross section relative to which it is measured. Improvements in the standard cause all measurements relative to that standard to be improved. This applies to measurements that have been, are being or will be made relative to that standard. This is the reason for the emphasis on increasing the quality of neutron cross section standards. They must be evaluated first in the process of developing a new version of an evaluated nuclear data file library. Measurement programs have continuously improved the database of the standards, and therefore it is important to re-evaluate these cross sections taking into account new experimental data and improved evaluation techniques.

There is also a need for additional data related to standards such as reference data and the extension in energy range of certain cross sections. These topics have been investigated during this project.

B. Work Leading to the New Evaluation

The standards have had quite an evolution going from ENDF/B-I to ENDF/B-VIII. When ENDF/B was in its infancy, the number of standards, their energy ranges of applicability, and their accuracy were not well established.

Prior to the ENDF/B-IV standards evaluation, evaluations were largely performed by drawing a smooth curve through the average of the data points on a graph. The uncertainties were very approximate and providing covariances was not even considered. Also a hierarchical approach was followed for the evaluations. The lighter element cross section standards were generally considered to be better known. The H(n,n) cross section was considered the best known standard and was evaluated first and independently of the other standards. The ^{6}Li(n,t) cross section evaluation was performed next. The only ^{6}Li(n,t) data which were used were absolute measurements or those measured relative to the H(n,n) standard which were converted to cross sections using the adopted hydrogen evaluation. Then the ^{10}B+n standard cross sections were evaluated. The only ^{10}B data which were used were absolute measurements and those relative to H(n,n) and ^{6}Li(n,t) which were converted using the new hydrogen and lithium evaluations. This process was continued for each of the standards. This method for using ratio measurements does not use all the information available. It does not include absolute and ratio data on the same basis as they were measured. For example, a ratio of the ^{10}B(n,α) to the ^{6}Li(n,t) cross sections would be used in the ^{10}B(n,α) cross section evaluation but not in the ^{6}Li(n,t) evaluation.

Some improvement occurred for the ENDF/B-IV standards evaluation in that *R*-matrix evaluations were introduced for the lighter element standards.

The movement towards more objective evaluations started with ENDF/B-V when a simultaneous evaluation of the ^{235}U(n,f) cross section was done by Poenitz. It was composed of an evaluation of the shape of the cross section and a separate evaluation of the normalization for the shape of the cross section. The members of the Normalization and Standards Subcommittee selected the experiments which were used for the determination of the normalization factor for the shape evaluation. This evaluation was a first step towards an evaluation process that would provide consistent sets of cross sections for all the standards.

The success obtained using the comprehensive objective data combination techniques in the ENDF/B-V standards evaluation led to the seeking out of a more global approach for the ENDF/B-VI standards evaluation than had been used earlier.

The previous complete evaluation of the neutron cross section standards was finished in October 2005 (often referred to as the 2006 evaluation) and made available as the NEANDC/INDC and ENDF/B-VII standards. *R*-matrix model fits for the light-element cross sections and non-model least-squares fits for all the cross sections employed were the basis of the combined fits for all of the data. Some important reactions and constants are not standards, but assist greatly in the determination of the standard cross sections and reduce their uncertainties; therefore, these data were also included in the combined fits. The largest experimental database used in the evaluation was prepared by Poenitz and included about 400 sets of experimental data with covariance matrices of uncertainties that account for all known cross-energy, cross-reaction and cross-material correlations. GMA is a least-squares code developed by Poenitz to fit all types of cross section (absolute and shape), their ratios, spectrum-averaged cross sections and thermal constants in one full analysis. It was observed in some cases that the GMA results appeared to be somewhat low compared with the majority of the experimental data being evaluated. This effect is called Peelle's Pertinent Puzzle [5, 6]. Study of this effect became an extensive investigation before the 2006 evaluation was completed. A "fix" was applied which basically removed the problem. The modified code is called GMAP.

Basically the process for the 2006 standards evalua-

tion involved using input from *R*-matrix analyses for the ^{6}Li(n,t), ^{10}B(n,α) and ^{10}B(n,$\alpha_1\gamma$) cross sections; a thermal constants evaluation as pre-evaluated data and direct experimental data for the ^{6}Li(n,t), ^{10}B(n,$\alpha_1\gamma$), ^{10}B(n,α), Au(n,γ), ^{235}U(n,f), ^{238}U(n,f), ^{238}U(n,γ) and ^{239}Pu(n,f) reactions in a combined fit with the generalized least-squares code GMAP [7, 8]. The H(n,n) evaluation was done separately as an *R*-matrix analysis.

C. Research Areas

Considerable effort was expended on obtaining experimental data for the evaluations. The data obtained were examined for possible problems or needed corrections before putting them in the database. Uncertainties were obtained and, when possible, correlations within a data set and correlations to other data were investigated. All uncertainties given in this paper are one standard deviation (k=1 or 68 % confidence interval). The work on cross section standards was extended into other areas related to standards: The work on the 30 keV Maxwellian spectrum averaged cross section for the Au(n,γ) cross section; cross sections for prompt γ-ray production in fast neutron-induced reactions; reference cross sections for very high energy fission cross sections; the ^{252}Cf spontaneous fission neutron spectrum and the ^{235}U thermal prompt fission neutron spectrum; and the thermal constants. Each of these quantities can be used in either a cross section measurement, to obtain neutron fluence, or to validate a cross section in a well characterized spectrum.

II. THE EXPERIMENTAL DATABASE – RECENT MEASUREMENTS

Measurements have been made relevant to each of the data being evaluated. For the 2006 evaluation there was only an initial effort on fission spectra and several new areas of research were only started. The present effort includes additional data related to standards such as reference data and the extension in energy of certain cross sections.

A. H(n,n) Cross Section Measurements

Measurements have been made by Moreh, Block and Danon [9] that show a possible anomalous drop of about 40 % in the n-p differential scattering cross section suggested by Ref. [10], compared with accepted values, for 100 eV to 200 eV neutrons does not exist. They measured scattered neutrons from CH_2 and separately from C. The ratio of these data shows the effect is not present for incident neutron energies of 100 eV to 140 keV.

Daub *et al.* [11] made measurements of the hydrogen total cross section where very few measurements of that cross section were available, at low neutron energies. The

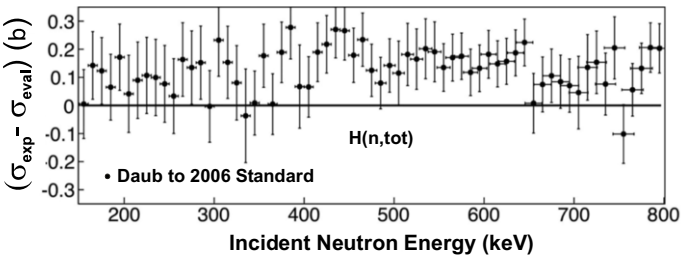

FIG. 1. Comparison of the hydrogen total cross section measurements of Daub *et al.* with the 2006 standards evaluation.

data were measured at the University of Kentucky Van de Graaff facility from 150 keV to 800 keV. The results are shown in Fig. 1 and are systematically about 1 % larger than the values from the 2006 evaluation but almost within their uncertainties of 1.1 % to 2 %.

Additional total cross section work at Kentucky has been done by Yang [12]. The focus was on lower neutron energies than those obtained by Daub *et al.* Data were obtained from 90 keV to 1.8 MeV with uncertainties of 1 %–2 %. Final data are not available. They are only shown in plots in a thesis document. So these data were not included in the standards evaluation.

The ongoing work at Ohio University on the hydrogen standard now emphasizes the small angles in the center-of-mass system (CMS) at about 14 MeV where few data are available. This work required detection of the recoil neutrons. Obtaining data over a large angular range is important since the data are relative measurements that are normalized to the accurately known total elastic cross section. Their earlier work [13], [14] at 10 and 14 MeV used proton recoil detection that limited the angular range to larger CMS angles. Work has also been done at 14 MeV by Kondo *et al.* [15] at Osaka University but their angular range was limited. Problems with the hydrogen scattering cross section still exist in the hundred MeV region and the prospects for new measurements there are very weak. Data have been obtained at about 200 MeV by Sarsour *et al.* [16] at Indiana University and by Rahm *et al.* [17] at Uppsala University. There are inconsistencies in these measurements as large as 10 % at CMS back angles. There has been an understanding amongst these authors that the Indiana University data are to be preferred due to the method used and the uncertainties obtained. There is a particular need for data in the higher energy regions that extend over a large angular range.

B. Work Related to the ^{3}He(n,p) Cross Section

This cross section is the least used of the cross section standards. It is not accepted as a standard by any libraries except for ENDF/B. Very few new measurements have been made of this cross section. There are data in the past that have been made relative to this standard so changes in this cross section through an evaluation can be important. Since so little experimental work had been

done on this cross section, no new evaluation was done. The last evaluation of this cross section was done for ENDF/B-VI. It was adopted for the 2017 standards.

C. ^{6}Li(n,t) Cross Section Measurements

Angular distribution measurements for that reaction at higher neutron energies have been completed by Zhang *et al.* [18] at Peking University and by Devlin *et al.* [19] at the Los Alamos Neutron Science Center (LANSCE). Excitation functions measured by Devlin *et al.* for tritons from the ^{6}Li(n,t) reaction for four angles are shown in Fig. 2. The R-matrix fit [19] shown in this figure was obtained using the Devlin *et al.* data and earlier measurements on the ^{7}Li compound system. Data such as these have an impact on the definition of the ^{6}Li(n,t) cross section since they provide information on the ^{7}Li compound nucleus that can be used in R-matrix evaluations.

At the NIST Neutron Center for Neutron Research a measurement was made by Yue *et al.* [20] of the ^{6}Li(n,t) cross section standard with a 0.3 % uncertainty at 3.3255 meV. Work continues on trying to determine the mass uncertainty of the ^{6}Li target. The original mass yielded a cross section in excellent agreement with the standards evaluation. The deposits were made at JRC Geel, however JRC Geel recently found an error so the mass changed by about 1 %. This leads to a cross section lower than the standard by about 1 %. Measurements have been made by Giorginis and Bencardino [21] at JRC Geel at 1.9, 2.0 and 2.1 MeV. The data were obtained relative to the ^{238}U(n,f) cross section. The data agree with the 2006 standards evaluation at 1.9 MeV but are 2.6 % higher at 2.0 MeV and 1.8 % higher at 2.1 MeV. However the results are in agreement with the 2006 standards evaluation within their uncertainties. Their measurements used a fission fragment loss correction given by Meadows. Giorginis found that a small change was required to that correction. It was incorporated in the final results of the Giorginis and Bencardino data.

A number of data sets having energies above the former standards energy range are included in the standards evaluation to improve *R*-matrix fits to the data sets.

D. ^{10}B(n,α) and ^{10}B(n,$\alpha_1\gamma$) Cross Section Measurements

Measurements of the ^{10}B(n,tot) cross section were made by Wasson [22]. Recently a complete analysis of those data was performed. They were then put into the GMAP analysis. The data are shown in Fig. 3 compared with the 2006 standards evaluation. In Ref. [22], comparison is made with the ENDF/B-VI standards evaluation. That comparison showed a larger measured cross section by about 5 % in the hundred keV energy region. The larger cross section in the hundred keV energy region was also observed by Brusegan *et al.* [23]. It is clear that the 2006 standards evaluation is an improvement over the ENDF/B-VI standards evaluation.

At JRC-Geel, Bevilacqua *et al.* [24] have made branching ratio, angular distribution and cross section measurements for the ^{10}B(n,α) reaction. Their new work extends the measurements to about 3 MeV. At the higher energies there is concern since there are large deviations from the 2006 standards evaluation. Work has also been done on the ^{10}B(n,α) cross section at Peking University by Zhang *et al.* [25] in the MeV energy region. They have made improvements to their experiment so ^{10}B(n,α) measurements with a minimum of "particle leaking" losses were obtained. Particle leaking losses [26] occur when both reaction products go into forward angles such that it is not possible to separate the particles. The detector sees a quasi-particle with an energy equal to the sum of the energies of the individual particles. Consequently, there will be a loss of events under these circumstances. The ^{10}B(n,α) data at these higher energies should eventually allow this standard to be extended to higher energies.

E. C(n,n) Cross Section Measurements

Carbon transmission measurements have been made by Gritzay *et al.* [27]. The results were shown to generally agree with the standards evaluation and are not dependent on the sample thickness. A motivation for this work was to determine if a strong resonance predicted by Canton *et al.* [28] is present in the 130-160 keV energy region. No evidence for a resonance was found. Filtered beam measurements have been made of the C(n,n) angular distribution for five angles at three energies by Gritzay *et al.* [29]. The data differ significantly from the standards evaluation. The data are relative to lead scattering. Daub *et al.* [11] also made measurements of the carbon total cross section. These data were obtained when the hydrogen total cross section measurements were made since carbon and polyethlyene samples were used in the measurements. They agree with the 2006 standard within uncertainties but are systematically lower. Measurements of the carbon total cross section have also been made by Danon *et al.* [30] at RPI that agree very well with the 2006 standards evaluation. The Daub *et al.* and Danon *et al.* measurements are shown in Fig. 4.

F. ^{197}Au(n,γ) and ^{238}U(n,γ) Cross Section Measurements

The work on the gold capture cross section was done in the standards energy region and also in support of astrophysics applications at lower neutron energies. New work on gold capture was done by Wallner *et al.* [31] who made a ^{238}U(n,γ)/Au(n,γ) cross section ratio measurement at 430 keV. The samples were irradiated and accelerator mass spectrometry was used to measure the ^{239}Pu resulting from the decay of ^{239}U. Activation was used for

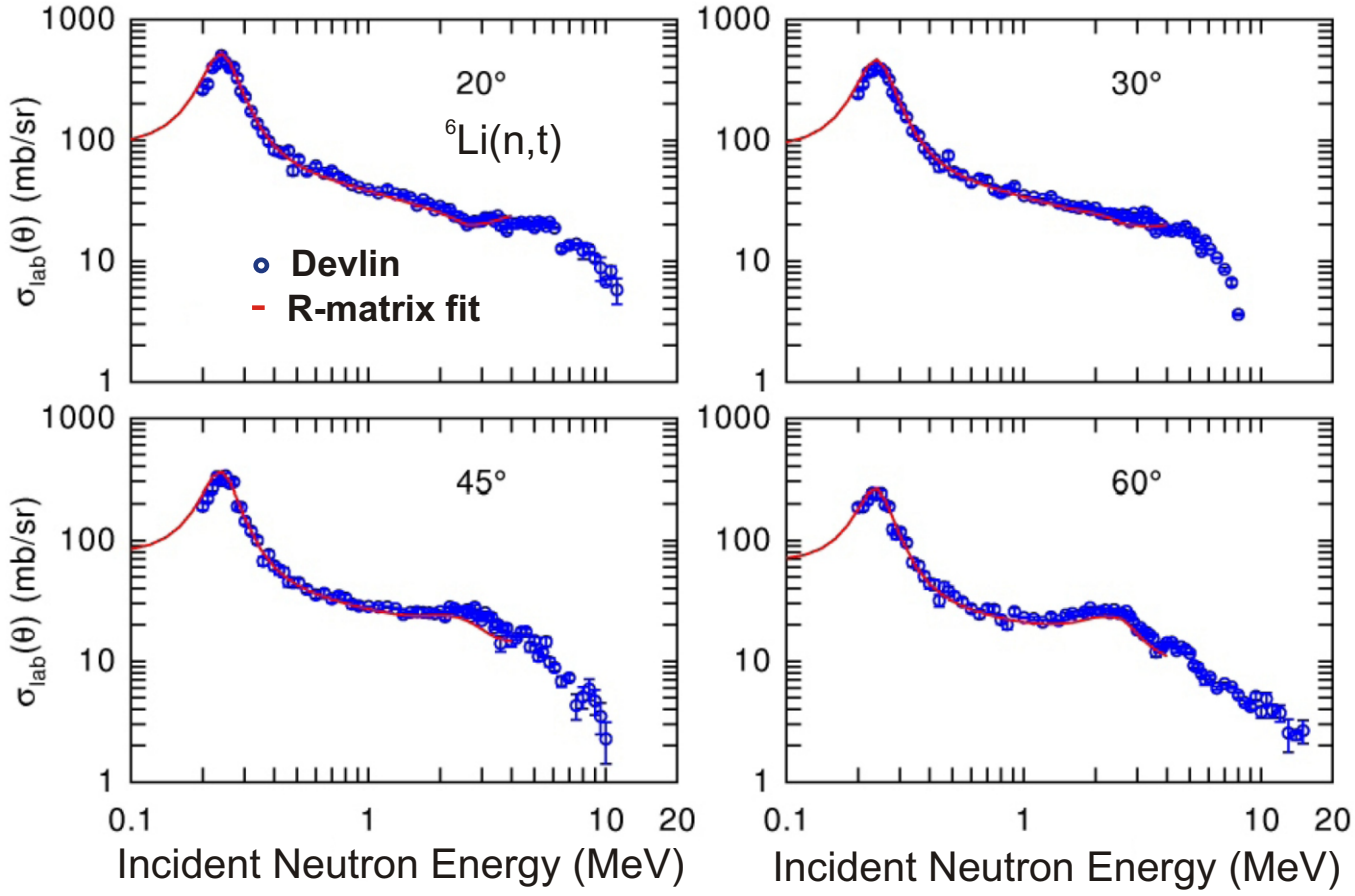

FIG. 2. (Color online) Excitation functions measured by Devlin *et al.* for tritons from the ^{6}Li(n,t) reaction for four angles compared with an R-matrix fit.

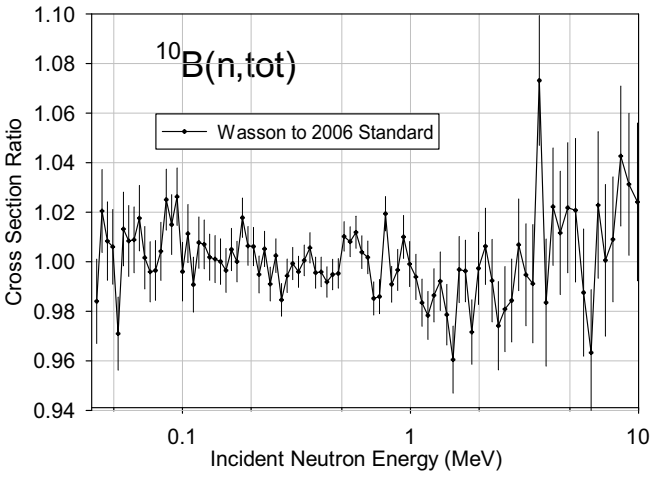

FIG. 3. Measurements of the ^{10}B total neutron cross section by Wasson *et al.* compared with the 2006 standard.

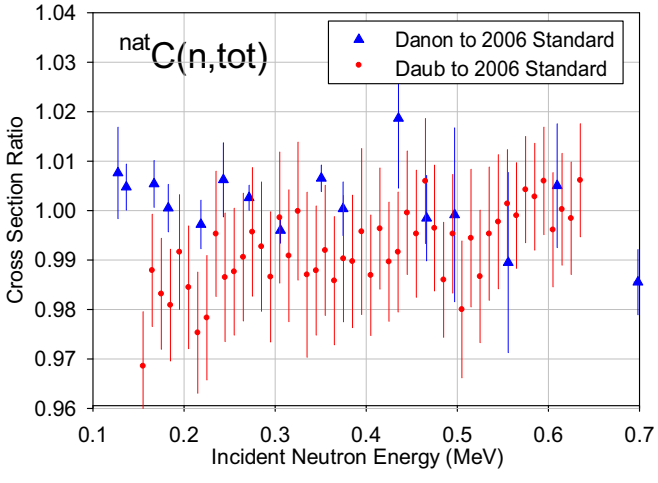

FIG. 4. (Color online) Carbon total cross section of Danon *et al.* and Daub *et al.* compared with the 2006 standards evaluation.

the gold measurements. The 430 keV measurement had a large (150 keV FWHM) energy resolution.

The cross section ratio obtained agrees with the standards evaluation. An extension of the n_TOF data by Massimi *et al.* [32] for the gold capture measurement up to about 400 keV was done by Lederer *et al.* [33]. In the standards energy region the Lederer *et al.* results, with uncertainties that are between 3.9 % and 4.5 % for a resolution of 10 bins per energy decade, generally agree well with the standards evaluation.

Measurements by Ullmann *et al.* [34] of the ^{238}U(n,γ) cross section were taken for the energy range from 10 eV to 500 keV. The data have only been reported from 1 keV to 500 keV. The measurements were relative to the ^{6}Li(n,t) and ^{235}U(n,f) cross section standards. The results from 200 keV to 500 keV agree well with the standards evaluation and were included in the evaluation. The data from 10 keV to 200 keV were not included in the evaluation due to unusual structure in the data. Very accurate measurements of the ^{238}U(n,γ) cross section in the resonance region and extending up to 80 keV were made at GELINA by Kim *et al.* [35] with a C_6D_6 detector. In Fig. 5 those data are shown compared with the results of the 2017 standards evaluation.

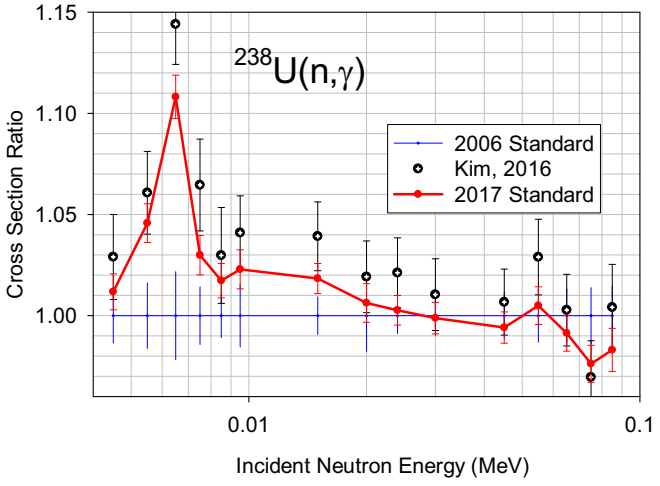

FIG. 5. (Color online) Measurements of the ^{238}U(n,γ) cross section by Kim *et al.* compared with the results of the 2017 standards evaluation, relative to 2006 standards.

At n_TOF, measurements were made with different C_6D_6 detectors [36], [37] and with a BaF_2 total absorption detector [38].

G. ^{197}Au(n,γ) Cross Section Measurements Related to the 30 keV Maxwellian Average Cross Section

The Maxwellian averaged cross section (MACS) for ^{197}Au(n,γ) is used in neutron capture cross section measurements as a reference for reactions important for astrophysics, reactor and dosimetry applications. This reference cross section was obtained from an evaluation by Ratynski and Käppeler [39].

The 2006 standards evaluation is approximately 6 % above the Ratynski and Käppeler evaluation.

Because of this discrepancy new experiments and reanalyses were done in an attempt to resolve the problem. The Lederer *et al.* data referred to previously include the energy region where this discrepancy exists. The results from that work generally agree with those obtained from the ^{197}Au(n,γ) standards evaluation within the uncertainty of the measurements. The MACS from these data at 30 keV is 2 % smaller than the MACS obtained from the standards evaluation and 4.7 % higher than the one obtained by Ratynski and Käppeler. The uncertainty of the Lederer *et al.* MACS at 30 keV is 3.6 %, thus there is very good agreement with the standards evaluation. All MACS values are compared for a temperature of 30 keV. Measurements by Wallner [31] of the ^{238}U(n,γ) cross section relative to the ^{197}Au(n,γ) cross section were made for a Maxwell-Boltzman simulated spectrum expected to be equivalent to that of Ratynski and Käppeler. Their ratio agrees with the standards evaluation. New measurements of the ^{197}Au(n,γ) cross section were made by Massimi *et al.* [40] at the GELINA facility. Large attention was paid to the measurements and analysis of the normalization, background, self-shielding and scattering corrections in this energy range. This led to a very small total measurement uncertainty of 1.5 %. The result agreed with the standards evaluation to within 2 %. It should be noted that these data are highly correlated with the Kim *et al.* [35] data. Earlier work at the GELINA facility by Borella *et al.* [41] are also in good agreement with the standards evaluation.

A spectrum averaged ^{197}Au(n,γ) cross section measurement by Feinberg *et al.* [42] at JRC-Geel is in good agreement with that calculated from the standards evaluation. It is about two standard deviations from the Ratynski and Käppeler value. All these experiments agree with the standards evaluation indicating a problem with the Ratynski and Käppeler result. Two measurements have been made of the simulated Maxwellian spectrum used in the Ratynski and Käppeler measurements. Both experiments used neutrons from the ^{7}Li(p,n) reaction for E_p=1912 keV (the same as that used by Ratynski and Käppeler). The spectrum measurements at PTB by Lederer *et al.* [43] are slightly softer, but have an effect of only 0.5 % on the averaged Au cross section. A comparison with thick target yields calculated using the PINO [44] code and evaluated microscopic differential cross sections give good agreement with the results of this experiment. Independently, measurements of the neutron spectrum at JRC-Geel by Feinberg *et al.* [42] showed good agreement with the findings of Ratynski and Käppeler and of Lederer. Martín Hernández *et al.* [45] made measurements related to the ^{7}Li(p,n) spectrum at threshold and found the calculated spectrum-averaged cross section (SACS) using the Ratynski and Käppeler spectrum is 6.5% higher than the cross section value measured by Ratynski and Käppeler. Their results indicate at least 8 of the 41 mb difference between the Ratynski and Käppeler activation measurement and the Ratynski and Käppeler SACS is probably due to the neutron spectrum uncertainty.

H. ^{235}U(n,f), ^{238}U(n,f) and ^{239}Pu(n,f) Cross Section Measurements

Measurements have been made of the ^{238}U(n,f)/^{235}U(n,f) cross section ratio by Paradela *et al.* [46] us-

ing fission chamber and parallel plate avalanche counter detectors. Data were taken with detectors in different orientations and special consideration was applied to determining losses due to the fission fragment angular distributions. The data extend to ≈ 1 GeV. The average of the data sets is in good agreement with the 2006 standards evaluation considering the uncertainties. In Fig. 6 the four measurements obtained in these experiments are shown. ^{238}U(n,f)/ ^{235}U(n,f) cross section ratio data were also obtained by Tovesson *et al.* [47] up to 198 MeV. The data are in fair agreement with the 2006 standards evaluation throughout most of the energy region.

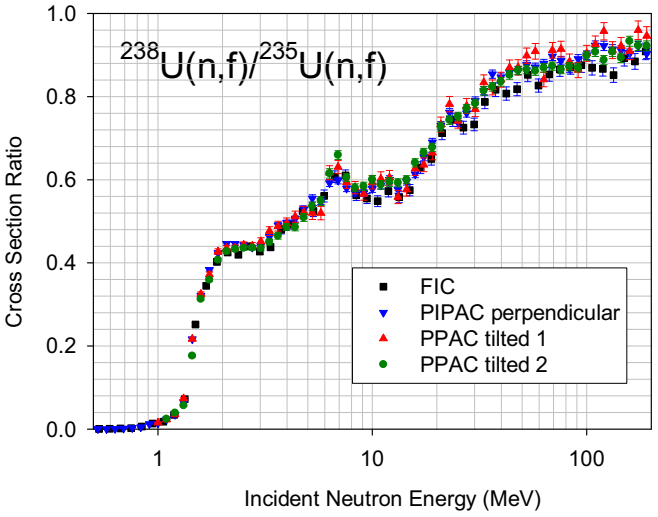

FIG. 6. (Color online) Measurements of the ^{238}U(n,f)/ ^{235}U(n,f) cross section ratio by Paradela *et al.*

Measurements have been made at LANL of the ^{239}Pu(n,f) cross section by Tovesson and Hill [48]. The data are relative to the ^{235}U(n,f) cross section. They are composed of 2 data sets. One set is for energies below 200 keV and the other for energies above 200 keV. There are large discrepancies for the lower energy set compared with most of the other experimental data so no data for the lower set were used in the evaluation. For the higher energy set they agree well with the standards evaluation up to about 13 MeV. Above that the measurements are somewhat lower than the standards evaluation. Very accurate fission cross section ratio measurements that include ^{239}Pu(n,f) data are being measured at the LANSCE facility. The data are being obtained with a Time Projection Chamber in a collaboration headed by the NIFFTE collaboration [49]. Data analysis is currently in progress. Their preliminary results are in excellent agreement with the 2006 standards evaluation.

I. High Energy Reference Fission Cross Section Measurements

Reference cross sections at high energies are needed for conversion of ratio measurements to cross sections at high energies where standards are not available.

The cross sections included here are for ^{209}Bi(n,f), ^{nat}Pb(n,f), ^{235}U(n,f), ^{238}U(n,f) and ^{239}Pu(n,f).

The database for these evaluations is rather limited.

An older experiment done at the LANSCE facility at LANL was re-analyzed by Miller and Kovash [50]. This led to a determination of the ^{238}U(n,f) cross section. The data were obtained relative to the hydrogen scattering cross section for neutron energies from 130 to 300 MeV. Unfortunately there were bubbles in the liquid hydrogen target that was used for the fluence determination so an absolute cross section could not be obtained. New measurements that have been made include: ^{238}U(n,f) to ^{235}U(n,f) cross section ratio measurements by Paradela *et al.* [46] up to 1 GeV; ^{239}Pu(n,f) to ^{235}U(n,f) cross section ratio measurements by Tovesson and Hill up to 200 MeV [48] and ^{209}Bi(n,f) to ^{nat}Pb(n,f) cross section ratio measurements by Tarrio *et al.* [51] up to 1 GeV.

J. Prompt γ-ray Production Reference Cross Section Measurements

There has been a need expressed for a reference cross section for use in measurements of γ-ray production cross sections. Such measurements are most easily performed using a reference cross section in which a discrete γ-ray is detected. Both (n,n'γ) and (n,2nγ) reactions were considered. Several candidates were investigated taking into account factors such as structure and magnitude of the cross section, status of the database, sample properties, typical experimental environments, and evaluations performed. In the past, inelastic scattering of neutrons on ^{56}Fe and ^{52}Cr, which produce 847 keV and 1434 keV prompt γ-rays, respectively, were considered. For ^{56}Fe the main drawbacks are the contribution from (n,p) reactions followed by beta decay to the 847-keV level in ^{56}Fe, the presence of resonance structure in the cross section below about 5 MeV, the non-isotropic angular distribution in γ yield which varies with the neutron energy, and the background from iron materials which are almost always present near experimental setups.

The database for the ^{52}Cr(n,n'γ) cross section is smaller than that for ^{56}Fe(n,n'γ). Cr suffers from drawbacks similar to Fe, and is difficult to fabricate into samples with uniform areal density.

Though more effort has been placed on the ^{56}Fe(n,n'γ) and ^{52}Cr(n,n'γ) cross sections, their inherent limitations suggest that other cross sections should be investigated to obtain better reference cross sections. ^{197}Au, ^{93}Nb, ^{48}Ti, ^{7}Li and ^{10}B were considered. It was decided that the use of the γ-production cross sections for ^{93}Nb and ^{197}Au is not suitable, because of feeding from isomers populated in the irradiation of the samples, and for ^{197}Au the presence of interfering γ-lines in the background.

The conclusion of this study is that the best candidates are ^{10}B, ^{7}Li, and ^{48}Ti. For the lower energies the ^{10}B(n,$\alpha_1\gamma$) reaction has a very large cross section and

varies smoothly with energy. It is a standard and it can be extended somewhat in energy over its use as a standard for its use as a reference. The ^{7}Li(n,n'γ) reaction, leading to the production of the same gamma-line as that from the ^{10}B(n,$\alpha_1\gamma$) reaction, has a yield that is isotropic in the CMS; has little structure in the energy region 1 to 4 MeV; and the cross section is reasonably large. For ^{48}Ti(n,n'γ) the cross section is very large and slowly changing with energy. It should be possible to use it as a reference to above 10 MeV.

Thus the reference reactions and their γ-rays are ^{10}B(n,$\alpha_1\gamma$) (E_γ = 0.478 MeV), ^{7}Li(n,n'γ) (E_γ = 0.478 MeV) and ^{48}Ti(n,n'γ) (E_γ = 0.984 MeV).

Recent measurements made of the ^{7}Li(n,n'γ) cross section at JRC-Geel [52] and LANSCE [53] are in good agreement. The most recent ^{48}Ti(n,n'γ) experiments have been carried out by LANSCE [54] and JRC-Geel [55]. They generally agree.

K. ^{252}Cf Spontaneous Fission and ^{235}U Thermal Neutron-induced Prompt Fission Neutron Spectra Measurements

There is only one recent measurement of the PFNS of ^{252}Cf(sf) which was by Kornilov at Ohio University [56]. It verified the standard evaluation [1] in the 2–20 MeV energy interval. There are two recent measurements of the PFNS of ^{235}U(n$_{th}$,f). These efforts were motivated by the lingering concern that evaluations of this spectrum do not agree in detail with measurements, particularly at high and at low energies. The first new measurement is by Kornilov *et al.* [57] in a JRC-Geel and IKI collaboration at the cold neutron facility (T=100 K) of the 10 MW Budapest Research Reactor. The PFNS for thermal neutrons was measured by the time-of-flight method. An ionization chamber containing a ^{235}U sample, as well as a ^{252}Cf reference sample outside of the neutron beam was used in the experiment. Three identical neutron detectors were used. Correction factors for multiple scattering and attenuation were calculated with the MCNP code as a ratio of a neutron spectrum emitted from the source surrounded by the real chamber to a spectrum calculated without chamber materials. Since data were obtained for both ^{252}Cf and ^{235}U deposits, it was possible with a proper evaluation procedure, to have an impact on the ^{252}Cf(sf) PFNS from this work also. However no changes were found to the Mannhart evaluation [58]. The experimental PFNS was normalized to unity and the average secondary neutron energy was calculated. A Maxwellian spectrum was fitted in the energy range of 0.7–1.5 MeV and 9–11 MeV to the measured spectrum and an extrapolation to zero and to 20 MeV was performed. The spectra measured with the three detectors are in excellent agreement and do not exhibit any angular dependence. The data obtained disagree in some respects with PFNS data for ^{235}U(n$_{th}$,f) from different evaluated data libraries. However, the data agree well with most experimental results. The results show that the spectrum is softer than the previous evaluation, having a higher yield in the energy range below 1 MeV. It also has a larger yield above about 9 MeV but the uncertainties are quite large in that energy region.

Measurements were also made of the ^{235}U(n,f) PFNS for thermal neutrons relative to the ^{252}Cf(sf) PFNS by Vorobyev *et al.* [59] at the Gatchina research reactor. The measurements of the prompt neutron spectra were performed at 11 fixed angles between the neutron and light fragment direction in the range from zero degrees to 180 degrees in 18 degree intervals. After the measured energy distributions for 11 fixed angles were corrected for the energy and angular resolution of the neutron detector, the total prompt neutron spectra were obtained by summing over all angles. Although the geometry for measurements with the ^{235}U and ^{252}Cf samples was the same, the corrections for the energy and angular resolutions do not cancel in the ratio. The total correction is energy dependent and amounts to no more than 3 % in the measured energy range. The comparison of the obtained data with experimental results obtained by other groups, which were normalized to the recommended value of the total average neutron multiplicity, $\overline{\nu}_{tot} = 2.421$, demonstrates that there is good agreement (within experimental errors) between all experimental data in the 1.5–8 MeV energy range. However, there is some discrepancy in the energy region below 1 MeV. Generally, the results obtained are consistent with the ENDF/B-VII.1 PFNS within the limits of the uncertainty. Again, the spectrum at low energies is softer than the evaluation however the agreement at high energies is quite good.

In addition to this recent work only three TOF experiments of the PFNS of ^{235}U(n$_{th}$,f) have been performed since 1975. The poor level of documentation of the older experiments [60–63] makes it difficult to generate quality covariance matrices of the data. The spectra for neutrons emitted at energies greater than 10 MeV are in contradiction to spectrum-averaged cross section data. Additionally, the same data above 10 MeV were statistically inconsistent as discussed in Ref. [64], therefore no PFNS differential data were considered in the evaluation above 10 MeV. The high energy PFNS tail, that represents less than 2 % of all emitted neutrons, was fixed by assuming a Maxwellian distribution that was matched smoothly to the least-square evaluation at 10 MeV; the Maxwellian temperature was selected to reproduce the evaluated spectrum-average cross section data for ^{90}Zr(n,2n) high-threshold reaction as explained in Ref. [64]. A typical uncertainty of the high-energy extrapolation is estimated to be around 7 % from 8–14 MeV and up to 30 % above 15 MeV.

III. NEUTRON STANDARDS EVALUATIONS

The standards evaluation includes work on each of the following: the neutron cross section standards; the thermal constants; the low energy gold capture cross section;

reference cross sections for prompt gamma-ray production; very high energy fission reference cross sections; the ^{235}U thermal neutron-induced prompt fission neutron spectrum; and the ^{252}Cf spontaneous prompt fission neutron spectrum. The reference cross sections have the role of standards but they are not as well known. They have the same properties as the standards such as smooth cross sections as a function of energy. The detailed documentation in this report contains the numerical values and uncertainties for these data. The standards and reference data with their energy ranges are shown in Table I.

TABLE I. Cross section standards and reference data, release 2017.

Neutron cross section standards	
Reaction	Standards incident neutron energy range
H(n,n)	1 keV to 20 MeV
^{3}He(n,p)	0.0253 eV to 50 keV
^{6}Li(n,t)	0.0253 eV to 1 MeV
^{10}B(n,α)	0.0253 eV to 1 MeV
^{10}B(n,$\alpha_1\gamma$)	0.0253 eV to 1 MeV
C(n,n)	10 eV to 1.8 MeV
Au(n,γ)	0.0253 eV, 0.2 to 2.5 MeV, 30 keV MACS
^{235}U(n,f)	0.0253 eV, 7.8-11 eV, 0.15 MeV to 200 MeV
^{238}U(n,f)	2 MeV to 200 MeV
High energy reference fission cross sections	
Reaction	Reference incident neutron energy range
^{nat}Pb(n,f)	$\approx$ 20 MeV up to 1 GeV
^{209}Bi(n,f)	$\approx$ 20 MeV up to 1 GeV
^{235}U(n,f)	200 MeV to 1 GeV
^{238}U(n,f)	200 MeV to 1 GeV
^{239}Pu(n,f)	200 MeV to 1 GeV
Prompt γ-ray production reference cross sections	
Reaction	Reference incident neutron energy range
^{10}B(n,$\alpha_1\gamma$)	0.0253 eV to 1 MeV
^{7}Li(n,n'γ)	0.8 MeV to 8 MeV
^{48}Ti(n,n'γ)	3 MeV to 16 MeV
Thermal neutron constants	
Prompt fission neutron spectra (PFNS)	
Reaction	Reference outgoing energy range
^{235}U($n_{\rm th}$,f)	0.00001 eV – 30 MeV
^{252}Cf(sf)	0.00001 eV – 30 MeV

A. Neutron Cross Section Standards

Improvements have been made in the very large database used for this standards evaluation. It includes the standards and ratios among them that can lead to improved evaluations of the standards. The cross sections evaluated were H(n,n), ^{6}Li(n,t), ^{10}B(n,$\alpha_1\gamma$), ^{10}B(n,α), C(n,n), Au(n,γ), ^{235}U(n,f) and ^{238}U(n,f). Also included in the evaluation process are the ^{238}U(n,γ) and ^{239}Pu(n,f) cross sections. Those data were included since there are many ratio measurements of those cross sections with the standards, and absolute data are available for them. The older measurements are given in Ref. [1] and the newer ones are given in Sec. II.

The experiments included in the GMAP database since the 2006 evaluation as direct input to GMAP are listed in Table II. In the table, "Data set number" refers to datasets in the GMA database. These data and those shown in Table II of Ref. [1] define the entire database used as direct input of experimental data to GMAP. In Table III, experiments included in the R-matrix analyses since the 2006 evaluation are listed. These data and those shown in Tables III and IV of Ref. [1] define the entire database used for the R-matrix analyses.

For details on the general evaluation process for the cross sections reactions, see Ref. [1]. Basically the process involved using the GMAP (GMA) code [7, 8] to combine input from EDA [65] and RAC [66] R-matrix analyses; also included are a thermal constants evaluation [67] and direct experimental measurements as input data to GMAP.

The procedure for evaluating the standards can be divided into four stages.

1. R-matrix analysis of the hydrogen cross section and subsequent renormalization of cross sections measured relative to that standard in the GMA database.

2. Independent evaluation of the ^{6}Li(n,t), ^{10}B(n,$\alpha_1\gamma$) and ^{10}B(n,α) reactions using the R-matrix model and experimental data available for all reactions that create ^{7}Li and ^{11}B compound systems. These data include various observables for all neutron- and charged-particle-induced reactions (integral and differential cross sections, and polarizations). Use of different R-matrix codes to fit the same data followed by analysis and minimization of the observed differences between the fits increases the reliability of the evaluation. Any differences in fits that cannot be eliminated by this analysis are accommodated when the R-matrix results are combined with the remaining data by a least-squares fit to produce the standards for the light and heavy nuclides.

3. Cross sections for the ^{6}Li(n,t), ^{6}Li(n,n), ^{6}Li(n,tot), ^{10}B(n,n), ^{10}B(n,$\alpha_1\gamma$), ^{10}B(n,α) and ^{10}B(n,tot) reactions and their covariance matrices (including cross-reaction covariances) obtained in the R-matrix evaluation were used in the combined least-squares fit with all other data from the GMAP database. These data include reactions with heavy nuclides and ratios between light and heavy nuclide cross sections. Finally, the outlying experimental data were analyzed and additional components of uncertainty were added to these data points to restore consistency and to bring the general chi-square per degree of freedom close to unity.

4. Refitting the derived GMAP fit for the lithium and boron standards using the R-matrix EDA code. The goal was to calculate standard cross sections for those reactions in any energy grid and produce a

TABLE II. Experimental data sets used in the final combined fit that were added to the GMA database since the 2006 standards evaluation.

Data set number	Reaction	Data type	First author	Reference
8050	^{235}U(n,f),^{238}U(n,f)	absolute	P. Salvador-Castiñeira	EPJ Web of Conferences 146, 04050 (2017)
8030	^{238}U(n,f)/^{235}U(n,f)	absolute ratio	F. Tovesson	Nucl. Sci. Eng. 178 (2014) 57
8002	^{239}Pu(n,f)/^{235}U(n,f)	absolute ratio	F. Tovesson	Nucl. Sci. Eng. 165 (2010) 224
8023	^{238}U(n,γ)	shape	J.L. Ullmann	Phys. Rev. C89 (2014) 034603
8022	^{238}U(n,γ)	shape	J.L. Ullmann	Phys. Rev. C89 (2014) 034603
8021	^{238}U(n,γ)	absolute	F. Mingrone	PhD (2014), C6D6 detector [36, 37]
8020	^{238}U(n,γ)	absolute	T. Wright	PhD (2014), TAC detector [38]
8019	^{238}U(n,γ)	absolute	H. Derrien	ENDF/B-VII.1, from R-M fit of high-resolution data not used in the GMA database below 10 keV
1450	^{238}U(n,γ)	absolute	M.C. Moxon	Report AERE-R6074, author's revision of the data
8013	^{238}U(n,γ)	absolute	H.I. Kim	EPJ A52 (2016) 170
8018	^{238}U(n,f)/^{235}U(n,f)	absolute	C. Paradela	Phys. Rev. C91 (2015) 024602 PPAC-TILT2 detector
8017	^{238}U(n,f)/^{235}U(n,f)	absolute	C. Paradela	Phys. Rev. C91 (2015) 024602 PPAC-TILT1 detector
8016	^{238}U(n,f)/^{235}U(n,f)	absolute	C. Paradela	Phys. Rev. C91 (2015) 024602 PPAC-PERP detector
8015	^{238}U(n,f)/^{235}U(n,f)	absolute	C. Paradela	Phys. Rev. C91 (2015) 024602 composition of FIC1 and FIC2 detectors
3332	Au(n, γ)	absolute	C. Massimi	EPJ/A 50 (2014) 124
8011	^{10}B(n,α_0)/^{10}B(n,α_1)	shape	F.-J.Hambsch	Nucl. Sci. Eng. 163 (2009) 1 28.4 m flight path
8010	^{10}B(n,α_0)/^{10}B(n,α_1)	shape	F.-J.Hambsch	Nucl. Sci. Eng. 163 (2009) 1 57.4 m flight path
8008	^{238}U(n,f)	absolute	R. Nolte	Nucl. Sci. Eng. 156 (2007) 197
3333	Au(n, γ)	absolute	C. Lederer	Phys. Rev. C83 (2011) 034608
8026	α of ^{235}U	absolute	V. Adamchuk	Atomnaya Energiya 65 (1988) 434 Thermal constant
8027	^{233}U(n,f)/^{235}U(n,f)	absolute	M. Calviani	Phys. Rev. C80 (2009) 044604 Thermal constant
8028	^{241}Pu(n,f)/^{235}U(n,f)	absolute	F. Tovesson	Nucl. Sci. Eng. 165 (2010) 224 Thermal constant
8029	^{239}Pu(n,f)/^{235}U(n,f)	absolute	F. Tovesson	Nucl. Sci. Eng. 165 (2010) 224 Thermal constant
	α of ^{233}U, ^{235}U and ^{239}Pu	absolute	M. Lounsbury	Nuclear Data for Reactors, Proc. Conf. Helsinki as corrected by Beer *et al.* [78]

TABLE III. Experimental data sets added to the R-matrix database since the 2006 standards evaluation.

The ^{7}Li system				
Reaction	Data used	First author	Energies	Reference
^{6}Li(n,t)	dσ/dΩ	Devlin	E_n=0.2 to 4.0 MeV	[19]
^{6}Li(n,n')^{6}Li*, ^{6}Li(n,n'd)α	σ	Batchelor	E_n=1.5 to 7.5 MeV	Nucl. Phys. 47 (1963) 385
^{6}Li(n,n')^{6}Li*	σ	Smith	E_n=3.5 to 4.0 MeV	Nucl. Phys. A373 (1982) 305
The ^{11}B system				
Reaction	Data used	First author	Energies	Reference
^{7}Li(α,n)^{10}B	σ	Macklin	E_α=4.45 to 5.14 MeV	Phys. Rev. 165 (1968) 1147
^{7}Li(α,n)^{10}B	dσ/dΩ	Sealock	E_α=4.4 to 5.1 MeV	Nucl. Phys. A357 (1981) 297
^{10}B(n,t)^{8}Be	σ	Kavanagh	E_n=25.3 meV, 420 keV	Phys. Rev. C36 (1987) 1194
^{10}B(n,t)^{8}Be	σ	Kornilov	E_n=sub threshold	Yad. Konst. Series 1 (1990) p.11
^{10}B(n,t)^{8}Be	σ	Cserpák	E_n=25.3 meV ^{252}Cf(sf) PFNS	Proc. Int. Conf. on Neutron Physics and Nuclear Data Harwell, p. 761 (1978)

table of those standard cross sections in a much denser grid than the one used in the GMA fit.

An analysis of unknown systematic uncertainties for these evaluations has been done based on the unrecog-

nized uncertainty-estimation method [68]. We define unrecognized (or unknown) systematic uncertainties as a practical minimum uncertainty that can be achieved using a given measuring method (or measuring tool). No matter how many times the measurements are repeated, if we use the same method, we can not get a result with lower uncertainty. The method allows the determination of some systematic data-uncertainties usually underestimated or neglected by the measurers that allow the establishment of implicit correlations of evaluated quantities. A similar approach was used in the BROND-3 library [69, 70].

The method of the unrecognized uncertainty estimation is based on the *a priori* assumption of equal reliability of all available experimental data, which excludes proven erroneous results. Some initial description of the data is required at the beginning and any deviations from it by individual experiments can be considered as related to systematic unknown uncertainties. The method can be applied in many ways. For our evaluation, each of the cross sections evaluated had the normalization quantities for absolute measurements statistically analyzed (considering weights) to obtain the standard deviation of that distribution regarded as an additional component of the unrecognized systematic uncertainty. Enough normalization components must be used to obtain good accuracy.

The unrecognized systematic uncertainty was estimated as an uncertainty of type B that follows a normal distribution [71]. In the particular case of a normal distribution we can estimate the type B uncertainty, $U_B = M/3$, where the distribution of sampled values is symmetric and extends from $-M$ to $+M$. It is assumed that the values are very certain. This condition is fulfilled if $M = 3\sigma$ for a Normal Distribution, therefore the unrecognized systematic uncertainty, $U_B = 3\sigma/3 = \sigma$ as we assumed.

The assumption is being made here that the unrecognized systematic uncertainty is not energy dependent. This method was not applied for thermal cross section data. Thus the unrecognized systematic uncertainty values listed in this document do not apply to the thermal cross section data. In Figs. 7 and 8 the determination of this quantity is shown for ^{235}U(n,f) and ^{197}Au(n,γ) data. In Tables IV–VIII data used to determine unrecognized systematic uncertainties for several quantities obtained in the standards evaluation are shown. The weights shown in these tables were determined from the uncertainties of the data for each experiment. Where weights are not shown equal weighting was used. More details of the method can be found in Ref. [68]. All determined unrecognized systematic uncertainties for standard and reference quantities are listed in Table IX.

The uncertainties on the results of the 2017 standards evaluation for the light-element standard cross sections are larger than in previous evaluations. This is due, in part, to a different prescription for determining parameter uncertainties, called *confidence intervals*. This procedure was first described by Avni [73] in an astrophysical setting, and later applied by some of us [74] to R-matrix data fitting. It essentially amounts to using in place of the usual

TABLE IV. Data used to determine the unrecognized systematic uncertainty for the evaluated $\overline{\nu}_{tot}$ of ^{252}Cf(sf). From the standard deviation of the distribution of these values, a value of 0.6 % was obtained. However it was decided to eliminate the two outliers labelled with * and then a value of 0.4 % was obtained. References for these data can be found in the report by Axton [67].

Author	Year	Value
Boldeman	1977(1)	3.75
Spencer	1982(1)	3.78
Hopkins	1963(1)	3.78
Asplund	1963(1)	3.79
White*	1968(1)	3.82
Axton	1985A(3)	3.75
Colvin/Axton*	1966(1)	3.73
Colvin/Ullo	1965(1)	3.74
Aleksandrov	1981(1)	3.76
Smith	1984(2)	3.77
Edwards	1982(1)	3.76
Bozorgmanesh	1977(1)	3.75
DeVolpi	1972(1)	3.75
Zhang	1981(1)	3.75
Spiegel	1981(1)	3.78

TABLE V. Data used to determine the unrecognized systematic uncertainty for the evaluated H(n,n) cross section. From the weighted standard deviation of the distribution of these values, a value of 0.34 % was obtained.

Author	Reference and Year	Weight	Value
Langsford	AERE-PR/NP 16 (Harwell) (1969)	10000	0.9945
Peterson	Phys. Rev. 120, 521 (1960)	1000	0.9780
Allen	Proc. Phys. Soc. London, A68, 1077 (1955)	1000	0.9885
Lisowski	PRL 49, 255 (1982)	10000	0.9927
Davis	PRC 4, 1061 (1971)	10000	0.9956
Bol	PRC 32, 623 (1985)	10000	0.9973
Larson	BNL-80, 277 (1980)	10000	0.9976
Clement	NPA 183, 51 (1972)	10000	0.9988
Fields	PR 94, 389 (1954)	4444.4	1.0000
Gordon	NPL-951, 40 (1983)	5000	1.0000
West	ORNL Rep. 3778, 94 (1965)	2500	1.0000
Engelke	PR 129, 324 (1963)	10000	1.0000
Groce	NP 83, 199 (1966)	1000	1.0004
Poenitz	NPA 383, 224 (1982)	10000	1.0007
Schwartz	Phys. Lett. B30, 36 (1969)	10000	1.0031
Brady	PRL 25 1628 (1970)	10000	1.0043
Abfalterer	PRC 63, 044608 (2001)	10000	1.0044
Cierjacks	PRL 23, 866 (1969)	10000	1.0099
Bowen	NP 22, 640 (1961)	1000	1.0285
Blair	Harwell Conf. 51 (1975)	625	1.0931
Clements	Phys. Lett. B 30, 25 (1969)	10000	0.9944
Phillips	Phys. Rev. C 22, 384 (1980)	10000	0.9838
Daub	Phys. Rev. C 87, 014005 (2013)	2500	0.9810

TABLE VI. Data used to determine the unrecognized systematic uncertainty for the evaluated ^{6}Li(n,t) cross section. From the weighted standard deviation of the distribution of these values, a value of 0.5 % was obtained. References for these data can be found in Ref. [1].

Author	Year	Weight	Value
Sowerby	1970	2500.0	1.0045
Sowerby	1970	2500.0	0.9953
Lamaze	1978	2500.0	1.0120
Poenitz	1974	2500.0	1.0104
Macklin	1979	2500.0	1.0059
Drosg	1994	2500.0	1.0033

TABLE VII. Data used to determine the unrecognized systematic uncertainty for the evaluated ^{10}B(n,$\alpha_1\gamma$) and ^{10}B(n,α) cross sections. From the weighted standard deviation of the distribution of these values, a value of 0.8 % was obtained. References for these data can be found in Ref. [1].

Author	Year	Weight	Value
Sealock	1976	100.0	0.9715
Davis	1961	100.0	1.0082
Schrack	1978	2500.0	1.0198
Schrack	1994	2500.0	1.0000
Schrack	1993	2500.0	1.0165

TABLE VIII. Data used to determine the unrecognized systematic uncertainty for the evaluated carbon total cross section. From the weighted standard deviation of the distribution of these values, a value of 0.65 % was obtained. References for these data can be found in the papers by Hale [72], Danon [30]. and Daub [11].

Author	Year	Weight	Value
Diment	1968	2500.0	1.0064
Danon	2007	4444.4	1.0037
Daub	2013	4444.4	1.0131
Auchampaugh	1979	3460.0	1.0202
Cierjacks	1968	5000.0	1.0199
Perey	1972	2500.0	1.0082

TABLE IX. Unrecognized systematic uncertainties from the analyses of the (weighted) standard deviations of the distributions for cross sections and $\overline{\nu}_{tot}$ for ^{252}Cf(sf). The $\overline{\nu}_{tot}$ for ^{252}Cf(sf) unrecognized systematic uncertainty was determined to be 0.4 %. All thermal neutron-induced $\overline{\nu}_{tot}$ unrecognized systematic uncertainties are also assumed to be 0.4 %.

Cross section	Unrecognized systematic uncertainty (%)
H(n,n) total	0.34
^{6}Li(n,t)	0.5
^{10}B(n,$\alpha_1\gamma$)	0.8
^{10}B(n,α)	0.8
C(n,n) total	0.65
Au(n,γ)	1.7
^{235}U(n,f)	1.2
^{238}U(n,f)	1.2
^{238}U(n,γ)	1.7 below 1 MeV
^{238}U(n,γ)	2.4 for 1 MeV and above
^{239}Pu(n,f)	1.2

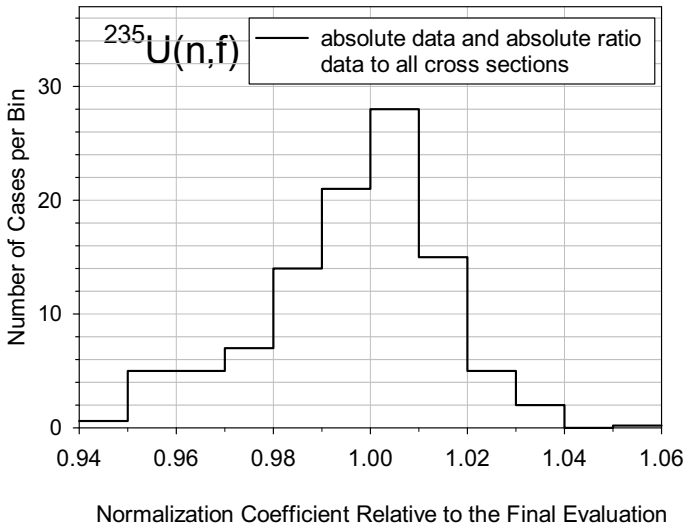

FIG. 7. Histogram as a function of deviation from unity for normalization coefficients of ^{235}U(n,f) absolute fission cross section and fission cross section ratio measurements. The standard deviation is 1.2 % which is interpreted as unrecognized systematic uncertainty that corresponds to all fission measurements of actinides that use fission chambers.

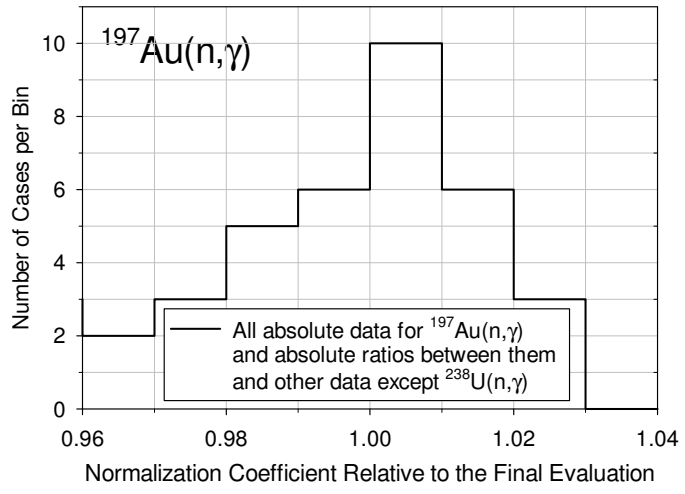

FIG. 8. Histogram as a function of deviation from unity for normalization coefficients of Au(n,γ) absolute cross section and absolute cross section ratio measurements with Au(n,γ) except data with ^{238}U(n,γ). The standard deviation is 1.7 % which is interpreted as unrecognized systematic uncertainty of neutron capture measurements on non-fissioning targets or actinides below the fission threshold.

$\Delta\chi^2 = 1$ criterion for defining parameter variances the condition $\Delta\chi^2 = k$, where k is the number of free R-matrix parameters. This scales up the parameter variances by a factor of $\sqrt{k}$, while leaving the correlations unchanged. This prescription accounts nicely for the empirical scaling factors (7–10) we have used for R-matrix uncertainties from analyses having 50–100 parameters.

In addition, we have included in quadrature estimates of the above-mentioned unknown systematic uncertainty by considering the variations in their normalization parameters, giving additional uncertainty components ranging from 0.34 % (for hydrogen) to 0.80 % (for boron).

As discussed above, the final stage involved refitting the results of the GMAP evaluation for each of the light element standards with EDA. This allowed the cross section

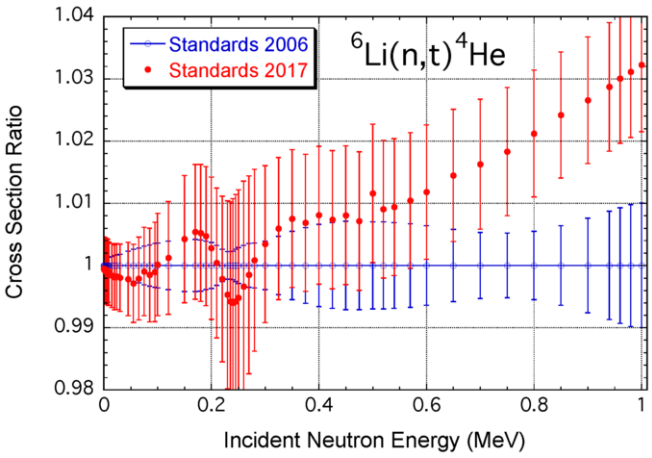

FIG. 9. (Color online) Comparison of the ^{6}Li(n,t) cross section from the 2017 evaluation with the 2006 standards evaluation. The baseline at 1.00 is the 2006 standards evaluation. At the highest energies the results are not within their uncertainties. The unrecognized systematic uncertainty of 0.5 % has been included in the 2017 data. It is possible that if the Parameter Confidence Interval and analysis of normalization for absolute measurements techniques had been available for the 2006 evaluation, those increased uncertainties would have provided agreement within uncertainties.

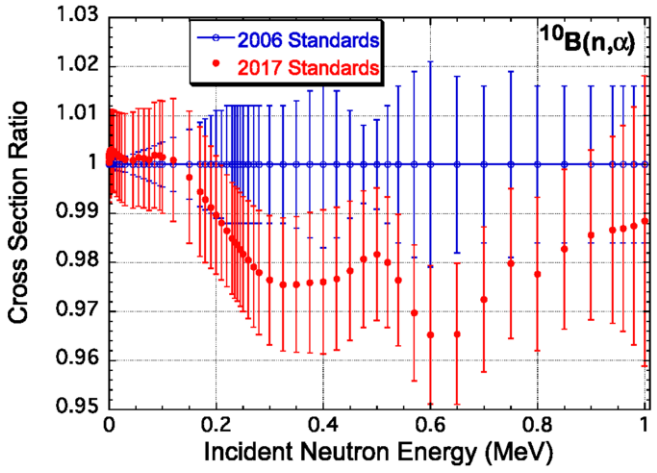

FIG. 10. (Color online) Comparison of the ^{10}B(n,α) cross section from the 2017 evaluation with the 2006 standards evaluation. The unrecognized systematic uncertainty of 0.8 % has been included in the 2017 data. The baseline at 1.00 is the 2006 standards evaluation.

to be accurately calculated with a finer mesh than what was used in the GMA code.

The 2017 standard cross sections obtained from the GMAP analysis are shown as ratios to the 2006 standards evaluation in Figs. 9–14. The non-standard ^{238}U(n,γ) and ^{239}Pu(n,f) cross sections are shown in Figs. 15 and 16 .

For each figure, comparison is made of the new result to the 2006 evaluated result [1]. Uncertainties are shown for the 2006 evaluation (the baseline at 1.00) and the 2017 evaluation. For clarity not all uncertainties are shown.

The integral cross section from 7.8 to 11 eV for ^{235}U(n,f) is frequently used for neutron fluence determination. It

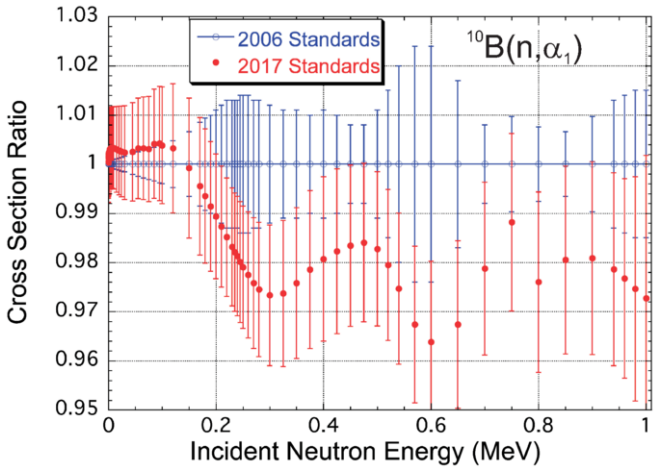

FIG. 11. (Color online) Comparison of the ^{10}B(n,$\alpha_1\gamma$) cross section from the 2017 evaluation with the 2006 standards evaluation. The unrecognized systematic uncertainty of 0.8 % has been included in the 2017 data. The baseline at 1.00 is the 2006 standards evaluation.

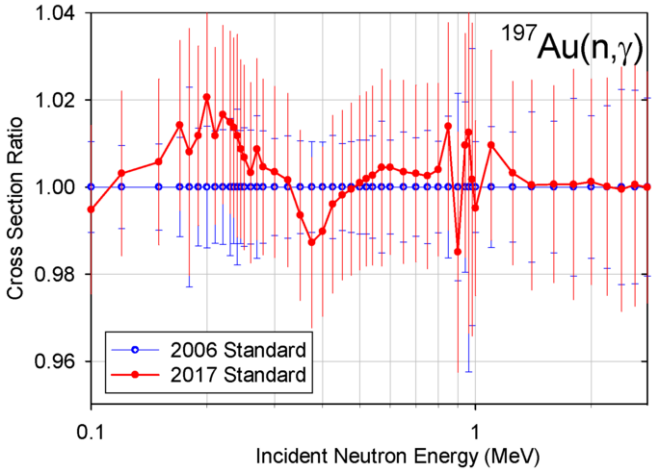

FIG. 12. (Color online) Comparison of the Au(n,γ) cross section from the 2017 evaluation with the 2006 standards evaluation. The unrecognized systematic uncertainty of 1.7 % has been included in the 2017 data. The baseline at 1.00 is the 2006 standards evaluation.

was used as a standard in that context. It has now been established as a standard. The value from the 2017 evaluation is 247.5 b-eV ± 3 b-eV. Including the unrecognized uncertainty of fission chamber measurements of 1.2% raised the estimated uncertainty of the integral from 1.1 b-eV to 3 b-eV (this corresponds to an average cross section of 77.3 b ± 0.9 b). For the 2006 evaluation the integral cross section is 246.4 b-eV ± 1.3 b-eV. There is agreement within the uncertainties. The increase in this cross section is largely a result of the increase in the ^{235}U(n,f) thermal cross section. The value in both the ENDF/B-VI and ENDF/B-VII.1 libraries is lower by 2 % than the 2006 standards evaluation recommended value, well outside the uncertainty band of 0.5 %. Preliminary work by Noguere [75] analyzing ^{235}U(n,f) data of Gwin, Wagemans and JRC-Geel measurements has provided a 7.8-11 eV in-

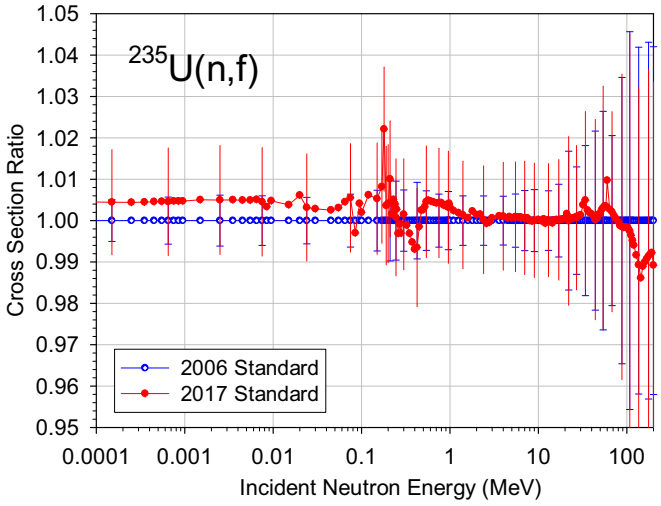

FIG. 13. (Color online) Comparison of the ^{235}U(n,f) cross section from the 2017 evaluation with the 2006 standards evaluation. The results from 1 keV up to 150 keV correspond to the average of low resolution experiments. The unrecognized systematic uncertainty of 1.2 % has been included in the 2017 data. The baseline at 1.00 is the 2006 standards evaluation.

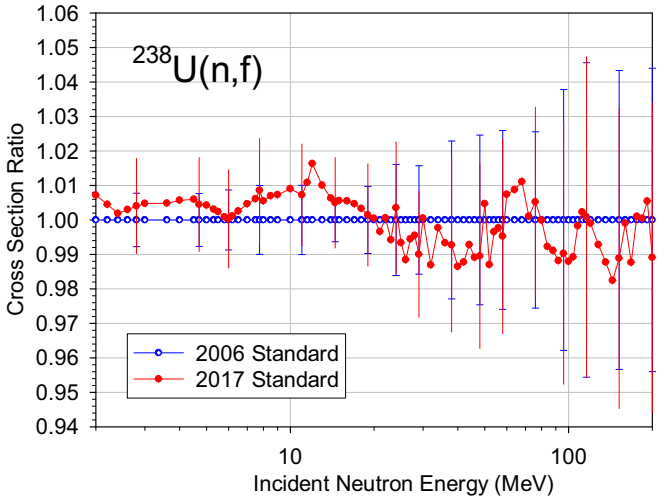

FIG. 14. (Color online) Comparison of the ^{238}U(n,f) cross section from the 2017 evaluation with the 2006 standards evaluation. The unrecognized systematic uncertainty of 1.2 % has been included in the 2017 data. The baseline at 1.00 is the 2006 standards evaluation.

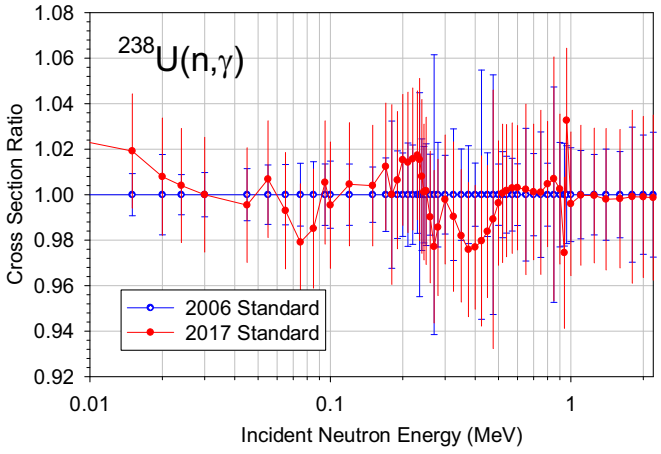

FIG. 15. (Color online) Comparison of the ^{238}U(n,γ) cross section from the 2017 evaluation with the 2006 evaluation resulting from the standards evaluation. The unrecognized systematic uncertainty has been included in the 2017 data. That uncertainty is 1.7 % below 1 MeV and 2.4 % at 1 MeV and above. The baseline at 1.00 is the 2006 standards evaluation.

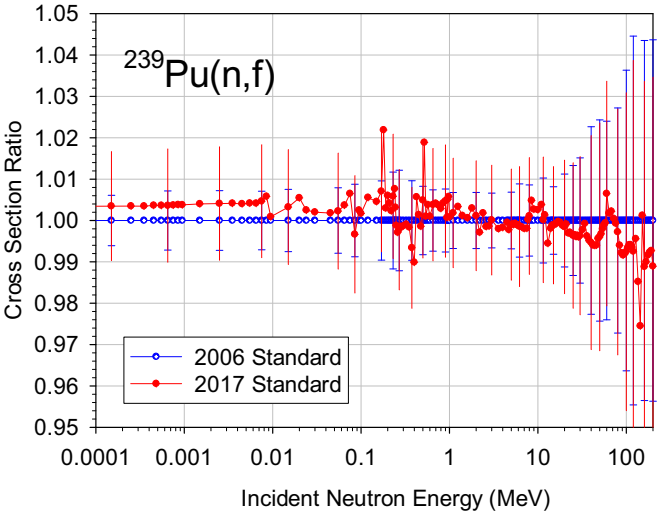

FIG. 16. (Color online) Comparison of the ^{239}Pu(n,f) cross section from the 2017 evaluation with the 2006 evaluation resulting from the standards evaluation. The unrecognized systematic uncertainty of 1.2 % has been included in the 2017 data. The baseline at 1.00 is the 2006 standards evaluation.

tegral of 245.7 b-eV ± 3.0 b-eV that is consistent with the 2017 standards value.

The H(n,n) evaluation was done separately as an *R*-matrix analysis by Hale and Paris. This standard is for the natural element but since ^{1}H is 99.9885 % of the natural element the evaluation is for ^{1}H only. The evaluation of the hydrogen standard is complete to 20 MeV. Efforts beyond the current evaluation are underway to extend it to 200 MeV. The C(n,n) evaluation was done by Hale. The carbon standard is also for the natural element. The C(n,n) evaluation is composed of separate ^{12}C(n,n) and ^{13}C(n,n) *R*-matrix evaluations. In Figs. 17 and 18 plots of the H(n,n) and C(n,n) cross sections are shown.

The changes in the n+C elastic scattering cross section come mainly from differences in the n+C total cross section, which approach 2 % at the upper end of the standards range. The increase results from a 2 % re-normalization of some of the total cross section data that were fitted at energies above about 1 MeV, in order to give better agreement with measurements of the differential elastic scattering cross section in the 1-2 MeV region.

No new evaluation was done for the ^{3}He(n,p) standard since little experimental work had been done on this cross section.

For the ^{6}Li(n,t) cross section, the EDA analysis was extended to 4 MeV and the RAC analysis to 20 MeV. The results obtained for the two evaluations differed above about 0.5 MeV. So the simple average of the two fits with increased uncertainties was used in the combined

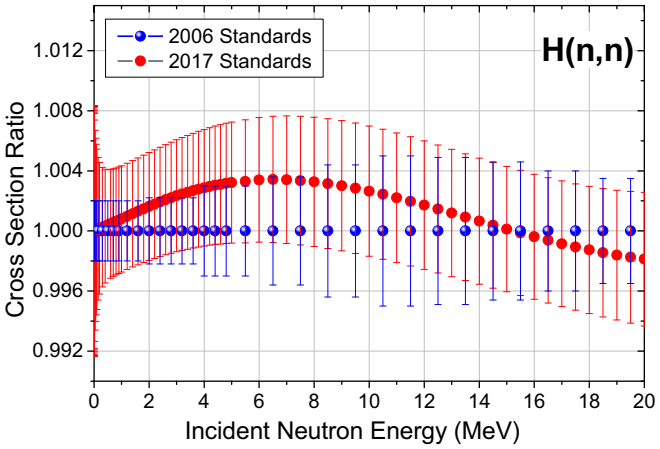

FIG. 17. (Color online) Comparison of the total neutron elastic cross section of hydrogen for the 2017 evaluation with the 2006 standards evaluation. The unrecognized systematic uncertainty of 0.34 % has been included in the 2017 data.

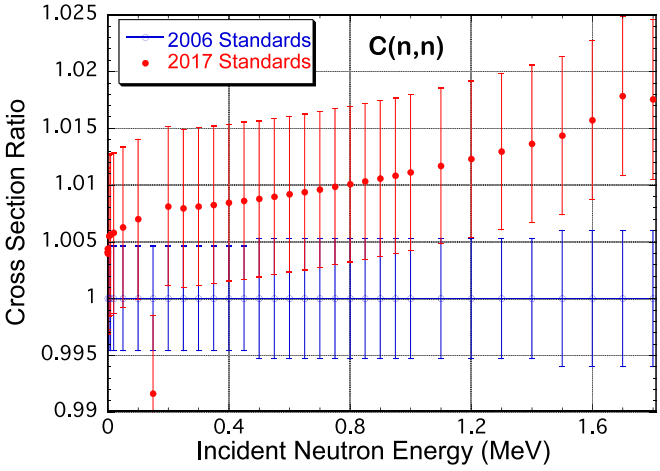

FIG. 18. (Color online) Comparison of the carbon total elastic cross section for the 2017 evaluation with the 2006 standards evaluation. The unrecognized systematic uncertainty of 0.65 % has been included in the 2017 data. The baseline at 1.00 is the 2006 standards evaluation. The structures at about 0.15 MeV and 1.76 MeV are a result of changes in the evaluated ^{13}C total cross section.

GMAP fit with the other data. The increased component of uncertainty equal to the difference between the two fits was used in the GMAP analysis. Larger uncertainty in the evaluations is observed in the region of the ^{6}Li(n,t) resonance at about 0.240 MeV and near the high energy boundaries of the standards region.

For the ^{10}B(n,$\alpha_1\gamma$) and ^{10}B(n,α) cross sections, there were concerns about the systematic uncertainties used in the RAC analysis. Thus it was decided to only use the EDA R-Matrix results for the B(n,$\alpha_1\gamma$) and ^{10}B(n,α) data in the GMAP analysis. Larger uncertainty in those evaluations is present near the high energy boundaries of the standards regions for these reactions.

For the ^{235}U(n,f) and ^{239}Pu(n,f) cross sections, the increases below 100 keV are a result of the increases in their thermal cross sections (see section B on the thermal neutron constants). There is a high degree of cross section correlation between thermal and the keV energy region. Also for those cross sections the increase in the ^{238}U(n,γ) cross section, resulting from measurements [35] with claimed high accuracy, led to an increase in the fission cross sections through the capture to fission cross section ratios. The ^{235}U(n,f) and ^{239}Pu(n,f) cross sections from 1 keV up to 150 keV, from this evaluation, correspond to the average of low resolution experiments.

B. Evaluated Light Element Cross Sections Changes

Since some relatively large changes have occurred for the evaluated light element standards over time compared with the quoted uncertainties, some discussion on the reason for those changes is needed. The evolution of the changes in evaluations of the light element standards is shown in Figs. 19–22. The changes in the $n-p$ scattering cross section at energies below 20 MeV shown in Fig. 19 are quite small (and within the uncertainties of the evaluations). The differences result from including new nucleon-nucleon scattering data.

For the ^{6}Li(n,t) cross section seen in Fig. 20, the trend to increasingly higher cross sections in the high-energy tail of the large resonance peak in successive versions of ENDF/B standards seems at first glance unsettling. Whereas the version V and VI evaluations are nearly identical at 1 MeV, that cross section increased by about 3 % between version VI and VII, and another 3 % between versions VII and VIII, for a total increase of 6 % over this period of time. This change resulted from an evolving theoretical and experimental understanding of the level structure in this reaction at energies above 1 MeV. The first experimental indication of a broad resonance around 2 MeV in this system actually came from $t+\alpha$ elastic scattering data at $E_t = 12.88$ MeV, and its effect was included in the EDA R-matrix analysis that was done for the 2006 Standards analysis (ENDF/B-VII.0). This resonance was confirmed directly in the ^{6}Li(n,t) differential cross section measurements of Devlin *et al.*, which were included in the R-matrix analyses that were done for the 2017 evaluation. Both of theses experiments indicated that the cross section should be again 3 % higher than obtained in the 2006 evaluation. The EDA analysis found, in fact, two broad resonances ($\frac{1}{2}^-$, $\frac{3}{2}^-$) in the region immediately above 1 MeV, and the tails of these resonances cause the increased cross section at 1 MeV, which is not inconsistent with the rather scattered and older measurements in this energy region. Thus, we find this 6 % increase since ENDF/B-VI justifiable, even though the earlier uncertainty estimates were much smaller than that, due to insufficient knowledge of the near-by resonances that resulted from the more limited range of the earlier R-matrix analyses.

The cross sections for the ^{10}B(n,α) reactions have changed by as much as 10-15 % from ENDF/B-V to the

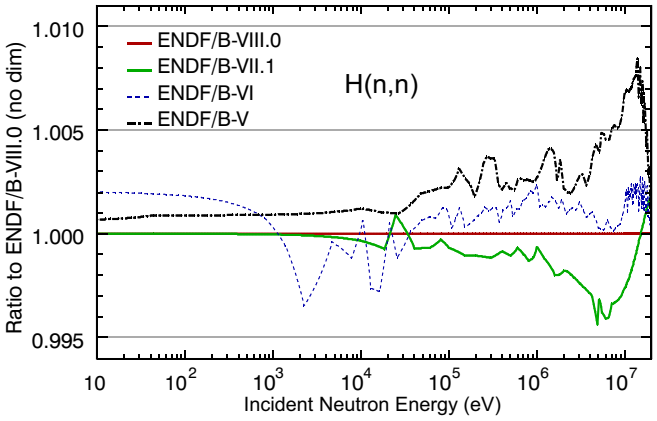

FIG. 19. (Color online) Comparison of evaluations of the hydrogen total elastic cross section. In the standards energy region, the ENDF/B-VII.1 and ENDF/B-VIII.0 evaluations are the 2006 and 2017 H(n,n) cross section standards, respectively.

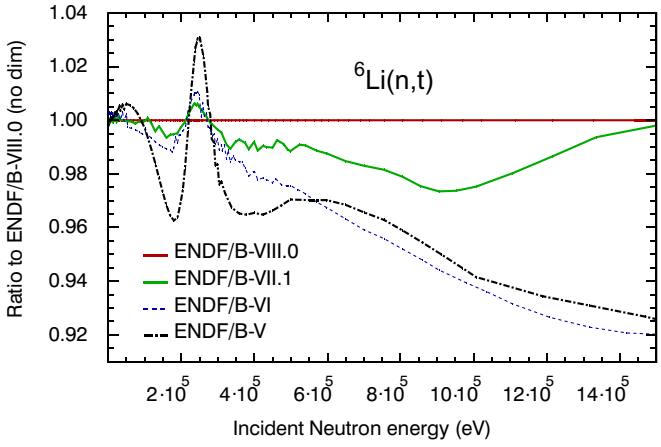

FIG. 20. (Color online) Comparison of evaluations of the ^{6}Li(n,t) cross section. In the standards energy region, the ENDF/B-VII.1 and ENDF/B-VIII.0 evaluations are the 2006 and 2017 ^{6}Li(n,t) cross section standards, respectively.

2017 evaluation, as can be seen in Figs. 21 and 22. Those changes became much smaller (≤ 5 %) for versions VI and VII.1, especially at low energies. This trend resulted from a better experimental data base, starting with ENDF/B-VI, which included better measurements of the (n, α_1) and (n, α_0) cross sections and their branching ratio. For the 2006 standards evaluation, we also had much better measurements of the neutron total cross section from Wasson *et al.* [22]. From version VII.1 to VIII.0, there were not large changes in the data base below 1 MeV, so the differences there come from the two different R-matrix fits to essentially the same data. For the 2006 standards evaluation, only the results from the RAC analysis were used, and for the 2017 standards evaluation, only the EDA results were used, and the differences are represented by the green curve above the red unity line in Figs. 21 and 22. Since these evaluations involve many cross sections combined in a consistent way, it is often difficult to point to the reason for changes in individual cross sections obtained in the evaluation process.

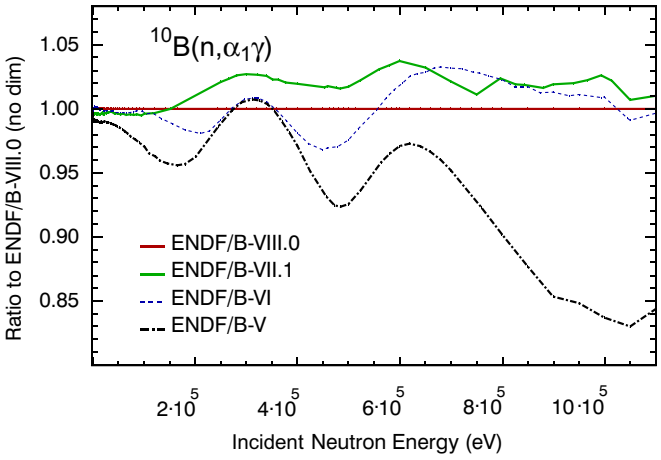

FIG. 21. (Color online) Comparison of evaluations of the ^{10}B(n,$\alpha_1\gamma$) cross section. In the standards energy region, the ENDF/B-VII.1 and ENDF/B-VIII.0 evaluations are the 2006 and 2017 ^{10}B(n,$\alpha_1\gamma$) cross section standards, respectively.

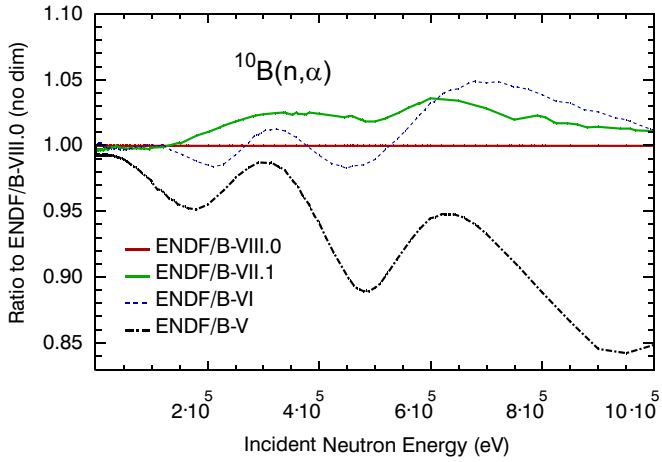

FIG. 22. (Color online) Comparison of evaluations of the ^{10}B(n,α) cross section. In the standards energy region, the ENDF/B-VII.1 and ENDF/B-VIII.0 evaluations are the 2006 and 2017 ^{10}B(n,α) cross section standards, respectively.

C. The Thermal Neutron Constants

Since thermal data are included in the standards evaluation, the thermal constants will have an impact on the results of the evaluation. Also the thermal constants themselves will be affected by the other data in the evaluation.

In the 2006 release of the standards evaluations [1], the Westcott factors for the fission and absorption processes were part of the Thermal Neutron Constants (TNC).

There were concerns about how well the temperatures were understood for Maxwellian (reactor) data and how close the thermal spectra agree with a Maxwellian. This led to a new evaluation [76]. Only one Maxwellian (reactor) experiment was used in the GMAP evaluation in addition to the microscopic data from Axton [67] to obtain the TNC for the 2017 evaluation. That Maxwellian experiment by Lounsbury *et al.* [77] used irradiation of samples containing ^{233}U, ^{235}U and ^{239}Pu for a year in a thermal column in the reactor. Then the samples were

analyzed by mass spectrometry to obtain α values (α is capture/fission). Beer *et al.* [78] utilized Monte Carlo techniques applied to the geometry of that reactor experiment to determine accurate thermal α values and uncertainties for those nuclides. This experiment had an important impact by lowering the uncertainties for capture for ^{233}U, ^{235}U and ^{239}Pu. The agreement of Beer's estimated ^{235}U thermal α value of 0.1697 ± 0.0029 with the only existing microscopic measurement of 0.1690 ± 0.0035 by Adamchuk [79] is excellent, which inspires confidence in using the unique Beer α data for ^{233}U and ^{239}Pu fissile targets.

The Westcott g-factors for fission and absorption normally given with the thermal constants were not evaluated for the GMAP evaluation.

However, Westcott [80] pointed out the importance of having up-to-date values of the g-factors for many nuclear applications with reliable estimates of their accuracy.

Therefore, as the macroscopic data reported by Axton represent a valuable source of information that cannot be ignored, we decided to extract Westcott factors from them by considering the Thermal Neutron Constants (neutron multiplicities and neutron cross sections) as fixed parameters with known uncertainties. The TNC uncertainties, provided by the GMA analysis, were propagated via the marginalization technique implemented in the CONRAD code [81]. For this work, a Monte-Carlo procedure was applied on 50 macroscopic data points identified as "mac" data in the Axton's report. The results are reported in Table X.

The results provided by the CONRAD code are in good agreement with the Westcott factors recommended in Ref. [1], except for the nuclear system ^{241}Pu+n. For this fissile isotope, the Monte-Carlo procedure of the CONRAD code gives relative uncertainties higher than 1 %, indicating that accurate g-factors cannot be extracted for ^{241}Pu from the analysis of the "mac" data reported by Axton. By contrast, the CONRAD code provides relative uncertainties ranging from 0.3 % to 0.7 % for the ^{233}U+n, ^{235}U+n and ^{239}Pu+n nuclear systems, confirming the low uncertainties previously released in Ref. [1].

$\overline{\nu}_{tot}$ for ^{252}Cf from the GMAP analysis is 3.7637 (or 3.764) ± 0.42 %. This includes a 0.4 % unrecognized systematic uncertainty. It was 3.7692 for the 2006 evaluation. The TNC results of this work are shown in Table XI. The quantities in square brackets in the bottom part of each cell are the values obtained in the 2006 standards evaluation [1]. The influence of the Maxwellian data on the 2006 evaluation was fairly strong, lowering the fission cross section and increasing the neutron multiplicity. In many cases changes in thermal constants are greater than the reported uncertainty. The ^{235}U(n,f) cross section at thermal in the ENDF/B-VII.1 library is 584.99 b. The ENDF/B-VIII.0 evaluated files are consistent with the new standards evaluation within the quoted uncertainties.

TABLE X. Westcott factors and their relative uncertainties for the absorption (g_a) and fission (g_f) processes calculated with the Monte Carlo formalism of the CONRAD code [81] and compared with the values recommended in Ref. [1].

Nuclear systems	g-factor	CONRAD results	Carlson *et al.* [1] (Standards 2006)
^{233}U+n	g_a	1.004 (0.7%)	1.000 (0.11%)
	g_f	0.998 (0.3%)	0.996 (0.14%)
^{235}U+n	g_a	0.979 (0.3%)	0.979 (0.01%)
	g_f	0.976 (0.3%)	0.977 (0.01%)
^{239}Pu+n	g_a	1.081 (0.4%)	1.078 (0.22%)
	g_f	1.053 (0.4%)	1.055 (0.21%)
^{241}Pu+n	g_a	1.021 (1.6%)	1.044 (0.19%)
	g_f	1.030 (0.6%)	1.045 (0.53%)

TABLE XI. The thermal neutron constants and their absolute uncertainties (in parentheses). For the $\overline{\nu}_{tot}$ values a 0.4 % unrecognized systematic uncertainty is included. For each of the other thermal constants the unrecognized systematic uncertainty has not been determined. The thermal constants in the bottom part of each cell in square brackets are those obtained from the 2006 standards evaluation.

Const.	^{233}U	^{235}U	^{239}Pu	^{241}Pu
σ_{nf}(b)	533.0 (2.2) [531.2]	587.3 (1.4) [584.3]	752.4 (2.2) [750.0]	1023.6 (10.8) [1014.0]
$\sigma_{n\gamma}$(b)	44.9 (0.9) [45.6]	99.5 (1.3) [99.4]	269.8 (2.5) [271.5]	362.3 (6.1) [361.8]
σ_{nn}(b)	12.2 (0.7) [12.1]	14.09 (0.22) [14.09]	7.8 (1.0) [7.8]	11.9 (2.6) [12.1]
$\overline{\nu}_{tot}$	2.487 (.011) [2.4968]	2.425 (.011) [2.4355]	2.878 (.013) [2.8836]	2.940 (.013) [2.9479]

D. Prompt Fission Neutron Spectra

The ^{235}U thermal prompt neutron fission spectrum (PFNS) is very important for reactor applications. It is also used as a reference for validating evaluated cross sections for neutron dosimeters used in many applications. Improvements in the evaluation of this spectrum were made by including measurements of the spectrum made relative to the ^{252}Cf spontaneous fission neutron spectrum. The evaluation was done with GMAP for which both those spectra together with ^{233}U and ^{239}Pu PFNS were evaluated simultaneously, and by considering all ratio measurements as shape data. Only spectra data were used in this evaluation.

Due to the much smaller uncertainties of the ^{252}Cf spectrum, the impact was largely on the ^{235}U spectrum. The ^{252}Cf spontaneous fission neutron spectrum evaluation of Mannhart was used in this evaluation. Those data are listed in Ref. [1]. The average energy of the ^{235}U thermal PFNS was determined to be 2.00 MeV ± 0.01 MeV[1]. In

[1] Unrecognized shape uncertainties were added that increased the uncertainty of the average energy of the ^{235}U(n_{th},f) PFNS from 5 keV to 10 keV.

Fig. 23 the results of this evaluation compared with the input data [57, 59, 61–63, 82, 83] are shown. The evaluation is fully documented in Ref. [64].

Concerning the PFNS evaluation for $E > 10$ MeV, it should be noted that in that energy region there are either no statistically consistent differential PFNS data measured for ^{235}U($n_{\rm th}$,f), or there are no measurements at all [64]. Therefore, a non-model least-square PFNS evaluation is not possible. An extrapolation of non-model PFNS evaluation was suggested and tested in Refs. [64, 84, 85] based on the evaluated SACS for the ^{90}Zr(n,2n) dosimetry reaction [86] and on the linear dependence of the SACS on $\overline{E}$. The suggested PFNS energy dependence above 10 MeV significantly improves the agreement with measured SACS for (n,2n) dosimetry reactions when IRDFF cross section evaluations [87, 88] are used to calculate the corresponding SACS. Much better agreement with recently measured SACS in the Rěz reactor [89] is also shown if the new standard PFNS (quoted as IAEA CIELO in Ref. [89]) is used.

E. High Energy Reference Fission Cross Sections

The neutron induced fission cross sections at high energies are recognised as a convenient reference for other reaction cross sections measurement where already established standards are not available yet. Since the relatively large number of independent experiments was carried out for the ^{209}Bi(n,f) and ^{nat}Pb(n,f) reactions in the past, the non-model evaluation by the GMA code [7, 8] has been performed for these reactions in 2015 [90] from effective threshold ≈ 20 MeV up to 1 GeV with provision of recommended reference cross sections.

As a part of that work the ^{235}U(n,f), ^{238}U(n,f) and ^{239}Pu(n,f) cross sections have been extended up to 1 GeV. The ^{235}U(n,f) and ^{238}U(n,f) cross sections which are standard up to 200 MeV can be now considered as potential reference cross sections from 200 MeV to 1 GeV. For this extention the selected ^{238}U(p,f) cross section data between 200 - 1000 MeV were also included in the GMA fit, that allowed us to lower the evaluated uncertainties, since no (n,f) measurements were available. The difference between (n,f) and (p,f) cross sections calculated by the CEM3.03 code [91], at that time, turned out to be small. Based on that difference, proper corrections were applied to all (p,f) measured data so they could be used as (n,f) data.

After 2015 the results of the ^{238}U(n,f) cross section measurement in the energy range 130 to 300 MeV at the LANSCE/LANL facility became available [50]. Since the author has normalized his data to the IAEA ^{238}U(n,f) standards at 130 MeV, we used them in our GMA fit as a shape. They are shown in Fig. 24. The dense energy grid between 200 and 300 MeV of the Miller experiment [50] notably differs from our previous evaluation. A similar problem was pointed out by Duran [92]. This forced us to include in the new fit, besides ^{238}U(n,f) of Ref. [50], also all ^{238}U(p,f) measurements above 200 MeV available in the EXFOR database [93] except for the obvious outliers.

The updated evaluation (GMA fit 2017) for ^{238}U(n,f) is shown in Fig. 24. For comparison, the high energy data from the FISCAL parameterization [94] are also shown in Fig. 24; however, after downscaling by factor 0.87. It is worth mentioning that inclusion of the new (n,f) and additional (p,f) data in the GMA fit has no impact on other (n,f) reactions, as is shown for ^{nat}Pb(n,f) in Fig. 25.

It should be noted that the region close to the minimum of the fission cross section around 150 MeV and above depends also on pion physics. For ^{238}U fission produced by protons, there is an increasing cross section for the production of pions competing with neutrons [95]. It will also be the case for the other reference fission cross sections. Uncertainties in modelling such physical effects add to the need to undertake new measurements to sort out discrepancies and potential inconsistencies in existing proton and neutron induced fission data.

In summary it is important to stress that additional measurements of the ^{238}U(n,f) and ^{235}U(n,f) cross sections, and proton induced fission reactions in the energy range 150 - 1000 MeV are necessary for a more reliable evaluation and extension of these reference cross sections.

F. Prompt γ-ray Production Reference Cross Sections

Measurements of neutron-induced γ-ray production cross sections are most easily performed relative to a cross section in which a discrete γ-ray is detected. Such cross sections are called "reference cross sections" because they do not meet the rigor of a standard must be evaluated. The reactions considered so far to be a potential reference are ^{10}B(n,$\alpha_1\gamma$) (E_γ = 0.478 MeV), ^{7}Li(n,n'γ) (E_γ = 0.478 MeV) and ^{48}Ti(n,n'γ) (E_γ = 0.984 MeV).

An evaluation of the ^{10}B(n,$\alpha_1\gamma$) cross section is described in the Section II.D. This section presents the evaluation results for the reactions ^{7}Li(n,n'γ) and ^{48}Ti(n,n'γ) as well as a recommendation for the energy intervals in which these three reactions can be used as references for γ-production cross section measurements.

The original experimental cross sections for the 2017 evaluation were taken from the EXFOR database [93], except for a few cases when data were received through private communications with authors.

The non-model evaluations of the discrete γ-ray production cross section for ^{7}Li and ^{48}Ti were performed by the least-squares method implemented in the GMA code [7, 8].

1. ^{7}Li(n,n'γ) 478 keV γ-ray Production Cross Section

The threshold for the inelastic neutron scattering on ^{7}Li is 546 keV when population of the first excited state at 478 keV in the target nucleus becomes kinematically

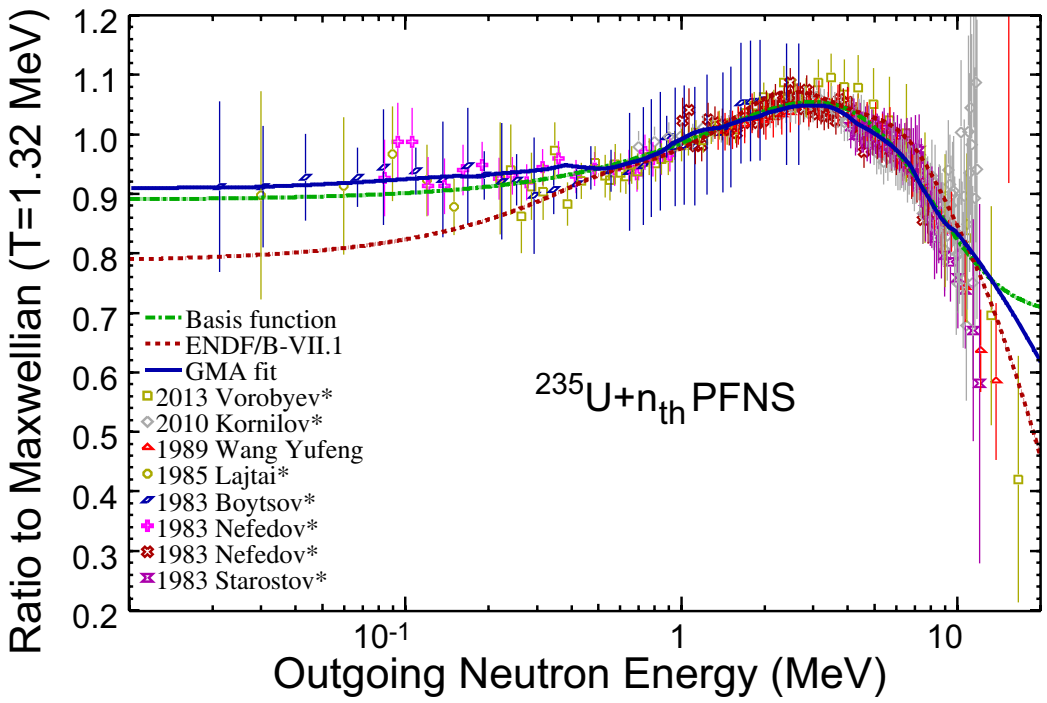

FIG. 23. (Color online) Comparison of the measurements of ^{235}U PFNS measurements with the 2017 evaluation (GMA fit) and the ENDF/B-VII.1 evaluation. Above 10 MeV the 2017 evaluation follows the "basis function" which is a Maxwellian with temperature fitted to reproduce the evaluated ^{90}Zr(n,2n) SACS and Maxwellian normalization fixed by a continuity requirement at 10 MeV.

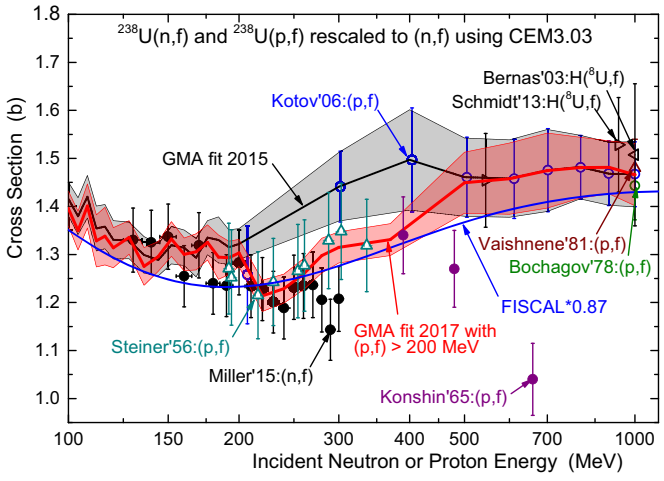

FIG. 24. (Color online) ^{238}U(n,f) cross section from 100 MeV to 1 GeV. Symbols: recent measurement of Miller [50] and selected known (p,f) experiments above 200 MeV after rescaling to (n,f) using CEM3.03 model. Curves: GMA fit made in 2015 [90] (black) and current fit (red) with uncertainties; FISCAL parameterization scaled by factor 0.87 (blue). Note that we quote the results of the FISCAL parameterization by Fukahori *et al.* [94] as the JENDL-HE values from 300 to 1000 MeV.

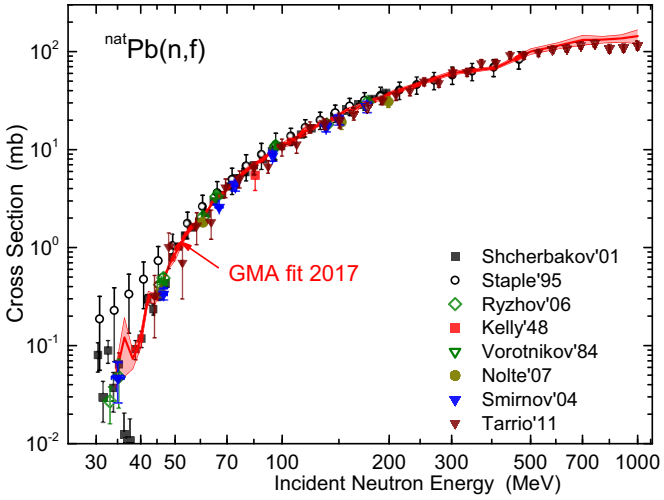

FIG. 25. (Color online) ^{nat}Pb(n,f) cross section from threshold up to 1 GeV: known measurements selected for the GMA evaluation (symbols) and GMA fit 2017 with uncertainties (red curve).

allowed. Since this first level is a single bound state of ^{7}Li (the unbound ones decay with emission only of tritons and α-particles), the cross sections for the 478 keV γ-ray production and inelastic scattering populating the first level are equal. Additionally, since the spin of the ^{7}Li first excited state is 1/2 , the angular distribution of the (n,n'γ) photons is isotropic in the CMS.

In total, 14 independent measurements of the 478 keV γ-ray yield and 5 measurements of inelastically scattered neutrons have been carried out since 1955. The most recent experiments were performed at JRC, Geel [52] and LANL, Los Alamos [53].

Approximately half of the known experiments have used enriched ^{7}Li samples thus providing the isotopic cross section. If the measurement was done with natural Li, the

authors usually made a proper correction for the 92.41 % abundance of ^{7}Li, otherwise we did the conversion ourselves.

Most of the reported measurements have provided an absolute cross section or absolute ratio to other standard cross sections, such as ^{1}H(n,n), ^{235}U(n,f) or ^{238}U(n,f), which are known with very low uncertainty (0.5 - 1.5) % in the energy range of interest.

Several measurements were excluded from the 2017 evaluation due to the use of extremely large Li samples, lacking documentation, or as obvious outliers. Finally the data from 12 experiments were fitted with the GMA code.

The GMA fit results are shown in Fig. 26, more details are available elsewhere [96]. The fit values and uncertainties ≈ (2–3) % are mainly defined by the recent and most precise measurements [52] and [53]. The comparison with the ENDF/B-VIII.0 evaluation [4] exhibits a difference (5–8) %.

2. ^{48}Ti(n,n'γ) 948 keV γ-ray Production Cross Section

The 984 keV γ-ray production channel opens at an energy of 1004 keV and is identical to the inelastic neutron scattering on ^{48}Ti up to 2344 keV when neutrons start to populate the second level at 2296 keV. ^{48}Ti is a dominant isotope (abundance 73.72 %) in natural titanium, other isotopes are ^{49}Ti (5.41 %), ^{50}Ti (5.18 %), ^{47}Ti (7.44%) and ^{46}Ti (8.25 %). The angular yield of 948 keV γ-rays is a result of a 2^{+} to 0^{+} transition in the nucleus. Consequently, it is symmetric around 90 degrees and the angular integrated cross section can be derived from differential cross section measurements at 55 degrees or 125 degrees by multiplying by 4π. For practically all experiments, which were used in the present evaluation, the yield of 948 keV γ-rays was measured at 55 degrees or 125 degrees. In two measurements where γ-ray detectors were located at other angles the correction for angular dependence was applied by the authors.

The 2017 evaluation of this reaction is an update of the evaluation performed in 2012 [97], which additionally used the results of nuclear reaction modelling, since the experimental database was insufficient at that time.

Since 1965 seven independent measurements of the 984 keV γ-ray yield and seven measurements of inelastically scattered neutrons have been carried out. Only two experiments used the enriched ^{48}Ti samples, the others used natural titanium. In most cases the absolute scale was derived from experimental comparison with the ^{1}H(n,n), ^{235}U(n,f) or ^{238}U(n,f) cross sections.

The most recent experiments with direct detection of 984 keV γ-rays were carried out by LANSCE [54] with enriched ^{48}Ti sample and by JRC-Geel [55, 98] with ^{nat}Ti. At energies above 9.314 MeV we reduced the JRC-Geel data for the contribution from ^{49}Ti(n,2n$\gamma_{\ 948keV}$)^{48}Ti reaction using the corresponding cross section from TENDL-2015 [99]. This correction amounts to ≈ 10 % at 14 MeV. After correction, the LANSCE and JRC-Geel measured data agree within declared uncertainties.

For the present non-model evaluation in the energy range of interest, we selected data from 8 experiments. These experimental data, the GMA fit and resulting uncertainty, ≈ (3–6) %, are shown in Fig. 27 (more details are available elsewhere [100]). The pronounced resonances with significant cross section changes become visible below 3 MeV, that restricts the usage of this reaction at lower energies. The comparison with the ENDF/B-VIII.0 evaluation [4] shows a difference of ≈ 4 % at the cross section maximum.

Recent relative cross section measurements [101] performed at LANL for Li, Ti, and Fe simultaneously, show inconsistency between the Li and Ti cross section results presented here. When combined with a revised Fe cross section (based on revised neutron flux values), these data improve agreement between the LANSCE and JRC Geel Li(n,n'γ) data within uncertainties, but indicate a lower Ti cross section by about 12 %. This work will be published when results are final. Because of this ongoing work, the Li data evaluation uses only the shape and not the magnitude of the LANSCE data, and the good agreement for the Ti cross section data of LANSCE and JRC Geel will be reduced.

3. Reference γ-ray Production Cross Section from Thermal Energy to 16 MeV

The information provided in this and Section II.D points to the impossibility to have a single discrete γ-ray production reaction which will meet the requirements for the reference cross section, *i.e.*, to be large and smooth in a broad energy domain.

Instead of one, we recommend for usage the combination of several reactions: ^{10}B(n,$\alpha_1\gamma$) from thermal up to 1.0 MeV, ^{7}Li(n,n'γ) from 0.8 to 8 MeV and ^{48}Ti(n,n'γ) from 3 to 16 MeV. The evaluated cross sections and uncertainties for them in the corresponding energy intervals are displayed in Fig. 28. The overlapping of energies allows covering practical applications from thermal to 16 MeV. For neutron energies up to 8 MeV the use of two reactions ^{10}B(n,$\alpha_1\gamma$) and ^{7}Li(n,n'γ) which produce a gamma-ray of the same energy, 478 keV, can be an additional convenience for detection.

G. Low Energy Au(n,γ) Cross Section

The MACS evaluation at kT=30 keV for ^{197}Au(n,γ) by Ratynski and Käppeler, that is used as an important reference for astrophysics applications, is based on their measurements of the ^{197}Au(n,γ) cross section and those of Macklin [102, 103]. The Ratynski and Käppeler measurements were made by averaging over that cross section with a Maxwellian-like experimentally simulated ^{7}Li(p,n) spectrum with temperature near 30 keV. The Macklin data were obtained as point-wise data that cover an en-

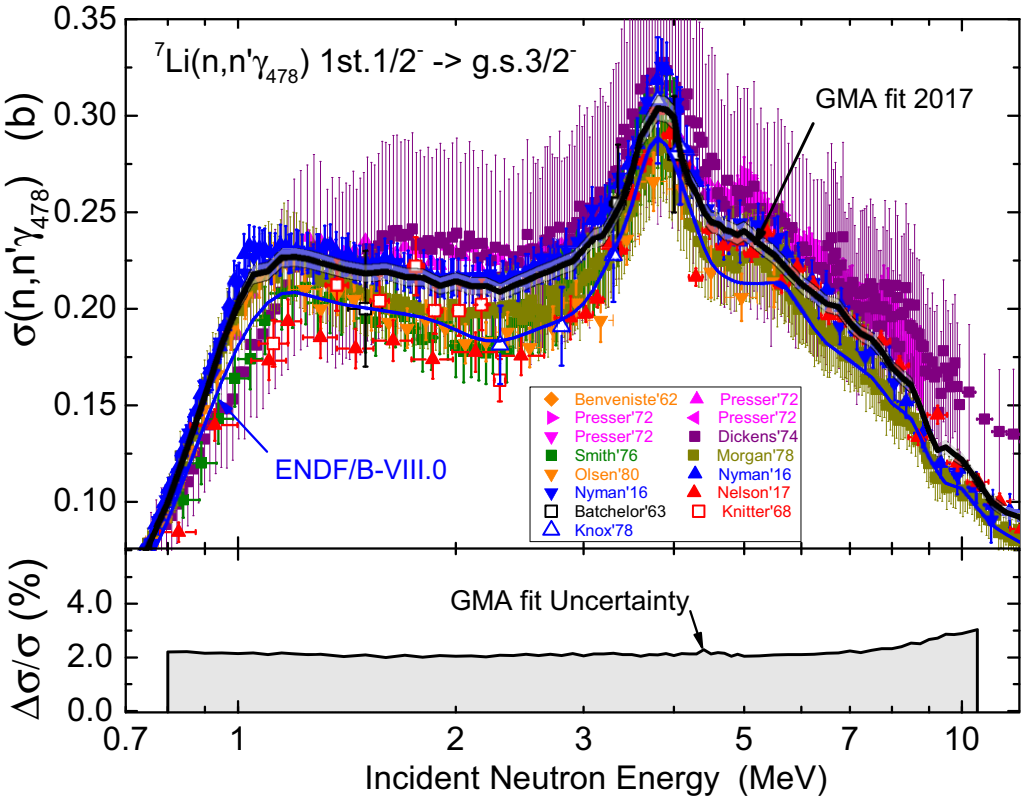

FIG. 26. (Color online) ^{7}Li(n,n'γ) reaction cross section in the neutron energy range 0.7–12 MeV. Top: existing and selected experimental (n,xγ) and (n,n$_1$) data (symbols); GMA fit 2017 (black curve) and ENDF/B-VIII.0 evaluation (blue). Bottom: uncertainty of the GMA fit.

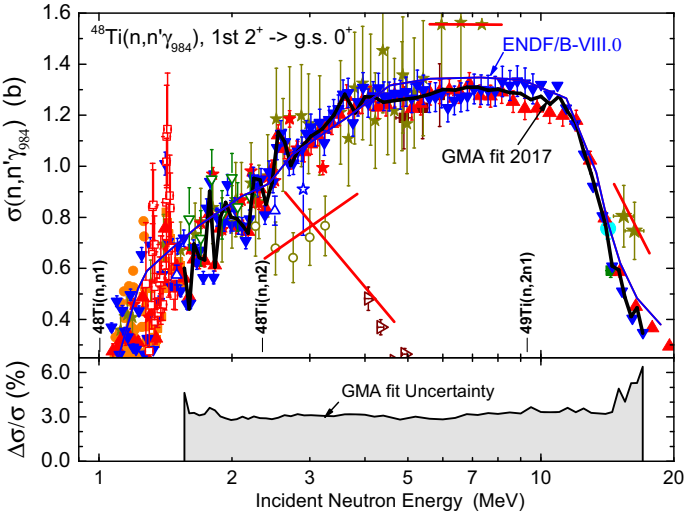

FIG. 27. (Color online) ^{48}Ti(n,n'γ) reaction cross section in the neutron energy range 1–20 MeV. Top: existing and selected (except crossed) experimental (n,xγ) and (n,n$_1$) data (symbols); GMA fit 2017 (black curve) and ENDF/B-VIII.0 evaluation (blue). Bottom: uncertainty of the GMA fit.

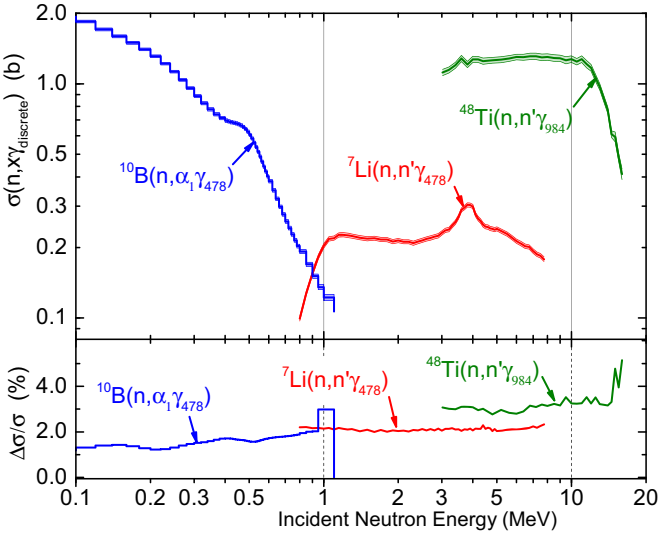

FIG. 28. (Color online) Evaluated discrete γ-ray production cross sections for the ^{10}B(n,α$_1$γ), ^{7}Li(n,n'γ) and ^{48}Ti(n,n'γ) reactions in the neutron energy ranges where they are recommended to use as references (top) and their uncertainties (bottom).

ergy region that includes that covered by the Maxwellian.

However, the 2006 standards evaluation of the gold capture cross section makes use of a large amount of data. In addition to gold capture cross section measurements, ratio measurements of that cross section to other standards are used. Then absolute measurements of those standards can have an impact on the gold cross section through those ratios. In effect, more than 400 cross section data sets had an impact to some degree on the gold standard capture cross section evaluation results. Accurate values

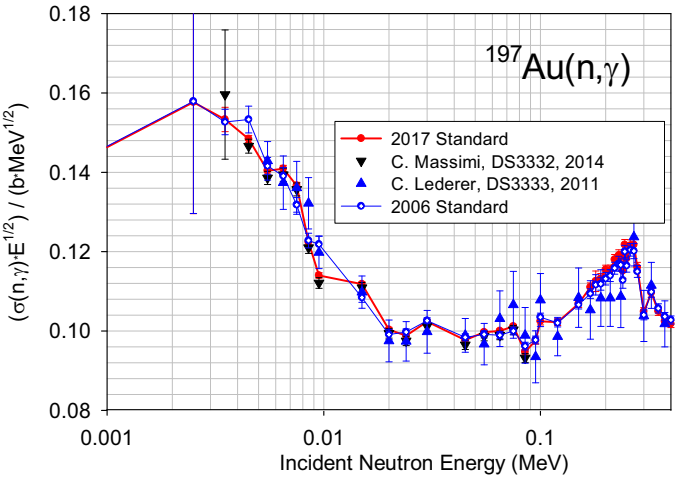

FIG. 29. (Color online) Comparison of recent measurements and evaluations of the ^{197}Au(n,γ) cross section from 1 keV up to 400 keV.

were obtained below 200 keV, from the 2006 standards evaluation process for the gold capture cross section, however they are not recommended for use as a standard due to structure in the cross section there. The 5 % to 7 % difference referred to in Sec. II.G between the 2006 standards evaluation result in the Maxwellian energy region and the Ratynski and Käppeler evaluation was also an important concern.

Experiments referred to in Sec. II.G were incorporated into the new GMAP evaluation along with the 2006 data in the standards database, resulting in the 2017 results. In Fig. 29, results of recent experiments [33, 40] are compared with the 2006 and 2017 standards evaluations. There is very good agreement. The Maxwellian averaged cross section at kT=30 keV for ^{197}Au(n,γ) is now a standard cross section. That cross section is 620 $\pm$ 4 mb before unrecognized uncertainty (see section III A) is taken into account. After taking that into account we obtain 620 $\pm$ 11 mb. The astrophysical database [104] (KADONIS 1.0) has changed the MACS for the ^{197}Au(n,γ) cross section. Their new preliminary value, 613 $\pm$ 7 agrees with the 2017 standards evaluation within one standard deviation.

IV. COMPARISONS OF THE NEW EVALUATION WITH EXPERIMENTAL DATA AND PREVIOUS STANDARDS

Figures 30–37 in this section show the results of the combined fits described above, which are the final standards evaluation results compared with the experimental data for the reaction cross sections and their ratios over various energy ranges. The standards evaluation final fits are shown by thick solid lines with evaluated uncertainties given at the nodes. The results of the 2006 standards evaluation are also shown. The experimental data shown in the figures are taken directly from the GMA database. "DS..." refers to datasets in the GMA database. In some cases the EXFOR [93] (Experimental Nuclear Reaction Data, sometimes abbreviated as X4) accession number is given that can be used to retrieve the data online.

Due to the large size of the database, only a subset of the data sets are plotted. For most of the figures, the dataset number, the name of the first author and the year of publication are given in the legend. The references for each dataset are given in Table II and those shown in Table II of Ref. [1]. Data are reduced to the original form in which they were obtained by the experimentalists: absolute cross sections, non-normalized (shape) cross sections, absolute ratio of cross sections and non-normalized (shape) ratio of cross sections. Absolute cross sections that had been normalized using the hydrogen-scattering standard were renormalized to the new standard. Data sets with shape cross sections and shape cross section ratios were renormalized with coefficients that give the best chi-square values relative to the final evaluation. Uncertainties in the experimental data shown in the figures are the original uncertainties assigned by the authors in virtually all cases. Expanded uncertainties for the outlying experimental data used in the final combined fit are not shown. However, they can easily be envisaged as uncertainty bars which restore consistency with the final evaluation. The GMA database also includes covariance matrices of the uncertainties of the experimental data generated from partial components of the uncertainties and their correlative properties. Many data sets obtained at the same laboratory, or with the same sample or detector, are combined in data blocks that account for correlations between sets. Except for the light element standards, the curves are not fits to the data, they simply follow the data points.

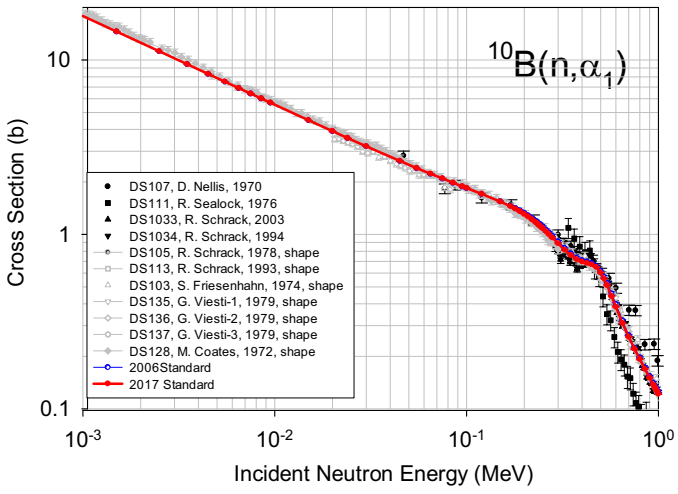

FIG. 30. (Color online) Comparison of the 2017 and 2006 standards evaluations, together with experimental data for the ^{10}B(n,$\alpha_1\gamma$) cross section for energies from 1 keV to 1 MeV.

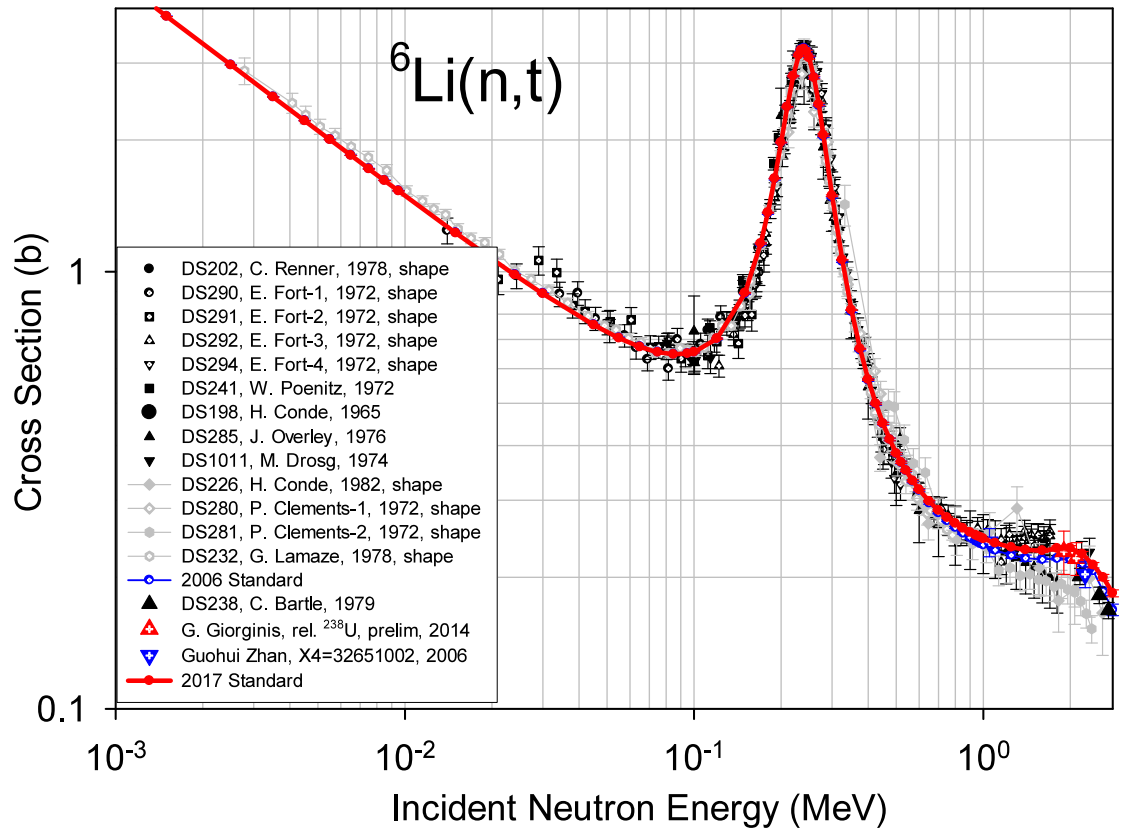

(a) Incident neutron energies from 1 keV to 3 MeV.

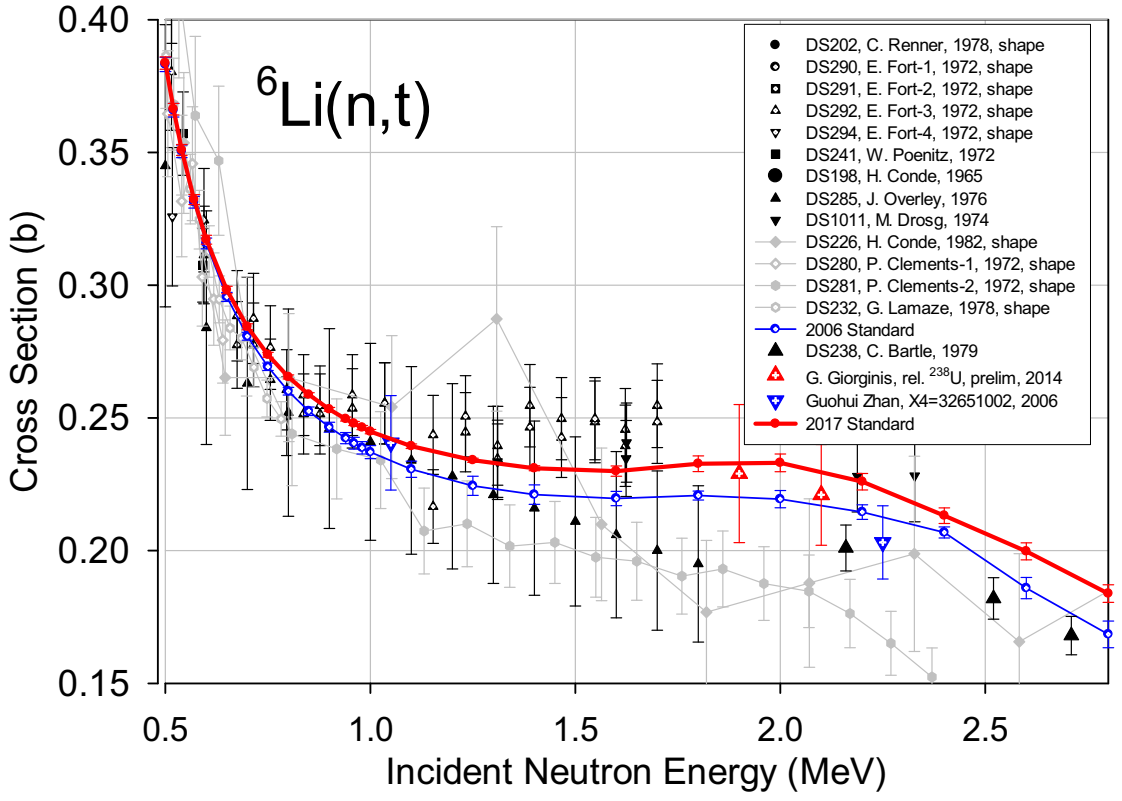

(b) Incident neutron energies from 0.5 MeV to 2.8 MeV.

FIG. 31. (Color online) Comparison of the 2017 and 2006 standards evaluations, together with experimental data for the ^{6}Li(n,t) cross section.

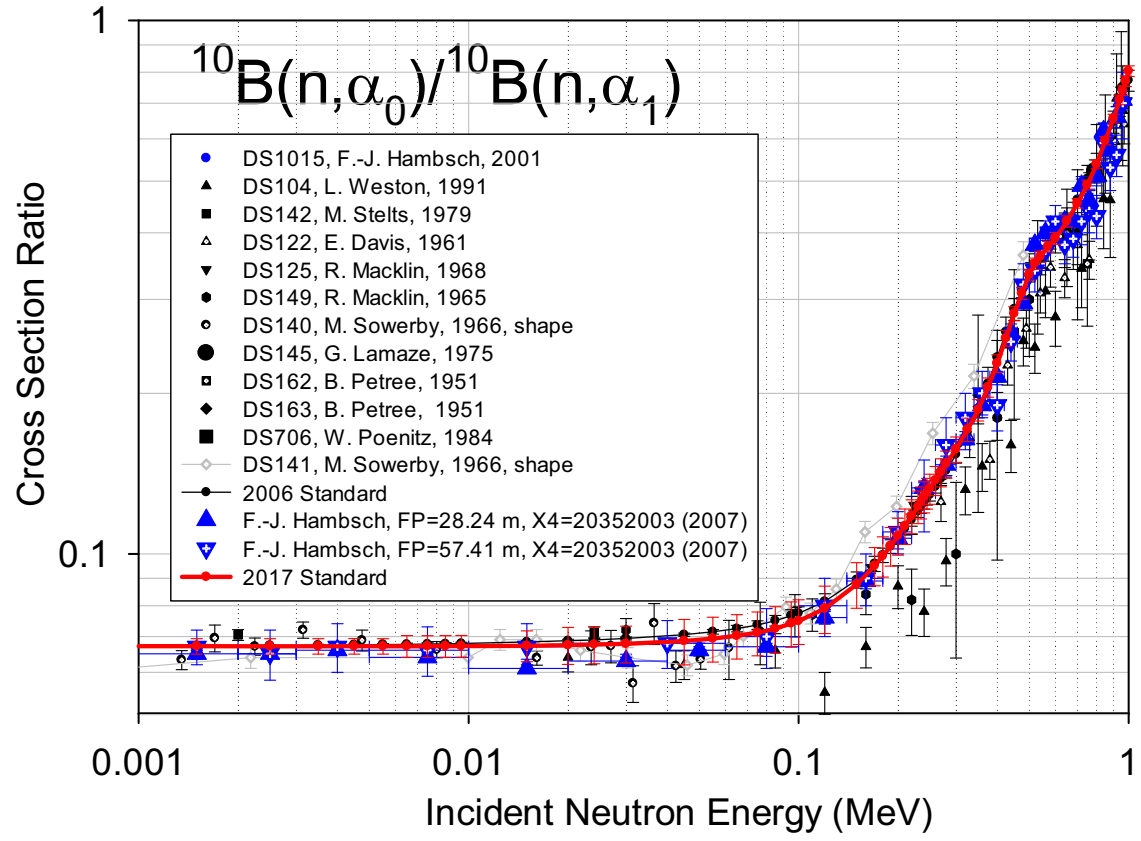

]

(a) Incident neutron energies from 1 keV to 1 MeV (Log. scale).

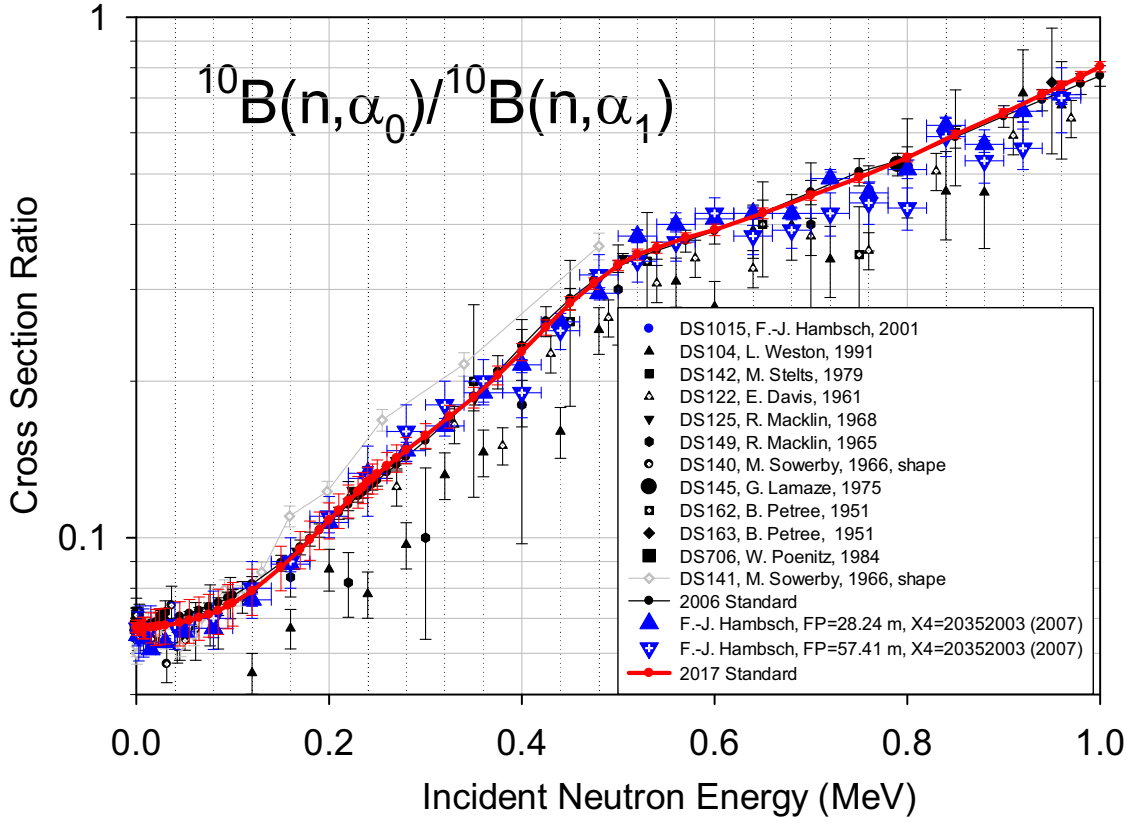

(b) Incident neutron energies up to 1 MeV (Linear scale).

FIG. 32. (Color online) Comparison of the 2017 and 2006 standards evaluations, together with experimental data for the ratio of the $^{10}B(n,\alpha_0)$ to $^{10}B(n,\alpha_1)$ cross section.

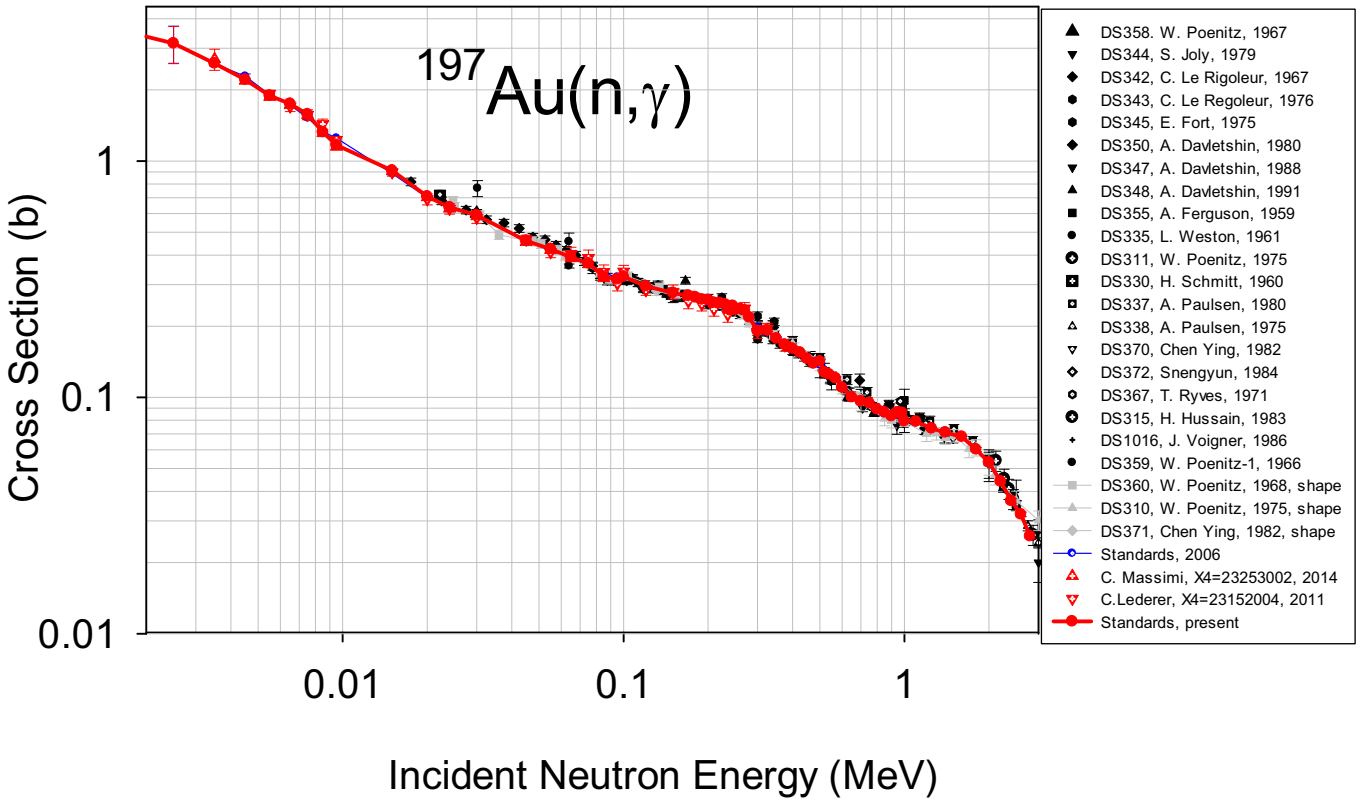

(a) Incident neutron energies from 2 keV to 2.8 MeV.

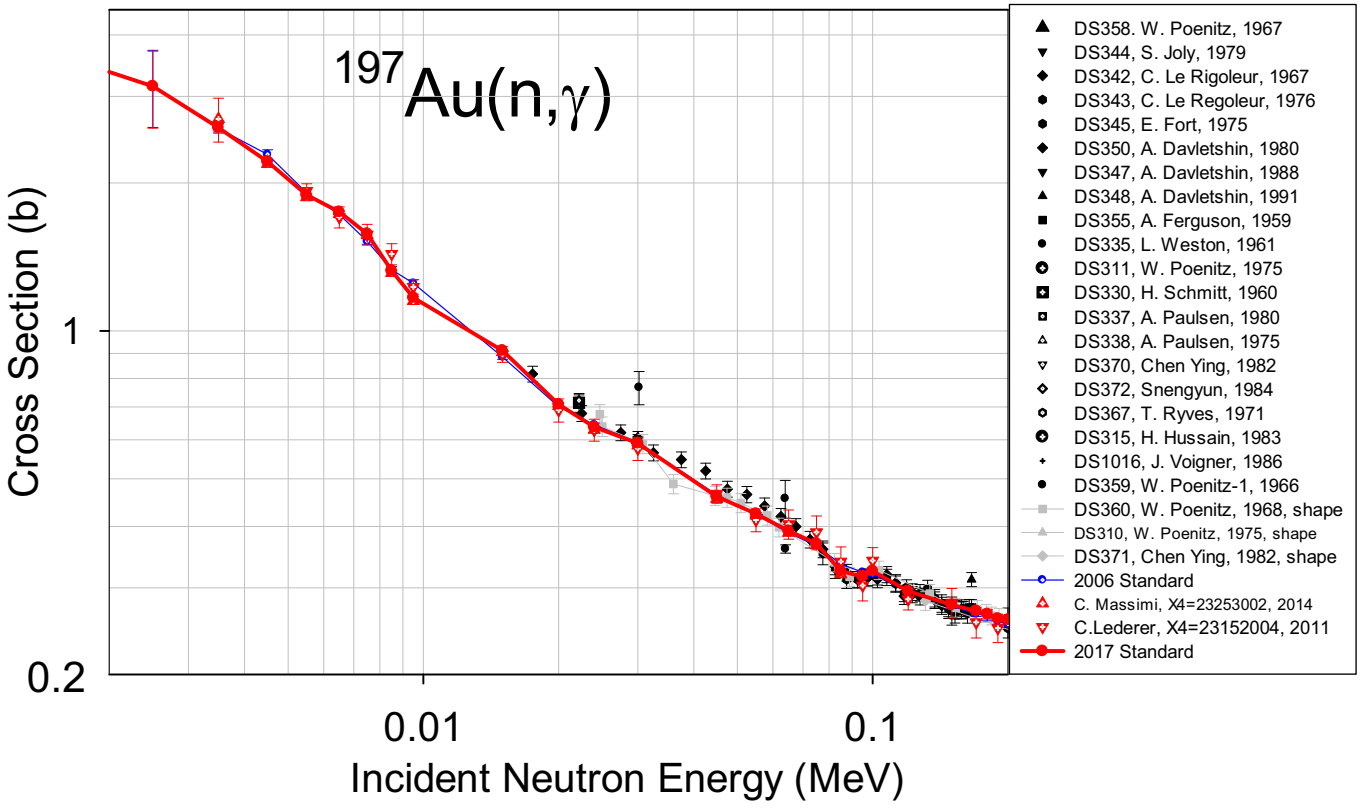

(b) Incident neutron energies from 2 keV to 200 keV.

FIG. 33. (Color online) Comparison of the 2017 and 2006 standards evaluations, together with experimental data for the Au(n,γ) cross section.

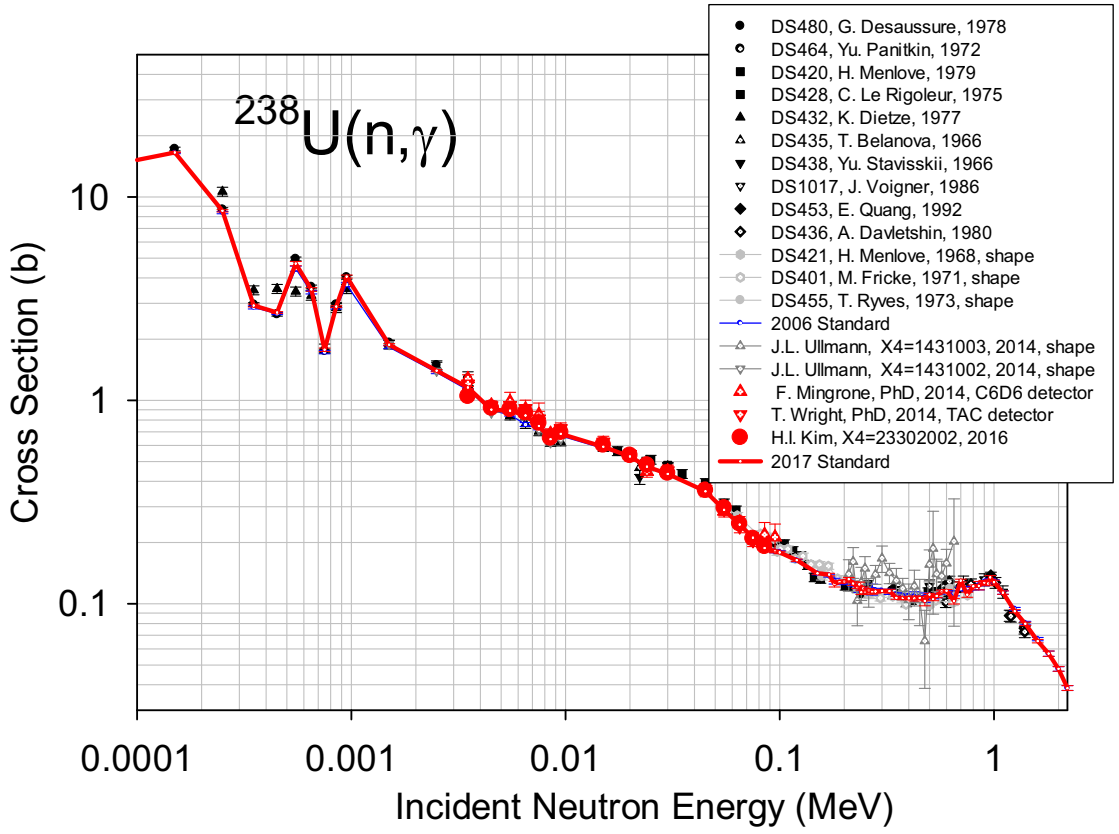

(a) Incident neutron energies from 100 eV to 2.2 MeV.

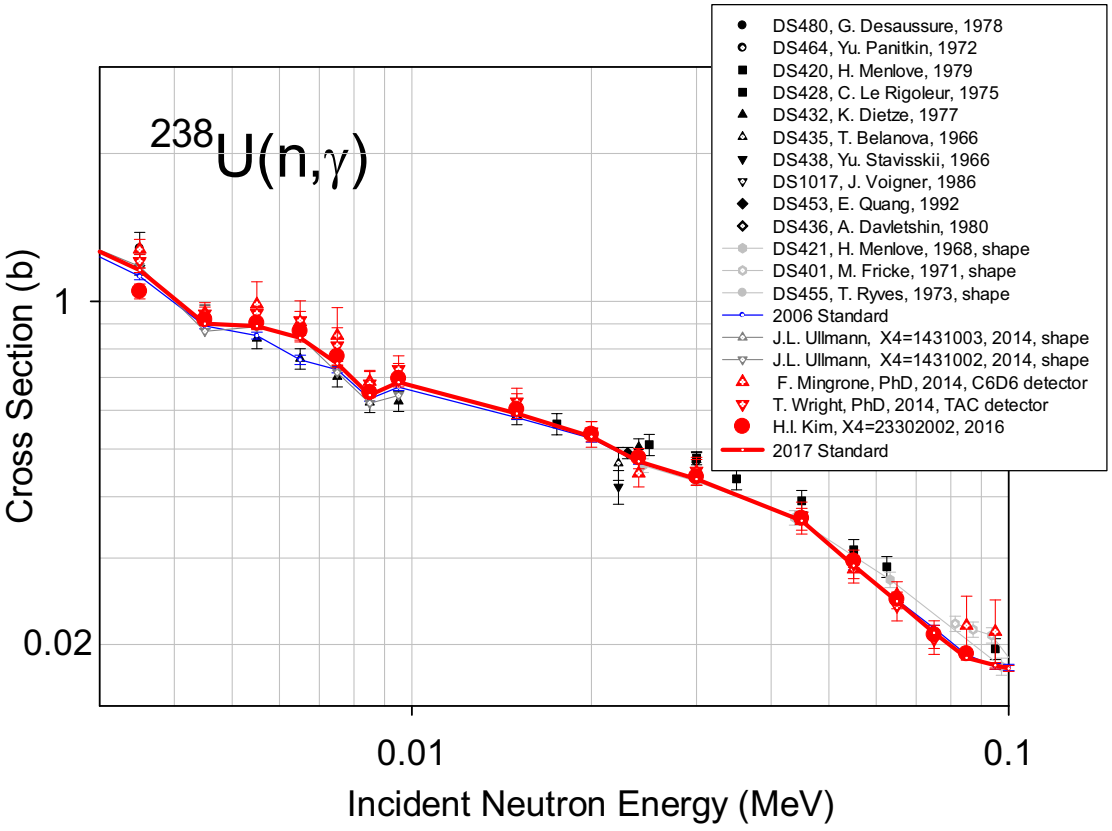

(b) Incident neutron energies from 3 keV to 100 keV.

FIG. 34. (Color online) Comparison of the 2017 and 2006 standards evaluations, together with experimental data for the ^{238}U(n,γ) cross section.

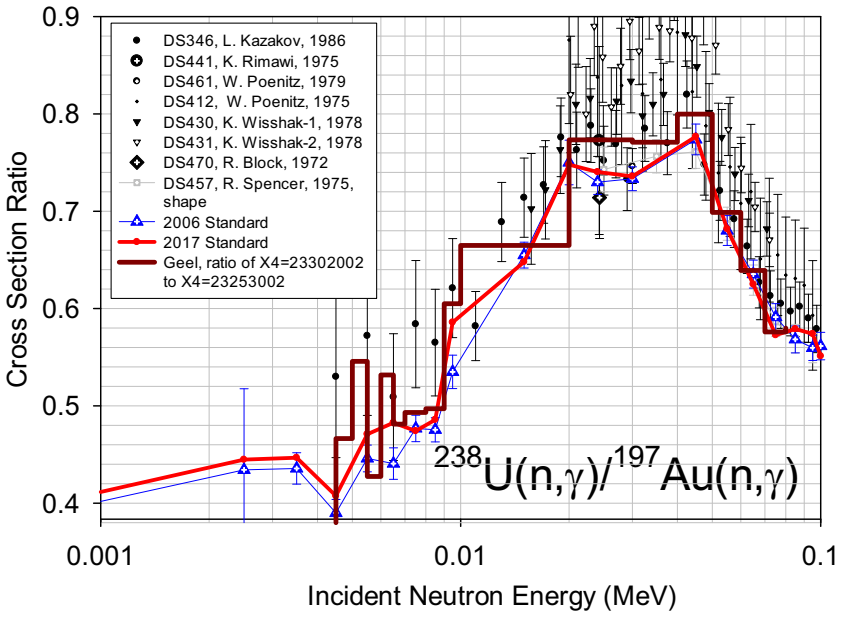

(a) Incident neutron energies from 1 keV to 100 keV.

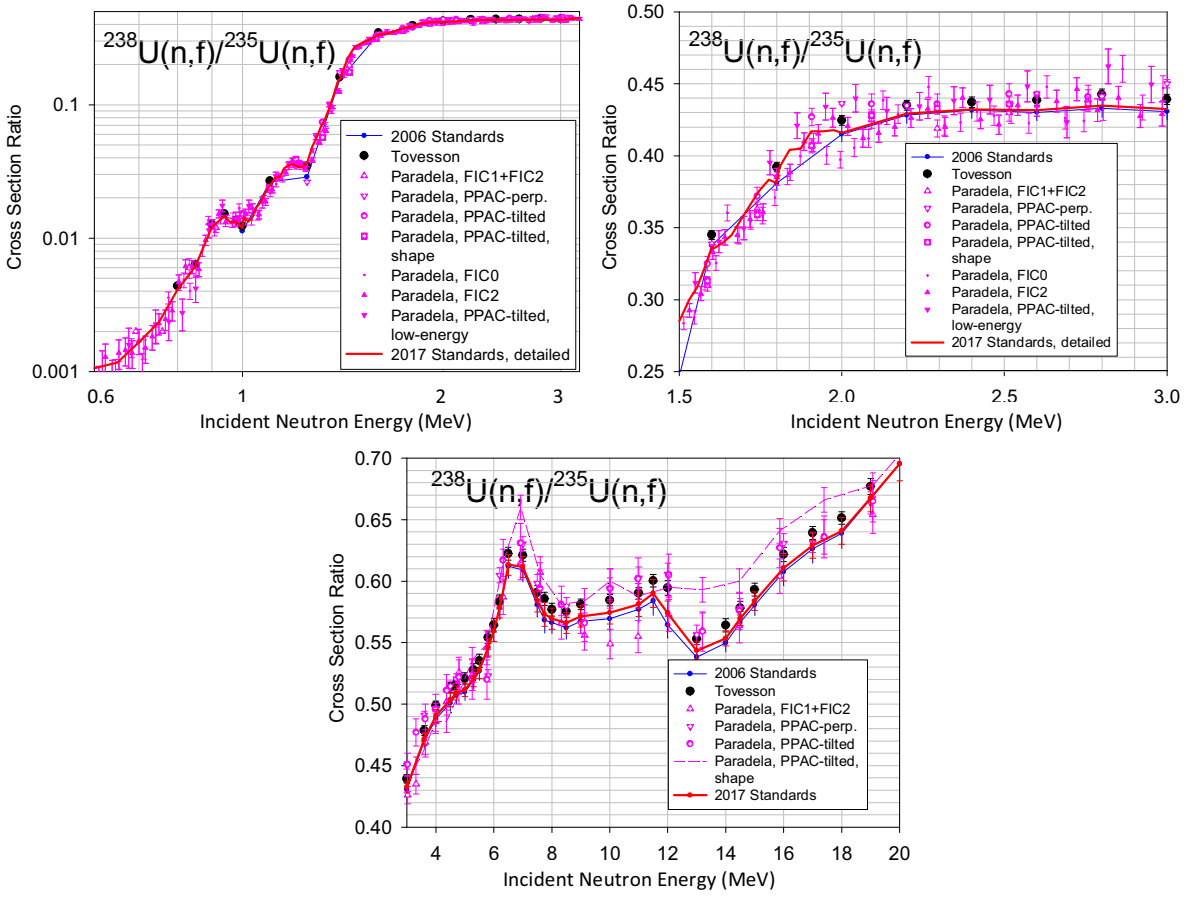

(b) Incident neutron energies from 600 keV to 20 MeV.

FIG. 35. (Color online) Comparison of the 2017 and 2006 standards evaluations, together with experimental data for the ^{238}U(n,γ) to Au(n,γ) cross section ratio (a), and for the ^{238}U(n,f) to ^{235}U(n,f) cross section ratio with the most recent data (b).

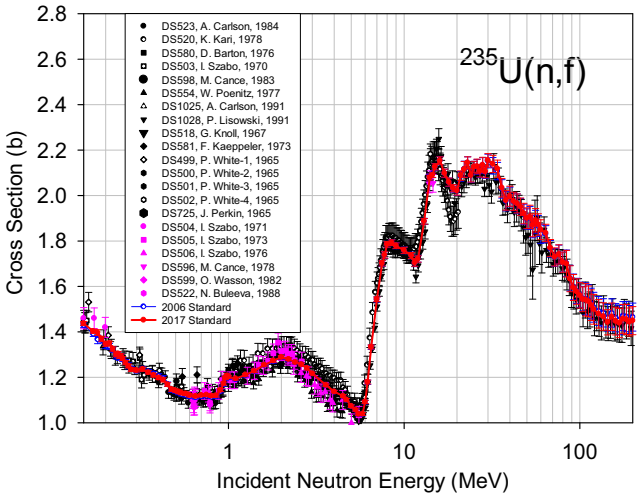

(a) First group of ^{235}U(n,f) experimental data from 0.1–200 MeV.

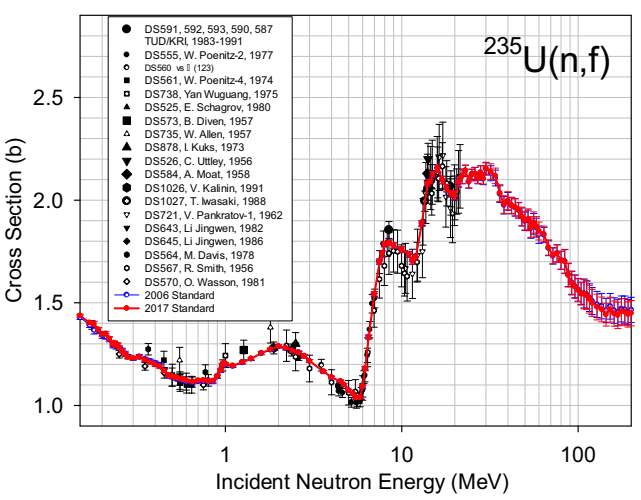

(b) Second group of ^{235}U(n,f) experimental data from 0.1–200 MeV.

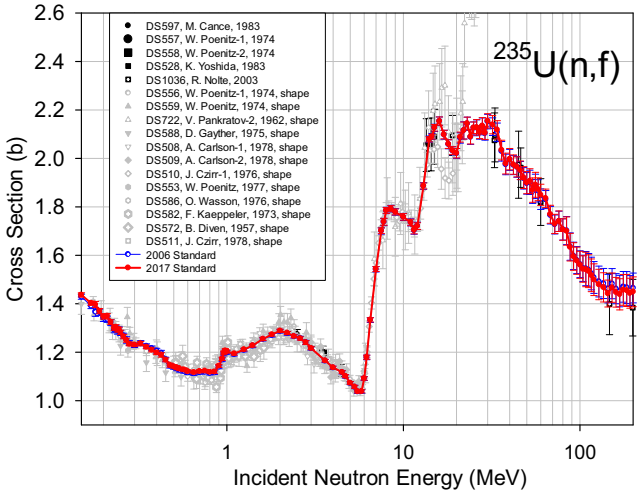

(c) Third group of ^{235}U(n,f) experimental data from 0.1–200 MeV.

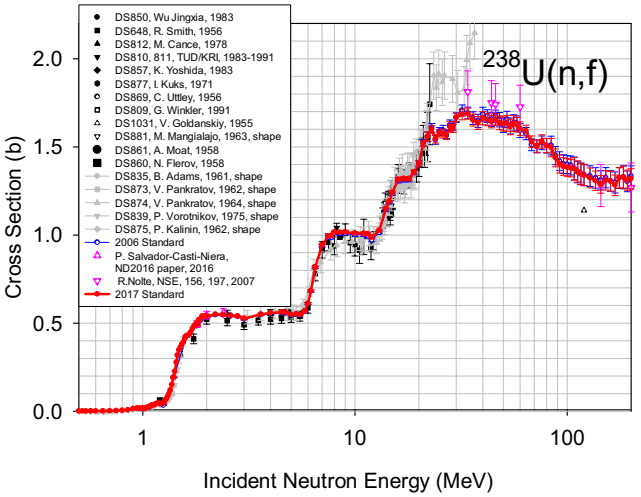

(d) ^{238}U(n,f) experimental data from 0.5–200 MeV.

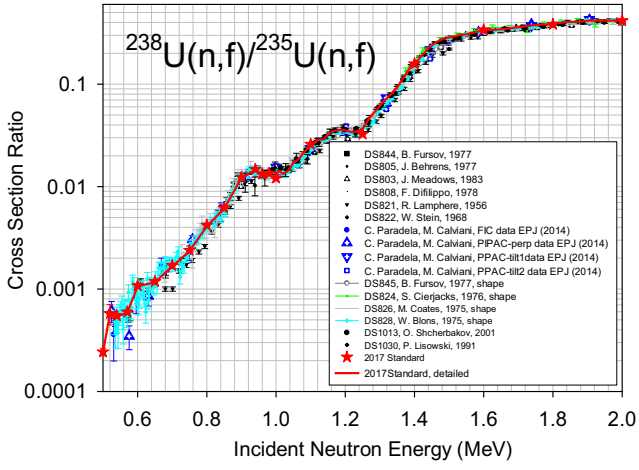

(e) ^{238}U(n,f) to ^{235}U(n,f) cross section ratio from 0.5–2 MeV.

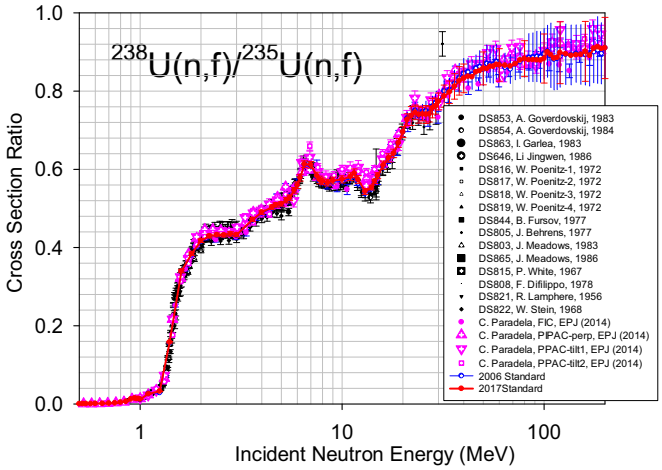

(f) ^{238}U(n,f) to ^{235}U(n,f) cross section ratio from 0.5–200 MeV.

FIG. 36. (Color online) Comparison of the 2017 and 2006 standards evaluations, together with experimental data for the ^{235}U(n,f) cross section (a,b,c), for the ^{238}U(n,f) cross section (d), and for the ^{238}U(n,f) to ^{235}U(n,f) cross section ratio from 0.5 MeV to 2 MeV (e), and from 0.5 MeV to 200 MeV (f).

V. TABULAR DATA FOR THE NEUTRON STANDARDS

Tabular data for each of the cross section standards and the additional cross sections obtained in the cross section standards evaluation process are given in the Tables XII–XX. For all the evaluations other than those for the light element standards, the tabular output is directly from GMAP. For the ^{6}Li(n,t), ^{10}B(n,α) and ^{10}B(n,$\alpha_1\gamma$) cross sections the GMAP output was fitted with EDA code as described in Sec. A. The tables for those cross sections were provided as point-wise values from EDA. The H(n,n) and C(n,n) cross sections had been evaluated using EDA and the tables are direct output from EDA as point-wise values.

The evaluation of the ^{252}Cf PFNS obtained from this work led to only very small changes in the spectrum obtained by Mannhart. It is recommended that the Mannhart evaluation be used for any applications. It is available at https://www-nds.iaea.org/standards/ref-spectra/ together with the evaluated ^{235}U thermal prompt fission neutron spectrum. The reference fission cross sections for ^{209}Bi(n,f), ^{nat}Pb(n,f), ^{235}U(n,f), ^{238}U(n,f) and ^{239}Pu(n,f); and the prompt γ-ray production reference Cross Sections for ^{7}Li(n,n'γ) and ^{48}Ti(n,n'γ) will be listed and updated on the site https://www-nds.iaea.org/standards/. As noted previously, the ^{3}He(n,p) cross section was not re-evaluated. The publication on the 2006 standards [1] contains the ^{3}He(n,p) evaluation.

The GMAP evaluation estimates a point-wise cross section and its uncertainty at energy E using experimental data in the energy range from E1 to E2. However, for the ^{235}U(n,f) cross section an integral from 7.8–11 eV is produced with a node average energy 9.4 eV. The interval corresponding to the node at 0.15 keV starts at 0.1 keV both for ^{235}U(n,f) and ^{239}Pu(n,f) cross sections. From there on, all intervals are located half-way between given GMA nodes. The results from 1 keV up to 150 keV correspond to the average of low resolution experiments. For the ^{238}U(n,f) cross section below 2 MeV (below the region where it is a standard) results with a denser grid are marked by "x" and one corrected point is labelled by "xx". Smoothing has been applied for regions where scatter of data needs to be removed since the standards should be smooth. For all the tabular data, the values in the standards energy region are recommended to be used as standards for measurements. The fitted unsmoothed values were included into the evaluated ENDF-B/VIII.0 general-purpose files in the standard region.

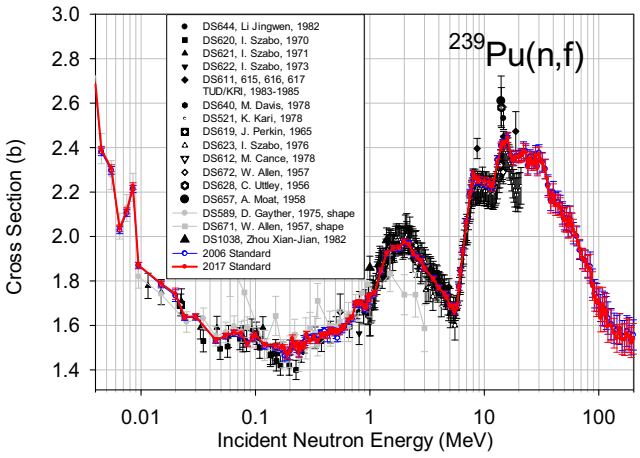

(a) ^{239}Pu(n,f) experimental data from 4 keV up to 200 MeV.

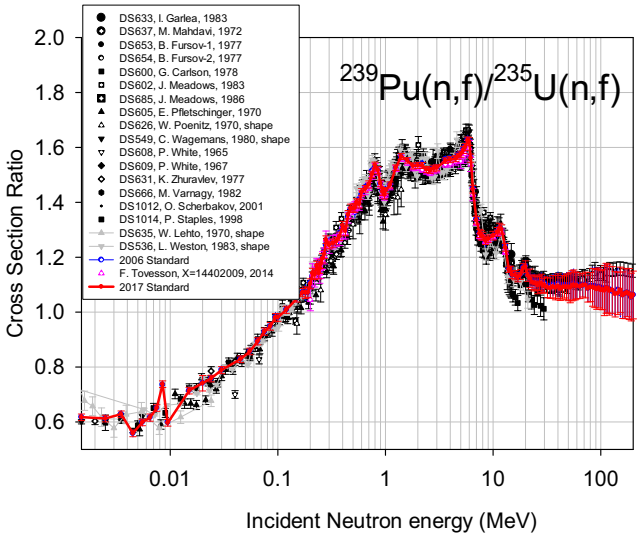

(b) ^{239}Pu(n,f) to ^{235}U(n,f) cross section ratio from 1 keV up to 200 MeV.

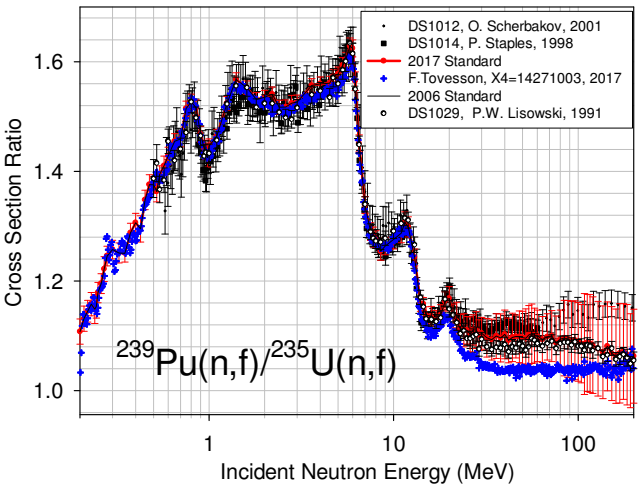

(c) ^{239}Pu(n,f) to ^{235}U(n,f) cross section ratio from 200 keV up to 200 MeV.

FIG. 37. (Color online) Comparison of the 2017 and 2006 standards evaluations, together with experimental data for the ^{239}Pu(n,f) cross section (a) and for the ^{239}Pu(n,f) to ^{235}U(n,f) cross section ratio (b,c).

TABLE XII. H(n,n) cross section data. It is a standard from 1 keV to 20 MeV. E_n is the incident neutron energy. CS is the cross section. ΔCS is the cross section uncertainty. The 0.34 % unrecognized systematic uncertainty is included in the uncertainties in the table. Linear interpolation between energies is recommended.

Recommended point-wise data		
E_n, MeV	CS, b	ΔCS, %
1.00E-11	20.436	0.83
2.00E-11	20.436	0.83
5.00E-11	20.436	0.83
1.00E-10	20.436	0.83
2.00E-10	20.436	0.83
5.00E-10	20.436	0.83
1.00E-09	20.436	0.83
2.00E-09	20.436	0.83
5.00E-09	20.436	0.83
1.00E-08	20.436	0.83
2.53E-08	20.436	0.83
1.00E-07	20.436	0.83
2.00E-07	20.436	0.83
5.00E-07	20.436	0.83
1.00E-06	20.436	0.83
2.00E-06	20.436	0.83
5.00E-06	20.435	0.83
1.00E-05	20.435	0.83
2.00E-05	20.433	0.83
5.00E-05	20.429	0.83
1.00E-04	20.423	0.83
2.00E-04	20.409	0.83
5.00E-04	20.369	0.83
1.00E-03	20.303	0.83
2.00E-03	20.171	0.82
4.00E-03	19.913	0.81
6.00E-03	19.663	0.80
8.00E-03	19.420	0.79
1.00E-02	19.184	0.78
2.00E-02	18.096	0.74
4.00E-02	16.296	0.67
6.00E-02	14.868	0.61
8.00E-02	13.707	0.57
1.00E-01	12.744	0.53
1.50E-01	10.925	0.47
2.00E-01	9.645	0.44
3.00E-01	7.954	0.40
4.00E-01	6.879	0.38
5.00E-01	6.128	0.37
6.00E-01	5.569	0.36
7.00E-01	5.135	0.36
8.00E-01	4.785	0.36
9.00E-01	4.495	0.35
1.00E+00	4.249	0.35
1.20E+00	3.854	0.35
1.40E+00	3.546	0.35

Recommended point-wise data		
E_n, MeV	CS, b	ΔCS, %
1.60E+00	3.296	0.36
1.80E+00	3.087	0.36
2.00E+00	2.908	0.36
2.20E+00	2.753	0.36
2.40E+00	2.617	0.36
2.60E+00	2.495	0.37
2.80E+00	2.386	0.37
3.00E+00	2.287	0.37
3.20E+00	2.196	0.38
3.40E+00	2.113	0.38
3.60E+00	2.037	0.38
3.80E+00	1.966	0.38
4.00E+00	1.900	0.39
4.20E+00	1.838	0.39
4.40E+00	1.781	0.39
4.60E+00	1.726	0.40
4.80E+00	1.676	0.40
5.00E+00	1.628	0.40
6.00E+00	1.423	0.41
7.00E+00	1.263	0.42
7.50E+00	1.195	0.43
8.00E+00	1.133	0.43
8.50E+00	1.077	0.43
9.00E+00	1.027	0.43
9.50E+00	0.980	0.43
1.00E+01	0.937	0.43
1.05E+01	0.897	0.43
1.10E+01	0.861	0.43
1.15E+01	0.827	0.43
1.20E+01	0.795	0.43
1.25E+01	0.765	0.43
1.30E+01	0.738	0.42
1.35E+01	0.712	0.42
1.40E+01	0.688	0.42
1.45E+01	0.665	0.42
1.50E+01	0.643	0.42
1.55E+01	0.623	0.42
1.60E+01	0.604	0.42
1.65E+01	0.586	0.42
1.70E+01	0.568	0.42
1.75E+01	0.552	0.42
1.80E+01	0.537	0.42
1.85E+01	0.522	0.43
1.90E+01	0.508	0.43
1.95E+01	0.495	0.44
2.00E+01	0.482	0.44

TABLE XIII. ^{6}Li(n,t) cross section data. It is a standard from 0.0253 eV to 1 MeV. E_n is the incident neutron energy. CS is the cross section. ΔCS is the cross section uncertainty. The 0.5 % unrecognized systematic uncertainty is included in the uncertainties in the table. Linear interpolation is recommended except below 0.03 MeV where log-log interpolation should be used.

Recommended point-wise data		
E_n, MeV	CS, b	ΔCS, %
2.53E-08	937.998	0.51
9.40E-06	48.636	0.51
1.50E-04	12.157	0.51
2.50E-04	9.412	0.51
3.50E-04	7.951	0.51
4.50E-04	7.010	0.51
5.50E-04	6.339	0.51
6.50E-04	5.830	0.51
7.50E-04	5.427	0.51
8.50E-04	5.097	0.51
9.50E-04	4.820	0.51
1.50E-03	3.834	0.51
2.50E-03	2.969	0.51
3.50E-03	2.509	0.51
4.50E-03	2.214	0.51
5.50E-03	2.004	0.51
6.50E-03	1.844	0.51
7.50E-03	1.718	0.51
8.50E-03	1.616	0.51
9.50E-03	1.530	0.51
1.50E-02	1.226	0.52
2.00E-02	1.070	0.52
2.40E-02	0.984	0.53
3.00E-02	0.891	0.54
4.50E-02	0.755	0.59
5.50E-02	0.705	0.63
6.50E-02	0.673	0.67
7.50E-02	0.654	0.71
8.50E-02	0.646	0.75
9.50E-02	0.649	0.80
1.00E-01	0.654	0.82
1.20E-01	0.702	0.91
1.50E-01	0.893	1.0
1.70E-01	1.161	1.1
1.80E-01	1.366	1.1

Recommended point-wise data		
E_n, MeV	CS, b	ΔCS, %
1.90E-01	1.635	1.1
2.00E-01	1.976	1.1
2.10E-01	2.380	1.2
2.20E-01	2.794	1.3
2.30E-01	3.115	1.5
2.35E-01	3.201	1.6
2.40E-01	3.224	1.7
2.45E-01	3.183	1.7
2.50E-01	3.085	1.7
2.60E-01	2.771	1.7
2.70E-01	2.395	1.6
2.80E-01	2.038	1.5
3.00E-01	1.485	1.3
3.25E-01	1.062	1.1
3.50E-01	0.817	1.1
3.75E-01	0.667	1.1
4.00E-01	0.569	1.1
4.50E-01	0.453	1.1
4.75E-01	0.416	1.1
5.00E-01	0.388	1.1
5.20E-01	0.369	1.1
5.40E-01	0.354	1.1
5.70E-01	0.335	1.1
6.00E-01	0.319	1.1
6.50E-01	0.300	1.0
7.00E-01	0.285	1.0
7.50E-01	0.274	1.0
8.00E-01	0.266	1.0
8.50E-01	0.259	1.0
9.00E-01	0.253	1.0
9.40E-01	0.249	1.0
9.60E-01	0.248	1.0
9.80E-01	0.246	1.0
1.00E+00	0.245	1.0

TABLE XIV. ^{10}B(n,$\alpha_1\gamma$) and ^{10}B(n,α) cross section data. E_n is the incident neutron energy. CS is the cross section. ΔCS is the cross section uncertainty. These cross sections are standards from 0.0253 eV to 1 MeV. The 0.8 % unrecognized systematic uncertainty for each cross section is included in the uncertainties in the table. Linear interpolation is recommended except below 0.03 MeV where log-log interpolation should be used.

Recommended point-wise data				
	^{10}B(n,$\alpha_1\gamma$)		^{10}B(n,α)	
E_n,MeV	CS, b	ΔCS, %	CS, b	ΔCS, %
2.53E-08	3602.029	0.83	3844.121	0.82
9.40E-06	186.598	0.83	199.140	0.82
1.50E-04	46.504	0.82	49.630	0.82
2.50E-04	35.963	0.82	38.379	0.82
3.50E-04	30.354	0.82	32.394	0.82
4.50E-04	26.740	0.82	28.537	0.82
5.50E-04	24.164	0.82	25.787	0.82
6.50E-04	22.208	0.82	23.700	0.82
7.50E-04	20.658	0.82	22.046	0.82
8.50E-04	19.391	0.82	20.693	0.82
9.50E-04	18.329	0.82	19.561	0.82
1.50E-03	14.542	0.82	15.519	0.82
2.50E-03	11.219	0.82	11.972	0.82
3.50E-03	9.454	0.82	10.089	0.82
4.50E-03	8.319	0.82	8.877	0.82
5.50E-03	7.511	0.82	8.015	0.82
6.50E-03	6.898	0.83	7.362	0.82
7.50E-03	6.414	0.83	6.845	0.83
8.50E-03	6.018	0.83	6.423	0.83
9.50E-03	5.688	0.84	6.070	0.83
1.50E-02	4.515	0.87	4.819	0.86
2.00E-02	3.908	0.90	4.172	0.89
2.40E-02	3.570	0.92	3.812	0.91
3.00E-02	3.199	0.95	3.417	0.94
4.50E-02	2.634	1.0	2.815	0.98
5.50E-02	2.400	1.0	2.567	1.0
6.50E-02	2.225	1.0	2.381	1.0
7.50E-02	2.088	1.1	2.237	1.0
8.50E-02	1.977	1.1	2.121	1.1
9.50E-02	1.885	1.2	2.025	1.1
1.00E-01	1.845	1.2	1.983	1.1
1.20E-01	1.707	1.3	1.842	1.3
1.50E-01	1.545	1.4	1.680	1.3
1.70E-01	1.450	1.4	1.587	1.3
1.80E-01	1.404	1.4	1.542	1.3

Recommended point-wise data				
	^{10}B(n,$\alpha_1\gamma$)		^{10}B(n,α)	
E_n,MeV	CS, b	ΔCS, %	CS, b	ΔCS, %
1.90E-01	1.357	1.3	1.497	1.2
2.00E-01	1.311	1.3	1.452	1.2
2.10E-01	1.265	1.2	1.407	1.2
2.20E-01	1.219	1.2	1.361	1.1
2.30E-01	1.172	1.2	1.316	1.1
2.35E-01	1.149	1.2	1.293	1.1
2.40E-01	1.127	1.2	1.270	1.1
2.45E-01	1.104	1.2	1.247	1.2
2.50E-01	1.082	1.2	1.225	1.2
2.60E-01	1.039	1.3	1.181	1.2
2.70E-01	0.997	1.3	1.139	1.2
2.80E-01	0.958	1.4	1.099	1.3
3.00E-01	0.887	1.4	1.026	1.3
3.25E-01	0.813	1.5	0.952	1.4
3.50E-01	0.758	1.5	0.899	1.4
3.75E-01	0.720	1.6	0.867	1.4
4.00E-01	0.697	1.7	0.855	1.5
4.25E-01	0.684	1.7	0.857	1.5
4.50E-01	0.671	1.6	0.860	1.4
4.75E-01	0.648	1.6	0.847	1.4
5.00E-01	0.605	1.6	0.806	1.4
5.20E-01	0.561	1.5	0.755	1.3
5.40E-01	0.512	1.5	0.696	1.3
5.70E-01	0.443	1.6	0.609	1.4
6.00E-01	0.384	1.6	0.534	1.4
6.50E-01	0.310	1.7	0.440	1.4
7.00E-01	0.258	1.8	0.375	1.5
7.50E-01	0.221	1.8	0.329	1.5
8.00E-01	0.192	1.8	0.296	1.6
8.50E-01	0.169	1.9	0.270	1.6
9.00E-01	0.151	2.0	0.249	1.7
9.40E-01	0.138	2.0	0.236	1.9
9.60E-01	0.133	2.0	0.230	2.1
9.80E-01	0.127	2.3	0.225	2.4
1.00E+00	0.122	2.9	0.220	3.0

TABLE XV. Au(n,γ) cross section. This is the GMAP output of point-wise cross sections. E_n is the incident neutron energy that corresponds to the GMA node. CS is the cross section. ΔCS is the cross section uncertainty. It is a standard at 0.0253 eV and between 0.2 MeV and 2.5 MeV. Linear interpolation between GMA nodes is recommended above the thermal energy (0.0253 eV). These data include a 1.7 % unrecognized systematic uncertainty. Data followed by "*" are smoothed values.

Recommended point-wise data		
E_n, MeV	CS, b	ΔCS, %
2.53E-08	98.659	0.14
2.50E-03	3.146	18.
3.50E-03	2.591	2.6
4.50E-03	2.210	1.8
5.50E-03	1.891	1.8
6.50E-03	1.746	1.8
7.50E-03	1.576	1.8
8.50E-03	1.326	1.8
9.50E-03	1.168	1.8
1.50E-02	0.912	1.8
2.00E-02	0.708	1.8
2.40E-02	0.637	1.8
3.00E-02	0.590	1.8
4.50E-02	0.460	1.8
5.50E-02	0.425	1.8
6.50E-02	0.392	1.8
7.50E-02	0.369	1.8
8.50E-02	0.334*	1.8
9.50E-02	0.320*	1.9
1.00E-01	0.318*	1.9
1.20E-01	0.296	1.9
1.50E-01	0.277	1.9
1.70E-01	0.269	2.0
1.80E-01	0.265	2.8
1.90E-01	0.260	2.1
2.00E-01	0.258	2.0
2.10E-01	0.252	2.0
2.20E-01	0.251	2.0
2.30E-01	0.247	2.1
2.35E-01	0.242*	2.1
2.40E-01	0.239*	2.3
2.45E-01	0.239*	2.1
2.50E-01	0.238*	2.1
2.60E-01	0.237	2.1
2.70E-01	0.233	2.1

Recommended point-wise data		
E_n, MeV	CS, b	ΔCS, %
2.80E-01	0.218	2.0
3.00E-01	0.191	2.0
3.25E-01	0.192	2.0
3.50E-01	0.178	2.0
3.75E-01	0.167	2.0
4.00E-01	0.161	1.9
4.25E-01	0.155	2.0
4.50E-01	0.146	2.0
4.75E-01	0.141*	2.0
5.00E-01	0.137*	2.0
5.20E-01	0.130*	2.0
5.40E-01	0.125	2.1
5.70E-01	0.120	2.3
6.00E-01	0.110	2.0
6.50E-01	0.100	2.1
7.00E-01	0.096	2.0
7.50E-01	0.095	2.1
8.00E-01	0.089	2.0
8.50E-01	0.086	2.4
9.00E-01	0.083	2.8
9.40E-01	0.086	2.6
9.60E-01	0.086	4.6
9.80E-01	0.086	3.6
1.00E+00	0.079	2.0
1.10E+00	0.079	2.2
1.25E+00	0.074	2.1
1.40E+00	0.071	2.4
1.60E+00	0.068	2.3
1.80E+00	0.060	2.6
2.00E+00	0.053	2.4
2.20E+00	0.044	2.5
2.40E+00	0.036	2.8
2.60E+00	0.032	2.8
2.80E+00	0.026	2.7

TABLE XVI. ^{235}U(n,f) cross sections. This is the GMAP output of point-wise cross sections. E_n is the incident neutron energy that corresponds to the GMA node. CS is the cross section. ΔCS is the cross section uncertainty. The energy interval for the point at 0.15 keV starts at 0.1 keV. From there on, all intervals are located half-way between given GMA nodes. The results from 1 keV up to 150 keV correspond to the average of low resolution experiments. Linear interpolation between GMA nodes is recommended above 0.15 keV. These data include a 1.2 % unrecognized systematic uncertainty. These data are recommended to be used as standards for measurements at the thermal point (0.0253 eV), and from 0.15 MeV to 20 MeV. **Recommended integral value for the GMA node at 9.4 eV for which the integral from 7.8 eV to 11 eV = 247.5 b-eV ± 3 b-eV.**

Recommended point-wise data		
E_n, MeV	CS, b	ΔCS, %
2.53E-08	587.288	0.23
1.50E-04	21.267	1.3
2.50E-04	20.782	1.3
3.50E-04	13.194	1.3
4.50E-04	13.845	1.3
5.50E-04	15.244	1.3
6.50E-04	11.566	1.3
7.50E-04	11.153	1.3
8.50E-04	8.252	1.3
9.50E-04	7.538	1.3
1.50E-03	7.339	1.3
2.50E-03	5.412	1.3
3.50E-03	4.808	1.3
4.50E-03	4.282	1.3
5.50E-03	3.857	1.3
6.50E-03	3.308	1.3
7.50E-03	3.251	1.3
8.50E-03	3.019	1.3
9.50E-03	3.135	1.3
1.50E-02	2.504	1.3
2.00E-02	2.353	1.8
2.40E-02	2.162	1.3
3.00E-02	2.080	1.3
4.50E-02	1.852	1.3
5.50E-02	1.814	1.3
6.50E-02	1.755	1.3
7.50E-02	1.682	1.3
8.50E-02	1.598	1.3
9.50E-02	1.577	1.3
1.00E-01	1.587	1.3
1.20E-01	1.500	1.3
1.50E-01	1.436	1.3
1.70E-01	1.402	1.4
1.80E-01	1.397	1.5
1.90E-01	1.369	1.4
2.00E-01	1.347	1.4
2.10E-01	1.349	1.4
2.20E-01	1.324	1.4
2.30E-01	1.299	1.4
2.35E-01	1.304	1.4
2.40E-01	1.294	1.4
2.45E-01	1.293	1.4
2.50E-01	1.282	1.4
2.60E-01	1.265	1.4
2.70E-01	1.250	1.4
2.80E-01	1.234	1.4
3.00E-01	1.231	1.3
3.25E-01	1.236	1.4
3.50E-01	1.216	1.3
3.75E-01	1.219	1.4
4.00E-01	1.186	1.4
4.25E-01	1.202	1.4
4.50E-01	1.165	1.4
4.75E-01	1.140	1.4
5.00E-01	1.142	1.3

Recommended point-wise data		
E_n, MeV	CS, b	ΔCS, %
5.20E-01	1.140	1.4
5.40E-01	1.123	1.4
5.70E-01	1.139	1.4
6.00E-01	1.110	1.3
6.50E-01	1.120	1.3
7.00E-01	1.117	1.3
7.50E-01	1.132	1.3
8.00E-01	1.111	1.3
8.50E-01	1.120	1.3
9.00E-01	1.144	1.3
9.40E-01	1.173	1.3
9.60E-01	1.197	1.4
9.80E-01	1.207	1.4
1.00E+00	1.203	1.3
1.10E+00	1.194	1.3
1.25E+00	1.211	1.3
1.40E+00	1.228	1.3
1.60E+00	1.255	1.3
1.80E+00	1.273	1.3
2.00E+00	1.289	1.3
2.20E+00	1.280	1.3
2.40E+00	1.266	1.3
2.60E+00	1.257	1.3
2.80E+00	1.240	1.3
3.00E+00	1.217	1.3
3.60E+00	1.165	1.3
4.00E+00	1.137	1.3
4.50E+00	1.118	1.3
4.70E+00	1.101	1.3
5.00E+00	1.073	1.3
5.30E+00	1.057	1.3
5.50E+00	1.038	1.3
5.80E+00	1.039	1.4
6.00E+00	1.092	1.4
6.20E+00	1.180	1.4
6.50E+00	1.334	1.4
7.00E+00	1.543	1.4
7.50E+00	1.701	1.4
7.75E+00	1.738	1.4
8.00E+00	1.785	1.4
8.50E+00	1.793	1.4
9.00E+00	1.779	1.4
1.00E+01	1.759	1.4
1.10E+01	1.736	1.4
1.15E+01	1.704	1.5
1.20E+01	1.721	1.4
1.30E+01	1.886	1.4
1.40E+01	2.079	1.3
1.45E+01	2.090	1.3
1.50E+01	2.126	1.4
1.60E+01	2.154	1.4
1.70E+01	2.098	1.5
1.80E+01	2.059	1.5
1.90E+01	2.032	1.4
2.00E+01	2.022	1.5

TABLE XVI. ^{235}U(n,f) cross sections (continued). This is the GMAP output of point-wise cross sections. E_n is the incident neutron energy that corresponds to the GMA node. CS is the cross section. ΔCS is the cross section uncertainty. All intervals are located half-way between given GMA nodes. Linear interpolation between GMA nodes is recommended. These data include a 1.2 % unrecognized systematic uncertainty. These data are recommended to be used as standards for measurements from 20 MeV to 200 MeV. Data followed by "*" are smoothed values.

Recommended point-wise data		
E_n, MeV	CS, b	ΔCS, %
2.00E+01	2.022	1.5
2.10E+01	2.088	1.6
2.20E+01	2.115	2.0
2.30E+01	2.145	1.7
2.40E+01	2.089	1.8
2.50E+01	2.127	1.6
2.60E+01	2.128	1.9
2.70E+01	2.108	1.8
2.80E+01	2.135	2.0
2.90E+01	2.105	1.8
3.00E+01	2.155	1.8
3.20E+01	2.139	2.2
3.40E+01	2.118	2.2
3.60E+01	2.035	2.3
3.80E+01	1.979	2.5
4.00E+01	1.997	2.5
4.20E+01	1.975	2.3
4.40E+01	1.965	2.4
4.60E+01	1.951	2.3
4.80E+01	1.921	2.6
5.00E+01	1.900	2.7
5.20E+01	1.906	3.0
5.40E+01	1.869	3.0
5.60E+01	1.891	3.0
5.80E+01	1.873	2.8
6.00E+01	1.850	2.7

Recommended point-wise data		
E_n, MeV	CS, b	ΔCS, %
6.40E+01	1.835	2.4
6.80E+01	1.770	2.4
7.20E+01	1.730	2.6
7.60E+01	1.741	2.7
8.00E+01	1.707	2.9
8.40E+01	1.700	3.6
8.80E+01	1.634	3.7
9.20E+01	1.595	3.8
9.60E+01	1.578*	3.7
1.00E+02	1.561*	3.8
1.04E+02	1.543*	3.7
1.08E+02	1.541*	4.8
1.12E+02	1.534*	4.6
1.16E+02	1.518*	4.6
1.20E+02	1.499*	4.6
1.28E+02	1.479	4.4
1.36E+02	1.468	4.3
1.44E+02	1.442	4.0
1.52E+02	1.467	4.3
1.60E+02	1.447	4.4
1.68E+02	1.439	4.7
1.76E+02	1.457	4.6
1.84E+02	1.455	4.8
1.92E+02	1.443	4.5
2.00E+02	1.449	4.5

TABLE XVII. C(n,n) cross section data. CS is the cross section. ΔCS is the cross section uncertainty. E_n is the incident neutron energy. The 0.65 % unrecognized systematic uncertainty is included in the uncertainties in the table. Linear interpolation between energies is recommended. It is a standard from 1 keV to 1.8 MeV.

Recommended point-wise data		
E_n, MeV	CS, b	ΔCS, %
1.00E-11	4.758	0.71
1.00E-09	4.759	0.71
2.53E-08	4.759	0.71
1.00E-07	4.759	0.71
1.00E-05	4.759	0.71
1.00E-03	4.755	0.71
5.00E-03	4.742	0.71
1.00E-02	4.726	0.70
2.00E-02	4.692	0.70
5.00E-02	4.595	0.70
1.00E-01	4.439	0.70
1.50E-01	4.304	0.70
2.00E-01	4.149	0.69
2.50E-01	4.014	0.69
3.00E-01	3.886	0.69
3.50E-01	3.765	0.69
4.00E-01	3.649	0.69
4.50E-01	3.538	0.69
5.00E-01	3.433	0.68

Recommended point-wise data		
E_n, MeV	CS, b	ΔCS, %
5.50E-01	3.333	0.68
6.00E-01	3.237	0.68
6.50E-01	3.146	0.68
7.00E-01	3.058	0.68
7.50E-01	2.974	0.68
8.00E-01	2.894	0.68
8.50E-01	2.818	0.68
9.00E-01	2.744	0.68
9.50E-01	2.674	0.68
1.00E+00	2.606	0.68
1.10E+00	2.479	0.68
1.20E+00	2.362	0.68
1.30E+00	2.254	0.68
1.40E+00	2.154	0.68
1.50E+00	2.062	0.69
1.60E+00	1.977	0.69
1.70E+00	1.899	0.69
1.80E+00	1.830	0.69

TABLE XVIII. ^{238}U(n,γ) cross section. This is the GMAP output of point-wise cross sections. E_n is the incident neutron energy that corresponds to the GMA node. The energy interval for the point at 0.15 keV starts at 0.1 keV. From there on, all intervals are located half-way between GMA nodes. CS is the cross section. ΔCS is the cross section uncertainty. Linear interpolation between GMA nodes is recommended above the thermal energy (0.0253 eV). Data followed by "*"are smoothed values. These data include a 1.7 % unrecognized systematic uncertainty below 1 MeV and 2.4 % at 1 MeV and above.

Recommended point-wise data		
E_n, MeV	CS, b	ΔCS, %
2.53E-08	2.678	0.59
1.50E-04	16.543	1.8
2.50E-04	8.544	2.1
3.50E-04	2.926	2.4
4.50E-04	2.704	1.9
5.50E-04	4.702	3.0
6.50E-04	3.512	2.6
7.50E-04	1.775	2.5
8.50E-04	2.892	1.9
9.50E-04	4.061	2.4
1.50E-03	1.877	2.1
2.50E-03	1.399	2.1
3.50E-03	1.157	2.0
4.50E-03	0.901	1.9
5.50E-03	0.890	2.0
6.50E-03	0.843	2.0
7.50E-03	0.747	2.0
8.50E-03	0.644	1.9
9.50E-03	0.684	2.0
1.50E-02	0.591	1.9
2.00E-02	0.530	1.9
2.40E-02	0.472	1.9
3.00E-02	0.434	1.9
4.50E-02	0.357	1.9
5.50E-02	0.290	1.9
6.50E-02	0.245	1.9
7.50E-02	0.211	1.9
8.50E-02	0.188	2.0
9.50E-02	0.182	2.1
1.00E-01	0.179	2.2
1.20E-01	0.164	2.1
1.50E-01	0.141	2.0
1.70E-01	0.139	2.2
1.80E-01	0.129*	3.6
1.90E-01	0.127*	2.5
2.00E-01	0.129*	2.3
2.10E-01	0.130*	2.6
2.20E-01	0.126*	2.6

Recommended point-wise data		
E_n, MeV	CS, b	ΔCS, %
2.30E-01	0.123*	2.3
2.35E-01	0.121*	3.1
2.40E-01	0.118*	2.9
2.45E-01	0.116*	2.5
2.50E-01	0.116*	2.8
2.60E-01	0.115*	2.3
2.70E-01	0.115*	2.9
2.80E-01	0.115*	2.5
3.00E-01	0.115*	2.3
3.25E-01	0.113*	2.8
3.50E-01	0.109*	2.4
3.75E-01	0.107*	2.4
4.00E-01	0.106*	2.1
4.25E-01	0.106*	3.3
4.50E-01	0.106*	2.4
4.75E-01	0.106*	5.4
5.00E-01	0.108*	2.1
5.20E-01	0.108*	2.5
5.40E-01	0.109*	2.4
5.70E-01	0.114*	2.3
6.00E-01	0.113*	2.1
6.50E-01	0.113*	3.3
7.00E-01	0.118*	2.5
7.50E-01	0.118*	3.2
8.00E-01	0.119*	2.2
8.50E-01	0.124*	5.1
9.00E-01	0.126*	2.8
9.40E-01	0.129*	2.8
9.60E-01	0.135	2.7
1.00E+00	0.128	2.7
1.10E+00	0.113*	3.2
1.25E+00	0.0943*	3.1
1.40E+00	0.0802*	3.3
1.60E+00	0.0669*	3.2
1.80E+00	0.0568*	3.9
2.00E+00	0.0478*	3.7
2.20E+00	0.0385	3.8

TABLE XIX. ^{238}U(n,f) cross section. This is the GMAP output of point-wise cross sections. E_n is the incident neutron energy that corresponds to the GMA node. CS is the cross section. ΔCS is the cross section uncertainty. All intervals are located half-way between given GMA nodes. Linear interpolation between GMA nodes is recommended. There is a denser grid below 2 MeV. Those nodes are marked by "x". A corrected node in that denser region is marked by "xx". These data include a 1.2 % unrecognized systematic uncertainty. These data are recommended to be used as standards for measurements from 2 MeV to 32 MeV.

Recommended point-wise data		
E_n, MeV	CS, b	ΔCS, %
5.00E-01	2.78E-04	7.7
5.20E-01	6.58E-04	22
5.40E-01	6.17E-04	4.0
5.70E-01	6.80E-04	4.0
6.00E-01	1.20E-03	3.5
6.50E-01	1.33E-03	2.6
7.00E-01	1.90E-03	2.7
7.50E-01	2.71E-03	2.2
8.00E-01	4.67E-03	2.0
8.50E-01	6.95E-03	1.8
9.00E-01	1.42E-02	1.6
9.40E-01	1.73E-02	1.6
9.60E-01	1.59E-02	1.9
9.80E-01	1.63E-02	1.7
1.00E+00	1.46E-02	1.5
1.01E+00	1.75E-02x	1.5
1.01E+00	1.74E-02x	1.5
1.02E+00	1.63E-02x	1.5
1.04E+00	1.75E-02x	1.5
1.05E+00	2.09E-02x	1.5
1.06E+00	2.30E-02x	1.4
1.08E+00	2.59E-02x	1.4
1.09E+00	2.94E-02x	1.4
1.10E+00	3.10E-02x	1.5
1.11E+00	3.23E-02x	1.4
1.12E+00	3.58E-02x	1.4
1.14E+00	3.60E-02x	1.4
1.15E+00	4.18E-02x	1.4
1.17E+00	4.38E-02x	1.4
1.19E+00	4.33E-02x	1.4
1.20E+00	4.28E-02x	1.4
1.22E+00	4.10E-02x	1.4
1.24E+00	4.25E-02x	1.4
1.25E+00	4.43E-02xx	1.4
1.27E+00	5.82E-02x	1.4
1.29E+00	6.85E-02x	1.4
1.31E+00	8.23E-02x	1.4
1.33E+00	9.91E-02x	1.4
1.35E+00	0.119x	1.4
1.37E+00	0.150x	1.4
1.39E+00	0.191x	1.4
1.40E+00	0.194x	1.4
1.42E+00	0.225x	1.4
1.44E+00	0.277x	1.4
1.46E+00	0.317x	1.4
1.48E+00	0.347x	1.4
1.51E+00	0.364x	1.3
1.53E+00	0.380x	1.3
1.56E+00	0.390x	1.3
1.58E+00	0.409x	1.3
1.60E+00	0.426x	1.3
1.61E+00	0.425x	1.3
1.63E+00	0.430x	1.3
1.66E+00	0.436x	1.3
1.69E+00	0.448x	1.3
1.72E+00	0.469x	1.3

Recommended point-wise data		
E_n, MeV	CS, b	ΔCS, %
1.75E+00	0.482x	1.3
1.78E+00	0.492x	1.3
1.80E+00	0.489x	1.3
1.81E+00	0.502x	1.3
1.84E+00	0.519x	1.3
1.87E+00	0.520x	1.3
1.91E+00	0.539x	1.3
1.94E+00	0.539x	1.3
1.98E+00	0.541x	1.3
2.00E+00	0.538	1.3
2.20E+00	0.550	1.3
2.40E+00	0.547	1.3
2.60E+00	0.543	1.3
2.80E+00	0.539	1.4
3.00E+00	0.526	1.3
3.60E+00	0.550	1.3
4.00E+00	0.558	1.3
4.50E+00	0.563	1.4
4.70E+00	0.561	1.4
5.00E+00	0.549	1.4
5.30E+00	0.551	1.4
5.50E+00	0.548	1.4
5.80E+00	0.567	1.4
6.00E+00	0.611	1.4
6.20E+00	0.682	1.5
6.50E+00	0.818	1.4
7.00E+00	0.944	1.4
7.50E+00	0.994	1.4
7.75E+00	0.996	1.5
8.00E+00	1.017	1.4
8.50E+00	1.015	1.4
9.00E+00	1.017	1.4
1.00E+01	1.010	1.5
1.10E+01	1.009	1.5
1.15E+01	1.005	1.5
1.20E+01	0.988	1.5
1.30E+01	1.025	1.4
1.40E+01	1.151	1.3
1.45E+01	1.190	1.3
1.50E+01	1.242	1.4
1.60E+01	1.315	1.5
1.70E+01	1.320	1.5
1.80E+01	1.320	1.5
1.90E+01	1.357	1.5
2.00E+01	1.406	1.6
2.10E+01	1.518	1.6
2.20E+01	1.558	2.1
2.30E+01	1.599	1.8
2.40E+01	1.545	1.9
2.50E+01	1.577	1.7
2.60E+01	1.576	2.0
2.70E+01	1.563	1.8
2.80E+01	1.615	2.1
2.90E+01	1.604	1.8
3.00E+01	1.667	1.9
3.20E+01	1.684	2.2

TABLE XIX. ^{238}U(n,f) cross section (continued). This is the GMAP output of point-wise cross sections. E_n is the incident neutron energy that corresponds to the GMA node. CS is the cross section. ΔCS is the cross section uncertainty. All intervals are located half-way between given GMA nodes. Linear interpolation between GMA nodes is recommended. These data include a 1.2 % unrecognized systematic uncertainty. Data followed by "*" are smoothed values. These data are recommended to be used as standards for measurements from 32 MeV to 200 MeV.

Recommended point-wise data		
E_n, MeV	CS, b	ΔCS, %
3.20E+01	1.684	2.2
3.40E+01	1.689	2.2
3.60E+01	1.652	2.4
3.80E+01	1.635	2.5
4.00E+01	1.663	2.5
4.20E+01	1.654	2.4
4.40E+01	1.643	2.5
4.60E+01	1.656	2.3
4.80E+01	1.637	2.7
5.00E+01	1.631	2.7
5.20E+01	1.634	3.0
5.40E+01	1.613	3.0
5.60E+01	1.632	3.0
5.80E+01	1.626	2.8
6.00E+01	1.604	2.7
6.40E+01	1.589	2.4
6.80E+01	1.529	2.5
7.20E+01	1.504	2.6
7.60E+01	1.531	2.7
8.00E+01	1.507	2.9

Recommended point-wise data		
E_n, MeV	CS, b	ΔCS, %
8.40E+01	1.496	3.7
8.80E+01	1.438	3.7
9.20E+01	1.403	3.8
9.60E+01	1.389*	3.8
1.00E+02	1.383*	3.8
1.04E+02	1.379*	3.8
1.08E+02	1.375*	4.8
1.12E+02	1.361*	4.6
1.16E+02	1.348*	4.6
1.20E+02	1.340*	4.6
1.28E+02	1.324	4.4
1.36E+02	1.308	4.3
1.44E+02	1.287	4.1
1.52E+02	1.311	4.4
1.60E+02	1.305	4.4
1.68E+02	1.282	4.7
1.76E+02	1.325	4.6
1.84E+02	1.328	4.9
1.92E+02	1.311	4.5
2.00E+02	1.319	4.4

TABLE XX. ^{239}Pu(n,f) cross section. This is GMAP output of point-wise cross sections. E_n is the incident neutron energy that corresponds to the GMA node. CS is the cross section. ΔCS is the cross section uncertainty. Linear interpolation between GMA nodes is recommended above 0.0253 eV. Interval corresponding to the node at 0.15 keV starts at 0.1 keV. From there on, all intervals are located half-way between give GMA nodes. These data include a 1.2 % unrecognized systematic uncertainty.

Recommended point-wise data		
E_n, MeV	CS, b	ΔCS, %
2.53E-08	752.371	0.29
1.50E-04	18.805	1.3
2.50E-04	18.060	1.3
3.50E-04	8.594	1.3
4.50E-04	9.623	1.3
5.50E-04	15.622	1.3
6.50E-04	4.547	1.4
7.50E-04	5.698	1.4
8.50E-04	5.063	1.3
9.50E-04	8.426	1.3
1.50E-03	4.528	1.4
2.50E-03	3.314	1.4
3.50E-03	3.019	1.4
4.50E-03	2.390	1.4
5.50E-03	2.307	1.4
6.50E-03	2.037	1.4
7.50E-03	2.116	1.4
8.50E-03	2.227	1.4
9.50E-03	1.871	1.4
1.50E-02	1.788	1.4
2.00E-02	1.743	1.9
2.40E-02	1.639	1.4
3.00E-02	1.641	1.4
4.50E-02	1.534	1.4
5.50E-02	1.554	1.4
6.50E-02	1.569	1.4

Recommended point-wise data		
E_n, MeV	CS, b	ΔCS, %
7.50E-02	1.563	1.4
8.50E-02	1.515	1.4
9.50E-02	1.546	1.5
1.00E-01	1.557	1.5
1.20E-01	1.514	1.4
1.50E-01	1.508	1.4
1.70E-01	1.503	1.5
1.80E-01	1.496	1.7
1.90E-01	1.466	1.6
2.00E-01	1.486	1.6
2.10E-01	1.541	1.6
2.20E-01	1.504	1.5
2.30E-01	1.520	1.5
2.40E-01	1.477	1.7
2.45E-01	1.498	1.5
2.50E-01	1.508	1.6
2.60E-01	1.513	1.6
2.70E-01	1.513	1.5
2.80E-01	1.560	1.5
3.00E-01	1.532	1.4
3.25E-01	1.546	1.5
3.50E-01	1.530	1.4
3.75E-01	1.556	1.5
4.00E-01	1.560	1.4
4.25E-01	1.558	1.6
4.50E-01	1.579	1.5

TABLE XX. ^{239}Pu(n,f) cross section (continued). This is the GMAP output of point-wise cross sections. E_n is the incident neutron energy that corresponds to the GMA node. CS is the cross section. ΔCS is the cross section uncertainty. Linear interpolation between GMA nodes is recommended. These data include a 1.2 % unrecognized systematic uncertainty.

Recommended point-wise data		
E_n, MeV	CS, b	ΔCS, %
4.50E-01	1.579	1.5
4.75E-01	1.572	1.5
5.00E-01	1.573	1.4
5.20E-01	1.573	1.5
5.40E-01	1.572	1.4
5.70E-01	1.589	1.5
6.00E-01	1.595	1.4
6.50E-01	1.624	1.4
7.00E-01	1.636	1.4
7.50E-01	1.700	1.4
8.00E-01	1.705	1.4
8.50E-01	1.699	1.4
9.00E-01	1.680	1.4
9.40E-01	1.687	1.4
9.60E-01	1.723	1.4
9.80E-01	1.723	1.4
1.00E+00	1.735	1.3
1.10E+00	1.747	1.3
1.25E+00	1.848	1.3
1.40E+00	1.924	1.3
1.60E+00	1.948	1.3
1.80E+00	1.951	1.3
2.00E+00	1.978	1.3
2.20E+00	1.963	1.3
2.40E+00	1.924	1.3
2.60E+00	1.906	1.3
2.80E+00	1.889	1.4
3.00E+00	1.856	1.3
3.60E+00	1.809	1.3
4.00E+00	1.769	1.3
4.50E+00	1.742	1.3
4.70E+00	1.726	1.3
5.00E+00	1.690	1.3
5.30E+00	1.682	1.4
5.50E+00	1.662	1.4
5.80E+00	1.688	1.4
6.00E+00	1.770	1.4
6.20E+00	1.841	1.4
6.50E+00	1.931	1.4
7.00E+00	2.061	1.4
7.50E+00	2.189	1.4
7.75E+00	2.225	1.5
8.00E+00	2.280	1.4
8.50E+00	2.259	1.4
9.00E+00	2.255	1.4
1.00E+01	2.249	1.5
1.10E+01	2.243	1.5
1.15E+01	2.226	1.5
1.20E+01	2.239	1.5
1.30E+01	2.331	1.4
1.40E+01	2.404	1.4
1.45E+01	2.419	1.3
1.50E+01	2.416	1.4
1.60E+01	2.444	1.5

Recommended point-wise data		
E_n, MeV	CS, b	ΔCS, %
1.70E+01	2.365	1.5
1.80E+01	2.341	1.5
2.00E+01	2.357	1.6
2.10E+01	2.366	1.6
2.20E+01	2.376	2.1
2.30E+01	2.377	1.8
2.40E+01	2.311	2.0
2.50E+01	2.351	1.8
2.60E+01	2.337	2.0
2.70E+01	2.331	1.9
2.80E+01	2.359	2.1
2.90E+01	2.307	1.9
3.00E+01	2.368	1.9
3.20E+01	2.331	2.2
3.40E+01	2.302	2.2
3.60E+01	2.223	2.4
3.80E+01	2.154	2.5
4.00E+01	2.186	2.6
4.20E+01	2.140	2.4
4.40E+01	2.142	2.5
4.60E+01	2.130	2.4
4.80E+01	2.097	2.7
5.00E+01	2.072	2.8
5.20E+01	2.076	3.0
5.40E+01	2.049	3.0
5.60E+01	2.078	3.0
5.80E+01	2.052	2.8
6.00E+01	2.028	2.7
6.40E+01	2.004	2.5
6.80E+01	1.943	2.5
7.20E+01	1.901	2.7
7.60E+01	1.890	2.8
8.00E+01	1.862	3.0
8.40E+01	1.854	3.7
8.80E+01	1.776	3.8
9.20E+01	1.728	3.9
9.60E+01	1.711*	3.9
1.00E+02	1.690*	3.8
1.04E+02	1.668*	3.8
1.08E+02	1.667*	4.8
1.12E+02	1.664*	4.7
1.16E+02	1.645*	4.7
1.20E+02	1.621*	4.6
1.28E+02	1.599	4.5
1.36E+02	1.564	4.4
1.44E+02	1.540	4.1
1.52E+02	1.585	4.4
1.60E+02	1.537	4.5
1.68E+02	1.536	4.8
1.76E+02	1.561	4.6
1.84E+02	1.551	4.9
1.92E+02	1.523	4.6
2.00E+02	1.540	4.6

A. Correlations in Neutron Standards

In Figs. 38–40 correlation matrices and relative uncertainties are shown for the uranium cross sections that were obtained in the 2017 standards evaluation effort from the fit of microscopic data as plotted by NJOY. These figures do not include the unrecognized systematic uncertainty. Including that uncertainty produces covariance matrices that are fully correlated almost everywhere.

Note that the GMA fit extensively used absolute and shape ratio data (*e.g.*, ^{238}U(n,γ)/Au(n,γ) cross section ratio in Fig. 35(a) and ^{238}U(n,f)/^{235}U(n,f) cross section ratio in Figs. 35(b) and 36(e,f)). Such microscopic ratio measurements lead to cross-reaction and cross-isotope correlations that are also derived from the fit. Covariance matrices including cross-reaction and cross-isotope correlations will be available at the IAEA website https://www-nds.iaea.org/standards/. For numerical applications full accuracy seven digit covariance matrices are needed.

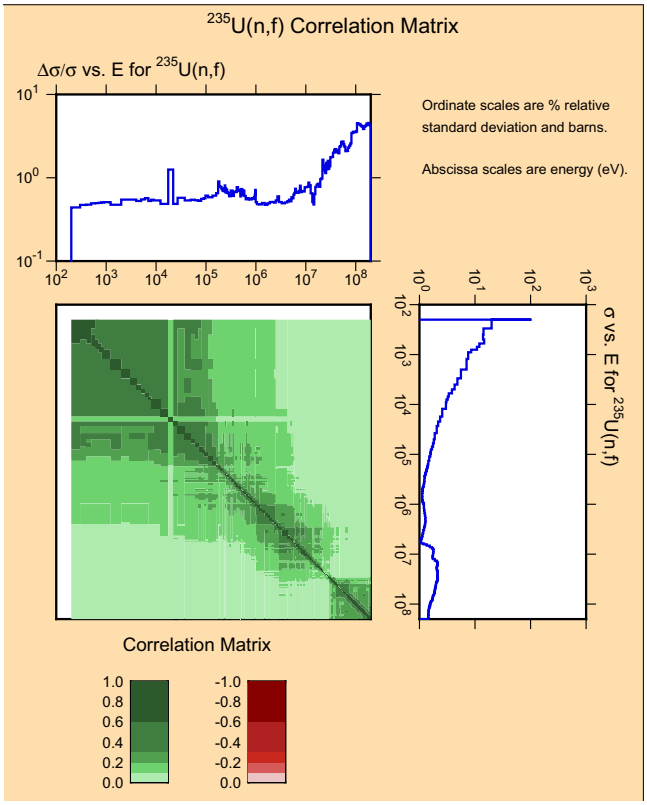

FIG. 38. (Color online) Correlation matrix and relative uncertainties for the ^{235}U(n,f) cross section.

B. Comparison with High-resolution Experimental Data and Data Normalization (Renormalization) to the Standards

To compare standards and experimental data, or for normalization of experimental data measured relative to a standard, experimental data should be reduced to the

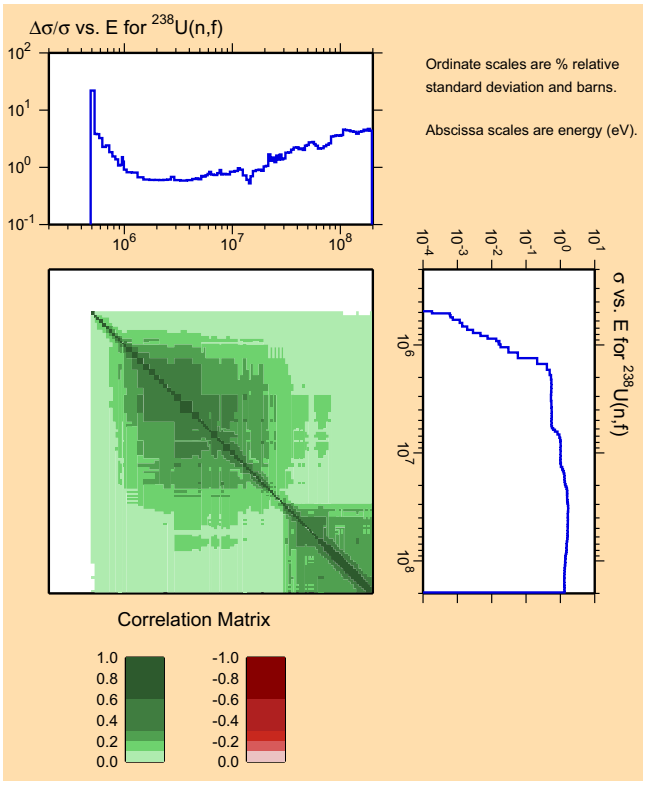

FIG. 39. (Color online) Correlation matrix and relative uncertainties for the ^{238}U(n,f) cross section.

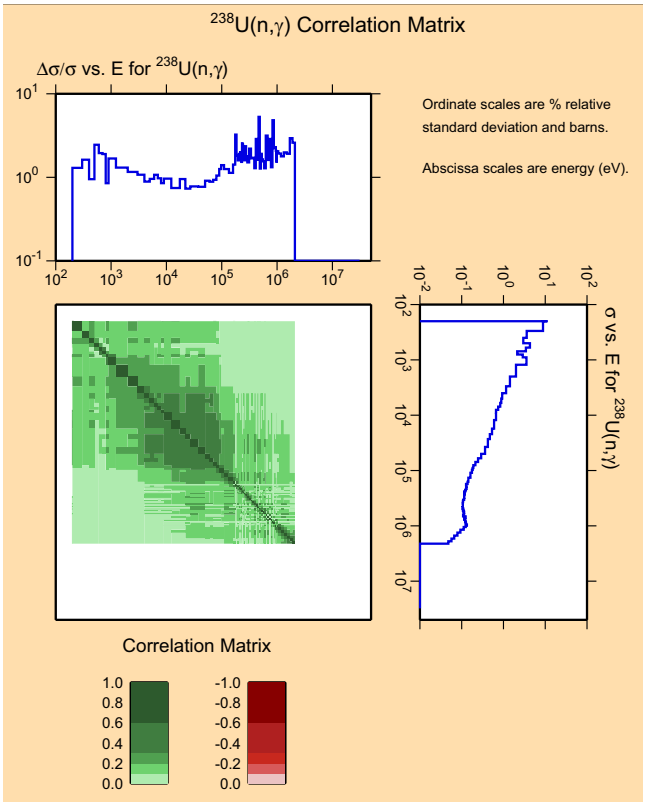

FIG. 40. (Color online) Correlation matrix and relative uncertainties for the ^{238}U(n,γ) cross section.

same resolution as the standard cross section (to the same nodes as in the standards). The best way to do this is to use the DAT code (an auxiliary code of GMA) for data reduction to the nodes. It reduces the experimental data to the nodes by interpolating according to the shape of a priori data for the full energy range of the data.

An alternative way for normalization (renormalization) of high-resolution data to the standards is to use the ratio of simple arithmetical group averaged values obtained for the bins between the GMA nodes for experimental data and the same for standards with required interpolation (for the standards - lin-lin interpolation for all cross sections above 30 keV and log-log interpolation for cross sections having 1/v energy dependence below 30 keV). For comparison of the group averaged values around the nodes, the averaging of the high-resolution experimental data and standard data can be done using midpoints between the nodes. For standard data these group averaged standard values can be different from the values evaluated in the nodes. The use of narrower bins, than those determined by the GMA nodes, in the comparison of the experimental cross sections with the standard, will lead to the comparison of data having different resolution.

C. Use of High-resolution Data in the GMA Fit

The boundaries for interpolation of experimental data to the nodes (determining the bin size) are the mid-points between the nodes. Lin-lin interpolation or log-log interpolation laws below 30 keV are used depending on the type of data. Above 30 keV, only lin-lin interpolation is used. It is not advisable to use data in GMAP which have a resolution larger than the typical bin-width in the energy region of the data. For example measurements with a lead slowing down spectrometer or with relatively broad energy spectra should not be used.

The results of the GMA fit are point-wise functions corresponding to the values in the nodes with the interpolation scheme determined in the data reduction. This is different from the statements given in the publications describing the 2006 Standards, where data for heavy nuclides below 20 keV were considered as group-wise at the mid-points of the energy interval. This last interpretation is wrong. High-resolution TOF experiments were not used in the GMA fit directly, but they can be used, if the number of points is not extremely large (*e.g.*, less than 200 per bin). In the region where the nodes have nearly the same width, the data averaged in the bin will be rather close to the data reduced to the node, if a prior data has its dependence close to linear inside the bin and the points averaged inside the bin are about equidistant. High-resolution data, obtained in TOF measurements, have channels varying in energy as $E^{3/2}$. Then, it will be advisable to average them in equal micro-bins with a number, say less than 100 per any GMA bin. During this averaging, as well as in the DAT data reduction procedure, the statistical components of uncertainties given at the points decrease according to the statistical law and systematic components are averaged over the points.

VI. CONCLUSION AND OUTLOOK

Results have been obtained for the nuclear data standards in this investigation. Concerns about the rather small uncertainties obtained for the standards in previous evaluations, led us to investigate one aspect of unknown systematic uncertainties. We realize that in some cases our previous uncertainties had been underestimated. The larger uncertainties now obtained result from unknown systematic uncertainties based on the spread in normalization factors of absolute measurements for each cross section type. Also improved determinations of the uncertainties obtained from R-matrix analyses were obtained using Parameter Confidence Intervals. Though there may also be unknown systematic uncertainties associated with the use of a certain type of detector (*i.e.*, fission chambers), technique, accelerator, etc. It is not clear how to determine those quantities. The GMAP code is capable of handling all uncertainties and the correlations between different experiments. In that respect we believe our evaluation methodology is accurate.

The IAEA with collaborative efforts will continue to maintain this evaluation project on the standards and important reference data.

ACKNOWLEDGMENTS

We greatly acknowledge support of this work by the IAEA Nuclear Data Section and the U.S. Department of Energy. We very much appreciate discussions with a number of colleagues on the measurements and analyses.

[1] A.D. Carlson, V.G. Pronyaev, D.L. Smith, N.M. Larson, Zhenpeng Chen, G.M. Hale, F.-J. Hambsch, E.V. Gai, Soo-Youl Oh, S.A. Badikov, T. Kawano, H.M. Hofmann, H. Vonach, S. Tagesen, "International Evaluation of Neutron Cross Section Standards," Nucl. Data Sheets **110**, 3215–3324 (2009).

[2] M.B. Chadwick, P. Obložinský, M. Herman *et al.*, "ENDF/B-VII.0: Next Generation Nuclear Data Library for Nuclear Science and Technology," Nucl. Data Sheets **107**, 2931–3060 (2006).

[3] M.B. Chadwick, M. Herman, P. Obložinský *et al.*, "ENDF/B-VII.1 Nuclear Data for Science and Technology: Cross Sections, Covariances, Fission Product Yields and

Decay Data," Nucl. Data Sheets **112**, 2887–2996 (2011).
[4] D.A. Brown, M.B. Chadwick, R. Capote *et al.*, "ENDF/B-VIII.0: The 8th Major Release of the Nuclear Reaction Data Library with CIELO-project Cross Sections, New Standards and Thermal Scattering Data," Nucl. Data Sheets **148**, 1 (2018).
[5] R.W. Peelle, "Peelle's Pertinent Puzzle," Memorandum dated 13 October 1987, Oak Ridge National Laboratory, TN, USA.
[6] D.L. Smith, "Probability, Statistics, and Data Uncertainties in Nuclear Science and Technology," American Nuclear Society, LaGrange Park, IL, USA (1991).
[7] W.P. Poenitz, "Data interpretation, objective evaluation procedures and mathematical techniques for the evaluation of energy-dependent ratio shape and cross section data,"Report **BNL-NCS-51363**, Vol. 1, p.249 (BNL, Brookhaven 1981).
[8] W.P. Poenitz, S.E. Aumeier, "The simultaneous evaluation of the standards and other cross sections of importance for technology,"Report **ANL/NDM-139** (ANL, Argonne 1997).
[9] R. Moreh, R.C. Block, Y. Danon, "Search for Anomalous n-p Scattering at 60 eV–140 keV," Proc. 13th Int. Conf. on Capture Gamma-Ray Spectroscopy and Related Topics (Cologne, Germany, 25–29 August 2008), AIP, Melville, NY, p.102 (2009).
[10] C. A. Chatzidimitriou-Dreismann, T. Abdul-Redah, M. Krzystyniak, "Anomalous neutron Compton scattering from molecular hydrogen," Phys. Rev. **B72**, 054123 (2005).
[11] B.H. Daub, V. Henzl, M.A. Kovash *et al.*, "Measurements of the neutron-proton and neutron-carbon total cross section from 150 to 800 keV," Phys. Rev. **C87**, 014005 (2013).
[12] H. Yang, Private communication (2016).
[13] N. Boukharouba, F.B. Bateman, A.D. Carlson *et al.*, "Measurement of the n-p Elastic Scattering Angular Distribution at E_n = 14.9 MeV," Phys. Rev. **C82**, 014001 (2010).
[14] N. Boukharouba, F.B. Bateman, C.E. Brient *et al.*, "Measurement of the n-p elastic scattering angular distribution at E_n=10 MeV," Phys. Rev. **C82**, 039901 (2010).
[15] K. Kondo *et al.*, "Charged-particle spectrometry using a pencil-beam DT neutron source for double-differential cross section measurement," Nucl. Inst. Meth. Phys. Res. **A568**, 723–733 (2006).
[16] M. Sarsour *et al.*, "Measurement of the absolute differential cross section for np elastic scattering at 194 MeV," Phys. Rev. **C74**, 044003 (2006).
[17] J. Rahm *et al.*, "np scattering measurements at 162 MeV and the πNN coupling constant," Phys. Rev. **C57**, 1077 (1998).
[18] G. Zhang *et al.*, "Measurement of differential and angle-integrated cross sections of the ^{6}Li(n,t)^{4}He reaction in the MeV neutron energy range," Nucl. Instr. Meth. Phys. Res. **A566**, 615–621 (2006).
[19] M. Devlin *et al.*, "Differential Cross Section Measurements for the ^{6}Li(n,t)alpha Reaction in the Few MeV Region," Proc. 13th Int. Conf. on Capture Gamma-Ray Spectroscopy and Related Topics (Cologne, Germany, 25–29 August 2008), AIP, Melville, NY, p.215 (2009).
[20] A. Yue, Private communication (2017).
[21] G. Giorginis, Private communication (2014).
[22] O.A. Wasson, A.D. Carlson, R.A. Schrack, "Total Neutron Cross Section Measurements of ^{10}B and ^{11}B," Proc. Int. Conf. on Nucl. Data for Sci. & Tech., Gatlinburg, TN, USA, ISBN 0-89448-194-0543 **Vol. 1**, p.50 (1994).
[23] A. Brusegan *et al.*, "The Total Neutron Cross Section of ^{10}B from 80 eV to 100 keV and from 1.5 to 1.8 MeV," Proc. Int. Conf. on Nucl. Data for Sci. & Tech., Gatlinburg, TN, USA, ISBN 0-89448-194-0543 **Vol. 1**, p.47 (1994).
[24] R. Bevilacqua *et al.*, "^{10}B and ^{6}Li Nuclear Data Measurements for Incident Neutron Energies up to 3 MeV," Nucl. Data Sheets **119**, 104–106 (2014).
[25] G. Zhang *et al.*, "Cross-section measurements for the ^{10}B(n,α)^{7}Li reaction at 4.0 and 5.0 MeV," Appl. Radiat. Isot. **66**, 1427–1430 (2008).
[26] G. Giorginis, V. Khriatchkov, "The effect of particle leaking and its implications for measurements of the (n,α) reaction on light elements by using ionisation chambers," Nucl. Instr. Meth. Phys. Res. **553**, 550–558 (2005).
[27] O. Gritzay *et al.*, "The total neutron cross section for natural carbon in the energy range 2 to 148 keV,"Proc. Int. Conf. on Nucl. Data for Sci. Tech. (April 22-27, 2007, Nice, France), eds. O. Bersillon, F. Gunsing, E. Bauge, R. Jacqmin, and S. Leray, EDP Sciences, 543–546 (2008).
[28] L. Canton *et al.*, "Particle-unstable light nuclei with a Sturmian approach that preserves the Pauli principle," Nucl. Phys. **A790**, 251–256 (2007).
[29] O. Gritzay *et al.*, "The Measurements of the Differential Elastic Cross Sections of Carbon for Energies from 2 to 133 keV," Proc. 13th Int. Symp. on Reactor Dosimetry (Akersloot, The Netherlands, 25-30 May 2008), 525–531 (2008).
[30] Y. Danon *et al.*, "High-accuracy filtered neutron beam and high-energy transmission measurements at the Gaerttner Laboratory," in Proc. Int. Conf. on Nucl. Data for Sci. Tech. (April 22-27, 2007, Nice, France), eds. O.Bersillon, F.Gunsing, E.Bauge, R.Jacqmin, and S.Leray, EDP Sciences, 401–402 (2008).
[31] A. Wallner, T. Belgya, M. Bichler *et al.*, "Novel Method to study Neutron Capture of ^{235}U and ^{238}U Simultaneously at keV Energies," Phys. Rev. Lett. **112**, 192501 (2014).
[32] C. Massimi *et al.* (the n_TOF Collaboration), "The ^{197}Au(n,γ) cross section in the resonance region," Phys. Rev. **C81**, 044616 (2010).
[33] C. Lederer *et al.*, "The ^{197}Au(n,γ) cross section in the unresolved resonance region," Phys. Rev. **C83**, 034608 (2011).
[34] J.L. Ullmann *et al.*, "Cross section and γ-ray spectra for ^{238}U(n,γ) measured with the DANCE detector array at the Los Alamos Neutron Science Center," Phys. Rev. **C89**, 034603 (2014).
[35] H.I. Kim *et al.*, "Neutron capture cross section measurements for ^{238}U in the resonance region at GELINA," Eur. Phys. J. **A52**, 170 (2016).
[36] F. Mingrone *et al.*, "Measurement of the ^{238}U Radiative Capture Cross Section with C_6D_6 at the CERN n_TOF Facility," Nucl. Data Sheets **119**, 18–21 (2014).

[37] F. Mingrone *et al.*, "Neutron capture cross section measurement of ^{238}U at the CERN n_TOF facility in the energy region from 1 eV to 700 keV," PHYS. REV. **95**, 034604 (2017).

[38] T. Wright *et al.*, "High-precision Measurement of the ^{238}U(n,γ) Cross Section with the Total Absorption Calorimeter (TAC) at n_TOF, CERN," NUCL. DATA SHEETS **119**, 26–30 (2014).

[39] W. Ratynski, F. Käppeler, "Neutron capture cross section of ^{197}Au: A standard for stellar Nucleosynthesis," PHYS. REV. **C37**, 595 (1988).

[40] C. Massimi *et al.*, "Neutron capture cross section measurements for ^{197}Au from 3.5 to 84 keV at GELINA," EUR. PHYS. J. **A50**, 124 (2014).

[41] A. Borella *et al.*, "Determination of the ^{232}Th(n,γ) Cross Section from 4 to 140 keV at GELINA," NUCL. SCI. ENG. **152**, 1–14 (2006).

[42] G. Feinberg *et al.*, "Quasi-stellar neutrons from the ^{7}Li(p,n)^{7}Be reaction with an energy-broadened proton beam," PHYS. REV. **C85**, 055810 (2012).

[43] C. Lederer *et al.* "Definition of a standard neutron field with the ^{7}Li(p,n)^{7}Be reaction," PHYS. REV. **C85**, 055809 (2012).

[44] R. Reifarth *et al.*, "PINO - a tool for simulating neutron spectra resulting from the ^{7}Li(p,n)^{7}Be reaction," NUCL. INSTR. METH. PHYS. RES. **A608**, 139–143 (2009).

[45] G. Martín Hernández, P. Mastinu, M. Maggiore *et al.*, "Excitation function shape and neutron spectrum of the ^{7}Li(p,n)^{7}Be reaction near threshold," PHYS. REV. **C94**, 034620 (2016).

[46] C. Paradela *et al.*, "High-accuracy determination of the ^{238}U/^{235}U fission cross section ratio up to $\approx$ 1 GeV at n_TOF at CERN," PHYS. REV. **91**, 024602 (2015).

[47] F. Tovesson, A. Laptev, T.S. Hill, "Fast Neutron-induced Fission Cross Sections of ^{233,234,236,238}Pu up to 200 MeV, " NUCL. SCI. ENG. **178**, 57–65 (2014).

[48] F. Tovesson, T.S. Hill, "Cross sections for ^{239,240}Pu(n,f) in the energy range E$_n$=0.01 eV–200 MeV," NUCL. SCI. ENG. **165**, 224–231 (2010).

[49] The Neutron Induced Fission Fragment Tracking Experiment collaboration, Private communication (2017).

[50] Z.W. Miller, "A Measurement of the Prompt Fission Neutron Energy Spectrum for ^{235}U(n,f) and the Neutron-induced Fission Cross Section for ^{238}U(n,f)," Ph.D. Thesis, Theses and Dissertations–Physics and Astronomy 29, University of Kentucky, Lexington (2015). Available online at https://uknowledge.uky.edu/physastron_etds/29/.

[51] D. Tarrio *et al.*, "Neutron-induced fission cross section of ^{nat}Pb and ^{209}Bi from threshold to 1 GeV: An improved parametrization," PHYS. REV. **C83**, 044620 (2011).

[52] M. Nyman, F. Belloni *et al.*, "Measurement of the 477.6-keV γ-ray production cross section following inelastic neutron scattering by ^{7}Li," PHYS. REV. **C93**, 024610 (2016); EXFOR 23288.002.

[53] R. Nelson, Private communication (2017).

[54] D. Dashdorj, G.E. Mitchell *et al.*, "Gamma-Ray Production Cross Sections in Multiple Channels for Neutron-induced Reaction on ^{48}Ti for E_n = 1 to 200 MeV," NUCL. SCI. ENG. **157**, 65–77 (2007); EXFOR 14162.002.

[55] A. Olacel, F. Belloni, C. Borcea *et al.*, "JRC data for the Ti-48 standard," JRC-Geel Report **EUR 27621 EN** (2015).

[56] N. Kornilov, "Verification of the ^{252}Cf(sf) standard in the energy range 2–20 MeV," Report **INDC(USA)-108** (IAEA, Vienna 2015).

[57] N. Kornilov, F.-J. Hambsch, I. Fabry *et al.*, "The ^{235}U(n,f) Prompt Fission Neutron Spectrum at 100K Input Neutron Energy," NUCL. SCI. ENG. **165**, 117–127 (2010).

[58] W. Mannhart, "Status of the ^{252}Cf fission-neutron spectrum evaluation with regard to recent experiments," PROC. CONSULT. MEETING ON PHYSICS OF NEUTRON EMISSION IN FISSION (Mito City, Japan, 24–27 May 1988), ed. H.D. Lemmel, p.305–336, Report **INDC(NDS)-220** (IAEA, Vienna 1989).

[59] A.S. Vorobyev, O.A. Shcherbakov, A.M. Gagarski *et al.*, "Investigation of the prompt neutron emission mechanism in low energy fission of ^{235,233}U(n$_{th}$,f) and ^{252}Cf(sf)," EPJ WEB OF CONF. **8**, 03004 (2010).

[60] B.I. Starostov, A.F. Semenov, V.N. Nefedov, "Measurement of Prompt Neutron Spectra for ^{233}U, ^{235}U and ^{239}Pu Thermal Neutron-induced Fission in the 0.01-5 MeV Energy Region and for ^{252}Cf Spontaneous Fission in the 0.01–10 MeV Region," Report **INDC(CCP)-164** (IAEA, Vienna 1981).

[61] V.N. Nefedov, B.I. Starostov, A.A. Boytsov, "Precision Measurements of ^{252}Cf, ^{233}U , ^{235}U and ^{239}Pu Prompt Fission Neutron Spectra (PFNS) in the Energy Range 0.04–5 MeV," PROC. 6-TH ALL-UNION CONF. ON NEUTRON PHYSICS (Kiev, 2–6 October 1983) Vol. 2, 285–289 (1983), in Russian); Report **INDC(CCP)-0457** (IAEA, Vienna 2014).

[62] B.I. Starostov, V.N. Nefedov, A.A. Boytsov, "Precision Measurements of ^{252}Cf, ^{233}U , ^{235}U and ^{239}Pu Prompt Fission Neutron Spectra (PFNS) in the Energy Range 2–11 MeV," PROC. 6-TH ALL-UNION CONF. ON NEUTRON PHYSICS (Kiev, 2–6 October 1983) Vol. 2, 290–293 (1983), in Russian; Report **INDC(CCP)-0458** (IAEA, Vienna 2014).

[63] A.A. Boytsov, A.F. Semenov, B.I. Starostov, "Relative Measurements of ^{233}U+n$_{th}$, ^{235}U+n$_{th}$ and ^{239}U+n$_{th}$ Prompt Fission Neutron Spectra (PFNS) in the Energy Range 0.04–5 MeV," PROC. 6-TH ALL-UNION CONF. ON NEUTRON PHYSICS (Kiev, 2–6 October 1983) Vol. 2, 294–297 (1983), in Russian; Report **INDC(CCP)-0459** (IAEA, Vienna 2014).

[64] R. Capote, Y.-J. Chen, F.-J. Hambsch *et al.*, "Prompt Fission Neutron Spectra of Actinides," NUCL. DATA SHEETS **131**, 1–106 (2016).

[65] G.M. Hale, "Use of R-Matrix Methods for Light Element Evaluations," PROC. CONF. ON NUCL. DATA EVAL. METHODS AND PROCEDURES (22–25 September 1980, New York, USA), Brookhaven National Laboratory Report **BNL-NCS-51363 Vol. 2**, p.509 (1981).

[66] Chen Zhenpeng, Sun Yeying, Zhang Rui, "Covariance Propagation in R-Matrix Model Fitting," HIGH ENERGY PHYS. AND NUCL. PHYS. **28**, 42–47 (2004).

[67] E.J. Axton, "Evaluation of the thermal constants of ^{233}U, ^{235}U, ^{239}Pu and ^{241}Pu, and the fission neutron yield of ^{252}Cf," Report **GE/PH/01/86** (Central Bureau for Nuclear Measurements, Geel 1986).

[68] E.V. Gai, "Some Algorithms for the Nuclear Data Evaluation and Construction of the Uncertainty Covariance Matrices," VOPR. ATOM. NAUKI I TECH., SER. NUCL. CONSTANTS, issue 1-2, pp. 56–65 (2007); in

Russian.
[69] E.V. Gai, A.V. Ignatyuk, "Uncertainties and Covariances of the Fission Cross Sections and the Fission Neutron Multiplicities for Actinides," Nucl. Data Sheets **109**, 2890–2893 (2008).
[70] A.I. Blokhin, E.V. Gai, A.V. Ignatyuk, I.I. Koba, V.N. Manokhin, V.G. Pronyaev, "New Version of Neutron Evaluated Data Library BROND-3," Vopr. Atom. Nauki i Tech., Ser. Nucl. Constants, issue 2, pp. 62–93 (2016); in Russian.
[71] JCGM 100, "Evaluation of measurement data: Guide to the expression of uncertainty in measurement,"BIPM publication available at https://www.bipm.org/utils/common/documents/jcgm/JCGM_100_2008_E.pdf (2008).
[72] G.M. Hale, P.G. Young, "n+^{12}C Cross Sections from an *R*-matrix Analysis of Reactions in the ^{13}C System," Nucl. Data Sheets **118**, 165–168 (2014).
[73] Y. Avni, "Energy Spectra of X-Ray Clusters of Galaxies," Ap. J. **210**, 642–646 (1976).
[74] G.M. Hale, M.W. Paris, "Data Covariances from *R*-Matrix Analyses of Light Nuclei," Nucl. Data Sheets **123**, 165–170 (2015).
[75] V.G. Pronyaev, A.D. Carlson, R. Capote Noy, Summary Report from the Technical Meeting on Current Status of Neutron Standards, **INDC(NDS)-0677** (IAEA, Vienna 2015).
[76] V.G. Pronyaev, R. Capote, A. Trkov, G. Noguere, A. Wallner, "New fit of Thermal Neutron Constants (TNC) for ^{233,235}U, ^{239,241}Pu and ^{252}Cf(sf): microscopic vs Maxwellian data,"(ND2016, Brugges, Belgium, September 2016), EPJ Web of Conf.**146**, 02045 (2017).
[77] M. Lounsbury, R.W. Durham, G.C. Hanna, "Measurements of Alpha and Fission Ratios for ^{233}U, ^{235}U and ^{239}Pu at Thermal Energies," in Proc. Second Int. Conf. organized by IAEA (Helsinki, 15-19 June 1970), *Nuclear Data for Reactors*, Report **STI/PUB/259**, Vol. 2, 287 (1972).
[78] M. Beer, M.H. Kalos, H. Lichtenstein, H.A. Steinberg, E.S. Troubetzkoy, "Monte Carlo Analysis of 2200 m/sec Alpha Values of Fissile Nuclides," Trans. Am. Nucl. Soc. **23**, 509 (1972); see also "A Monte Carlo Analysis of a Chalk River Experiment on Cross Sections of Fissile Nuclides,"Report **EPRI-NP-163**, Electric Power Research Institute (1975).
[79] Yu.V. Adamchuk, M.A. Voskanyan, G. Georgiev, A.L. Kovtun, G.V. Muradyan, N. Stancheva, N. Chikov, N. Yaneva, Yu.G. Shchepkin, "Measuring of ^{235}U α Values at a Thermal Point," At. Energiya **65**, 434 (1988); in Russian.
[80] C.H. Westcott, "A study of the accuracy of g-factors for room-temperature Maxwellian spectra for U and Pu isotopes," Report **INDC(CAN)-005** (IAEA, Vienna 1969).
[81] P. Archier, C. De Saint Jean, O. Litaize, G. Noguere, L. Berge, E. Privas, P. Tamagno, "CONRAD evaluation code: development, status and perspectives," Nucl. Data Sheets **118**, 488–490 (2014).
[82] Y. Wang, X. Bai, A. Li *et al.*, "Experimental study of the prompt neutron spectrum of U-235 fission induced by thermal neutrons," Chin. J. Nucl. Phys. (Beijing) **II**, 47 (1989).
[83] A. Lajtai, J. Kecskemeti, J. Safar *et al.*, "Energy Spectrum Measurements of Neutrons for Energies 30 keV–4 MeV from Thermal Fission of Main Fuel Elements," Proc. Nucl. Data for Basic and Applied Sci., Santa Fe, NM, Gordon and Breach Publishers, p.613 (1985).
[84] A. Trkov, R. Capote, "Evaluation of the Prompt Fission Neutron Spectrum of Thermal-neutron Induced Fission in U-235," Phys. Procedia **64**, 48–54 (2015).
[85] A. Trkov, R. Capote, V.G. Pronyaev, "Current Issues in Nuclear Data Evaluation Methodology: ^{235}U Prompt Fission Neutron Spectra and Multiplicity for Thermal Neutrons", Nucl. Data Sheets **123**, 8–15 (2015).
[86] W. Mannhart, "Status of the Evaluation of the Neutron Spectrum of ^{235}U," Report **INDC(NDS)-0540**, presentation link in Appendix C (IAEA, Vienna 2008).
[87] E. M. Zsolnay, R. Capote, H. Nolthenius, A. Trkov, "Summary description of the new international reactor dosimetry and fusion file (IRDFF release 1.0)," Report **INDC(NDS)-0616** (IAEA, Vienna 2012). Data available online at https://www-nds.iaea.org/IRDFF/.
[88] R. Capote, K. I. Zolotarev, V. G. Pronyaev, A. Trkov, "Updating and Extending the IRDF-2002 Dosimetry Library," J. ASTM Internat. **9**, JAI104119 (2012). Data available online at https://www-nds.iaea.org/IRDFF/.
[89] M. Kostal, E. Losa, P. Baron *et al.*, "Measurement of ^{89}Y(n,2n) spectral averaged cross section in LR-0 special core reactor spectrum," Rad. Phys. Chem. **141**, 22–28, 2017.
[90] B. Marcinkevicius, S.P. Simakov, V.G. Pronyaev, "^{209}Bi(n,f) and ^{nat}Pb(n,f) Cross Sections as a New Reference and Extension of the ^{235}U, ^{238}U and ^{239}Pu(n,f) Standards up to 1 GeV," Report **INDC(NDS)-0681** (IAEA, Vienna 2015).
[91] S.G. Mashnik, A.J. Sierk, R.E. Prael, "MCNP6 Fission Cross Section Calculations at Intermediate and High Energies," Nucl. Data Sheets **118**, 320–322 (2014).
[92] I. Duran, A. Ventura, S. Lo Meo, D. Tarrío, L. Tassan-Got, C. Paradela, "On the search for a (n,f) cross-section reference at intermediate energies," EPJ Web of Conf.**146**, 02032 (2017) and "Current Status of Neutron Standards Summary," Report **INDC(NDS)-0677** (IAEA, Vienna 2015), available at https://www-nds.iaea.org/index-meeting-crp/TM-neutron-std/docs/Duran-2014.pdf.
[93] N. Otuka, E. Dupont *et al.*, "Towards a More Complete and Accurate Experimental Nuclear Reaction Data Library (EXFOR): International Collaboration Between Nuclear Reaction Data Centres (NRDC)," Nucl. Data Sheets **120**, 272–276 (2014); data are available at https://www-nds.iaea.org/exfor/exfor.htm.
[94] T. Fukahori, O. Iwamoto, S. Chiba,"Unified Description of Neutron-, Proton- and Photon-induced Fission Cross Sections in Intermediate Energy Region," Proc. of 2009 Fall Meetings of Atomic Energy Society of Japan, Report **JAERI-Conf 2003-019**, p.603 (2003) and Private communication (2016).
[95] A.S. Iljinov, M.V. Mebel, "Induced nuclear fission accompanied by pion emission," Phys. At. Nucl. **64**, 1386–1391 (2001).
[96] S.P. Simakov, R. Capote, R.O. Nelson *et al.*, "Evaluation of the ^{7}Li(n,n'γ) 478 keV γ-ray production cross section for Standards,"Report **INDC(NDS)-0739** (IAEA, Vienna, to be published in 2018).
[97] S.P. Simakov, V.G. Pronyaev, R. Capote, R.O. Nelson, "^{48}Ti(n,n'γ) gamma production cross sec-

tion as a candidate for a reference cross section," PROC. 13TH INT. CONF. ON NUCLEAR REACTION MECHANISMS (Varenna, 11–15 June 2012), **CERN-Proceedings-2012-002**, p.321 (2012). Available at http://cds.cern.ch/record/1495183/files/cern-proceedings-2012-002.pdf.

[98] A. Olacel, F. Belloni, C. Borcea *et al.*, "Neutron inelastic scattering measurements on the stable isotopes of titanium," PHYS. REV. **C96**, 014621 (2017); Private communication.

[99] A.J. Koning, D. Rochman, J. Kopecky, J.-Ch. Sublet *et al.*, "TENDL-2015: TALYS-based evaluated nuclear data library,"available at https://tendl.web.psi.ch/tendl2015/tendl-2015.html.

[100] S.P. Simakov, R. Capote, R.O. Nelson *et al.*, "Evaluation of the ^{48}Ti(n,n'γ) 948 keV γ-ray production cross section for Standards," Report **INDC(NDS)-0740** (IAEA, Vienna, to be published in 2018).

[101] R.O. Nelson, Private communication (2017).

[102] R.L. Macklin, J. Halperin, R.R. Winters, "Gold Neutron-capture Cross Section from 3 to 550 keV," PHYS. REV. **C11**, 1270 (1975).

[103] R.L. Macklin, "Gold Neutron Capture Cross Section from 100 to 2000 keV," NUCL. SCI. ENG. **79**, 265–268 (1981).

[104] Karlsruhe Astrophysical Database of Nucleosynthesis in Stars (KADONIS), Test version 1.0. Available at http://exp-astro.physik.uni-frankfurt.de/kadonis1.0/.